



Aalto-yliopisto  
Insinöörیتieteiden  
korkeakoulu

Mikko Nurkka

## **Restoration of Load-Bearing Timber Members Subjected to Fungal Growth: A Case Study of Louhisaari Manor's Roof Truss Structure**

Master's thesis submitted for evaluation in order to finalize master's degree in Building Technology.

Espoo, 21<sup>st</sup> of September, 2019

Supervisor: Professor Gerhard Fink

Instructor: M. Eng. Antti Haikala

---

<b>Author</b> Mikko Nurkka		
<b>Title of thesis</b> Restoration of Load-Bearing Timber Members Subjected to Fungal Growth: A Case Study of Louhisaari Manor's Roof Truss Structure		
<b>Master programme</b> Building Technology	<b>Code</b> CIV	
<b>Thesis supervisor</b> Professor Gerhard Fink		
<b>Thesis advisor</b> M. Eng. Antti Haikala		
<b>Date</b> 21.09.2019	<b>Number of pages</b> 75+62	<b>Language</b> English

---

### Abstract

The Louhisaari estate, located in Askainen, has high historical and artistic value. It dates all the way back to the 1650s, which is when the construction works of Louhisaari manor started. The roofs in the ancillary buildings of Louhisaari manor have recently been repaired, and in a few years the manor's roof truss structures are also going to be repaired. This is the reason for the commissioning of this master's thesis.

This thesis studies the original roof truss structures of Louhisaari manor. The aim of this study is to gain knowledge on the conditions of roof truss members that are embedded into the masonry wall; solve the normal forces that are acting in the connections of timber members inside the masonry wall; and investigate possible intervention materials and methods that could be applied to repair the decayed structures penetrating the outer masonry wall.

This study is based on the available literature, interviews, field studies and structural analysis. The field studies include visual inspection, infrared thermography imaging and resistance drillings. These investigations were mainly subjected to the parts of timber members in the truss that penetrate the outer masonry walls. As a result, a "Rot Report on Louhisaari Manor's Roof Structures" was prepared.

Investigations showed that the timber members (rafters, posts and tie beams) that are partly inside the outer masonry wall are severely rotten and the repair of the roof structures is essential. The applicability of available repair materials and methods was evaluated based on the "Principles for the Conservation of Wooden Built Heritage" and specific characteristics of Louhisaari manor. It was found that timber and steel as repair materials could be applied to maintain the valuable characteristics of the manor, such as the original decorative paintings on the surfaces of the tie beams.

The roof truss structure consists of rafter frames, which distribute a major part of the loads to the leaning trestles that stiffen the roof structures and prevent it from collapsing. The normal forces acting in the embedded parts of timber members were received from finite element analysis. The analysis of members indicate that the cross sections of undamaged timber members embedded into the masonry wall are able to fulfill the existing design requirements with the normal forces received. However, the load history and other characteristics in timber members that might have changed during time were not included in the structural performance analysis.

The received internal forces from the finite element analysis, the rot report and the analysis of possible repair methods can be used as a foundation for further investigations and for the forthcoming restoration process.

**Keywords** deterioration assessment method, finite element analysis, historic, intervention method, IRT, Louhisaari manor, resistance drillings, timber roof truss, rot, wood destroying fungi

---

<b>Tekijä</b> Mikko Nurkka		
<b>Työn nimi</b> Lahonneiden kantavien rakenteiden restaurointi: tapaustutkimuksena Louhisaaren kartanon kattoristikkorakenne		
<b>Maisteriohjelma</b> Building technology	<b>Koodi</b> CIV	
<b>Työn valvoja</b> Professori Gerhard Fink		
<b>Työn ohjaaja</b> DI Antti Haikala		
<b>Päivämäärä</b> 21.09.2019	<b>Sivumäärä</b> 75+62	<b>Kieli</b> Englanti

### Tiivistelmä

Askaisissa sijaitseva Louhisaari on merkittävä historiallista ja taiteellista arvoa sisältävä kokonaisuus, jonka juuret juontuvat 1650-luvulle asti. Louhisaaren päärakennuksen kahden sivurakennuksen vesikattorakenteet on restauroitu edeltävien vuosien aikana, ja Louhisaaren kartanon kattorakenteiden korjaus on tarkoitus toteuttaa muutaman vuoden päästä, mikä on syy tämän maisterin työn toteuttamiseen.

Tämä maisterin tutkielma tutkii Louhisaaren kartanon alkuperäisiä vesikattorakenteita. Työn tarkoituksena on saada tietoa kattorakenteiden osien kunnosta, jotka ovat tiilimuurien sisällä; selvittää muurin sisällä olevien puurakenteiden liitoksissa vaikuttavat normaalivoimat; ja tutkia mahdollisia materiaaleja ja menetelmiä, joilla tiilimuriin tunkeutuvia puurakenteita voitaisiin korjata.

Tämä tutkimus perustuu olemassa olevaan kirjallisuuteen, haastatteluihin, kenttätutkimuksiin ja rakenneanalyysiin. Kenttätutkimukset sisältävät visuaalisen havainnoinnin, lämpökuvauksen ja vastusporaukset. Nämä kenttätutkimukset kohdennettiin pääasiassa kantavien kattorakenteiden puuosille, jotka työntyvät tiilimuurien sisälle. Tuloksena valmistui ”Lahoraportti Louhisaaren kartanon kattorakenteista”.

Tutkimustulokset osoittivat, että osittain ulkotiiliseinän sisällä olevat kattorakenteiden osat (selkäpuut, pukin jalat ja alapaarteet) olivat pääsääntöisesti lahonneita, ja kattorakenteiden korjaus olisi välttämätöntä. Mahdollisia korjausmateriaaleja ja -metodeja arviointiin ”Principles for the Conservation of Wooden Built Heritage” ja Louhisaaren kartanon ominaispiirteiden perusteella. Tutkimusten perusteella voidaan todeta, että käyttäen puuta ja terästä korjausmateriaaleina voitaisiin säilyttää kartanon arvokkaat ominaispiirteet, kuten koristeelliset maalaukset alapaarteiden pinnoissa.

Kattotuolirakenteen selkäpuuparit jakavat suurimman osan katolle tulevista kuormista pukkirakenteille, jotka jäykistävät kattorakennetta ja estävät sen romahtamisen. Tiiliseinän sisällä olevissa puurakenteissa vaikuttavat normaalivoimat ratkaistiin elementtimenetelmänalyysin avulla. Rakenteiden analyysi osoitti, että vahingoittumattomat puurakenteiden poikkileikkaukset, jotka ovat tiilimuurien sisällä, täyttävät olemassa olevat suunnitteluvaatimukset ratkaistuilla normaalivoimilla. On huomioitava, että rakenteiden kuormitushistoriaa, eikä muita puun ominaisuuksia, jotka ovat saattaneet muuttua ajan kuluessa otettu huomioon rakenteiden kestävyuden analysoinnissa.

Elementtimenetelmänalyysistä saatuja sisäisiä voimia, lahoraporttia sekä mahdollisten korjausmenetelmien analyysia voidaan käyttää lähtötietoina jatkotutkimuksissa sekä tulevassa rakenteiden restaurointiprosessissa.

**Avainsanat** elementtimenetelmänalyysi, historiallinen, korjaustapa, laho, lahottajasieni, Louhisaaren kartano, lämpökuvaukset, puukattoristikko, vaurioitumisen arviointikeino, vastusporaus

## Acknowledgements

*I would like to thank all the people who have assisted me during this master's thesis. Especially, I would like to thank my instructor Antti Haikala from HP Insinöörit Oy and my supervisor Gerhard Fink from Aalto University who both guided and supported me throughout the work. Antti Haikala and Juhani Pentinmikko from HP Insinöörit Oy deserve my special thanks for inventing the subject for this master's thesis.*

*Selja Flink from Senaattikiinteistöt provided me this unique opportunity to study one of the most valuable roof structures located in Finland, which I am very grateful of. I would also like to thank Pekka Tukiainen from HP Insinöörit who pondered the problems that arised during the process and shared his ideas with me.*

*Finally, I would like to thank Kaisa for her linguistic support, love and encouragement.*

In Espoo 21<sup>st</sup> of September, 2019



Mikko Nurkka

# Contents

Abstract	
Tiivistelmä	
Acknowledgements	
Contents .....	5
Introduction.....	7
1.1 Background .....	7
1.2 Research area .....	7
1.3 Outline and objectives.....	8
2 Literature review .....	9
2.1 Wood-destroying fungi .....	9
2.1.1 Brown rot .....	10
2.1.2 White rot .....	12
2.1.3 Soft rot .....	13
2.1.4 Typical structural timber parts degraded due to fungal growth.....	13
2.2 Deterioration assessment methods for historic load-bearing timber members .....	14
2.3 Intervention materials.....	18
2.3.1 Timber.....	18
2.3.2 Steel .....	18
2.3.3 Fibre-reinforced polymer .....	19
2.3.4 Adhesives.....	21
2.4 Intervention methods.....	24
2.4.1 Replacement.....	26
2.4.2 Timber prosthesis.....	26
2.4.3 Gap-filling adhesive.....	30
2.4.4 Consolidation .....	32
2.4.5 Partial substitution with steel .....	33
2.4.6 Circumvention .....	34
3 Louhisaari manor .....	36
3.1 Structural system.....	36
3.1.1 The leaning trestles .....	39
3.1.2 The rafter frames.....	40
3.1.3 Eave structures .....	41
3.1.4 Third floor ceiling .....	41
3.2 Structural analysis .....	43
3.2.1 Structural system.....	43
3.2.2 Loads.....	43
3.2.3 Supports .....	45
3.2.4 Internal forces .....	45
3.2.5 Structural performance .....	48
4 Investigations .....	50
4.1 Visual inspections .....	50
4.2 Resistance drillings .....	54
4.3 Infrared thermography imaging .....	59
4.4 Discussion .....	60
5 Intervention method for the rotten timber structures .....	62
5.1 Boundary conditions .....	62

5.2	Analysis of intervention methods.....	62
5.2.1	Timber prosthesis with all-timber/metal fastener connections .....	63
5.2.2	Glued-in steel and FRP rods .....	64
5.2.3	Gap-filling adhesive.....	65
5.2.4	Partial substitution with steel.....	65
5.2.5	Circumvention .....	65
5.3	Recommendation for the intervention method.....	66
5.4	Additional measures.....	66
6	Conclusions.....	67
	Bibliography .....	70
	Appendixes .....	75
	A. Structural calculations	
	B. Rot Report on Louhisaari Manor´s Roof Structures	

# Introduction

## 1.1 Background

The recent investigations on Louhisaari manor's roof structures were started in the autumn 2017 by a group of students and researchers from five different universities in Finland. The roof structures of Louhisaari were investigated although the main focus was at that time in the roof structures of the eastern ancillary building of Louhisaari manor. This repair process was completed in the beginning of summer 2019. The investigations that were performed in 2017 are presented in "Ruotsin suurvalta-ajan vesikattorakenteet Suomessa". It was found that the roof had been leaking and the roof truss structures were rotten in parts where the timber members are penetrating to the outer masonry walls from the attic. [1, p. 25, 143-144] Based on these investigations the need for the repair of the roof structures was clear. However, the amount of rot in timber members was unclear as the timber members are partly embedded to the external masonry walls [1, p. 143].

The repair of the roof structures in Louhisaari manor are planned to take place in the near future and the need to carry on the investigations on Louhisaari roof structures was essential. Antti Haikala from HP Insinöörit Oy suggested to Selja Flink from Senaatti-kiinteistöt in the end of 2018 that a thesis could be implemented relating to the roof truss structures of Louhisaari which led to the commissioning of this master's thesis.

## 1.2 Research area

Louhisaari manor is located in Masku and its construction started in the 1650s. The load-bearing roof structures are known to be original from the beginning of 1660s. The roof structure is based on a rafter frame and leaning trestle structure. These roof truss structures are not typical in Finland, and only two other similar type of roof structures from the same era are known to be found in Finland. These other roof structures can be found in the church of Askainen and the old church of Uusikaupunki which are both located close to Louhisaari. The roof structure type came to Finland from Sweden. Similar type of roof construction based on leaning trestles has been used in other European countries as well. The roof structures in Louhisaari manor have high historical and archeological value and the preserving of these structures is important. [1, p. 25, 164]

The decorative paintings located in the ceiling of third floor banqueting hall are known to be original from 1650s. These paintings have high artistic and historical value and preserving these paintings is of importance. The ceilings in other rooms in the third floor have been painted, but they are more heavily restored, although some of these are very impressive. It is also possible that the decorative paintings in one room have not been investigated. [1, p. 14-15] All these paintings are also on the surfaces of tie beams, which tie the roof structures together and support the third-floor ceiling. The tie beam ends are inside the outer masonry wall where they connect to the rafters of rafter frames and to the posts of the leaning trestles.

### **1.3 Outline and objectives**

Most general wood destroying fungi in buildings are investigated to understand the reactions that occur in decaying timber and to figure out the environmental conditions that have to prevail in order for the fungal growth to take place in timber. The understanding of required environmental conditions for fungal growth guides the structural engineer to minimize the possibility of fungal growth when designing the repair for timber structures.

The normal forces that are used in the structural design phase for the repairs are solved in the connections of timber members (tie beams, rafters and posts) that are embedded into the masonry wall. The performance of these existing timber members from their embedded parts are evaluated in ULS (ultimate limit state) with the existing design guidelines.

The conditions of timber members that are partly embedded into the outer masonry wall are investigated with the most suitable timber assessment methods.

Intervention materials and methods that can be applied to repair rotten timber members are investigated. The applicability of these repair methods is evaluated based on the requirements specific to Louhisaari manor and the “Principles for the Conservation of Wooden Built Heritage”.



## 2 Literature review

### 2.1 Wood-destroying fungi

Micro-organisms occupying wood are divided into four different groups that are wood-staining, surface moulds, bacteria and wood-destroying. Wood-destroying fungi are able to change the chemical and physical composition of wood and break the cell walls to smaller pieces, which makes it the most destructive wood occupying micro-organism. [2, p. 107] Wood-destroying fungi can be categorized into three main groups based on their enzyme systems (visual appearance and the type of damage they produce) [2, p. 109; 3, p. 442]. These groups are soft rot, white rot and brown rot fungi [3, p. 442]. Brown rot, white rot and some soft rots are also called wet rot when dry rot (brown rot species) is not included [2, p. 109-110; 3, p. 442; 4, p. 80; 5, p. 331; 6, p. 427]. The reason for this many reference relating to fungal definition is that different researchers have different ways of categorizing them and there is no commonly accepted practice how different fungi should be categorized into kingdoms and other systematic groups [7, p.68]. Microscopic hyphae of the fungus consist of threads with cross sections of 1 to 10  $\mu\text{m}$  thick that penetrate the wood. [3, p. 442]

Certain environmental conditions must exist for the fungal growth to take place in wood. These environmental conditions required are suitable substrate (wood), source of infection (spores or invasion by fungal mycelium), adequate moisture supply, suitable temperature and absence of poisonous substances or inhibiting substances including preservative chemicals and toxic heartwood components from the substrate. Adequate moisture, oxygen, moderate temperatures and food are the essence of continued fungal growth. Furthermore, acidic pH level is a factor for wood-destroying fungi. pH values between 4.5 to 5.5 are optimal for the growth of brown and white rot fungi. Furthermore, in the process of metabolizing white rot and especially brown rot increase the acidity of wood which improves the fungal growth. In addition, only a few types of fungi require light to grow. [2, p. 105-108]

The temperatures which favour fungal growth are generally between 20 to 25°C. Fungal growth slows down in temperatures higher than 30°C and lower than 10°C. Lethal temperatures depend on the type of fungi. Fungi can be killed with high or low temperatures, but it does not protect the wood from new fungal attack if the lethal temperature is not sustained. [2, p. 106]

Air and moisture inside the wood are necessity for fungal activity and growth. Thus, when wood is near or at fibre saturation point (28 to 30% moisture content) it is vulnerable to fungal attack. However, the exact moisture content requirement depends on the species of fungi. Instead of dying at low moisture levels the fungus stays dormant, and if beneficial moisture conditions appear it can start growing again. However, particular species are resistant to drying and others can even transport water from distances to increase moisture content for decomposition of wood. Lack of oxygen inside the voids of wood due to high moisture content can affect negatively on the growth and infiltration of fungi. [2, p. 106-107]

In fungal attack, hemicellulose and cellulose are disintegrated into simple compound sugars by the enzymes exuded by the fungi. The degrading organisms of fungi then absorb and metabolize these simple compound sugars. Apart from most rot species, white rot has the ability to degrade lignin. Typically, if the lignin is attacked by most of the rot species, cellulose and hemicellulose are already degraded and it is the only element left. [2, p. 108] Fungi

can spread in two different ways e.g. by sexually or asexually produced spores. When spreading sexually the spores are formed in a fruiting body, inside tubes or on the surface of lamellae. [3, p. 442]. Each wood species contains extractives. The amount of extractives define the resistance against fungal attack, that is, the higher the amount the higher the resistance. [2, p. 108] The amount of extractives in wood in temperate regions vary typically between 1-10% [8, p. 35]. For example, Scots pine (*Pinus sylvestris*) has an extractive content between 2.5 to 4.5% depending on the growth conditions [9, p. 10-11]. However, in some tropical species the amount of extractive concentration can be up to 40% [8, p. 35].

### 2.1.1 Brown rot

Brown rot is the most common type of rot found in buildings and it is a subdivision of Basidiomycota fungi [10, p. 128; 2, p. 109]. There are more than 100 types of known brown rot found. The common ones are dry rot (*Serpula Lacrymans*) known as the floor fungus, cellar fungus (*Coniophora puteana*) and *Fibroporia Vaillantii* (and other *Poria* species) [3, p.442; 4, p. 81]. The strength of the wood is weakened in the process where brown rot exudes oxalic acid that hydrolyzes the hemicelluloses which induce the disarranging of cellulose fibres. The weight loss in wood occurs in later stages of fungal activity when the cellulose fibres are disintegrated. When the disintegration is complete only lignin is left “in the form of brown humic acids”, as Bech Anderssen describes. [3, p. 442] Cracks that are along and across the grain are caused by brown rot which also turns the wood darker in colour. Very decayed wood colonized by brown rot will crumble to dust when dry. [5, p. 331] Two types of Brown rot that are relevant for this study are expanded on below, because the other one is most destructive and the other is the most common.

#### Dry rot (*Serpula Lacrymans*)

Dry rot lives inside wet masonry. However, the type of masonry has an impact on the growing ability of the fungus because it needs calcium and iron for the decaying process. The moisture is absorbed to wood when contacted to wet masonry. [6, p. 426] If the wet masonry is contaminated by dry rot it spreads to the wood parts in contact that excess of 20% moisture content [11, p. 426].

There is a vast amount of altering data concerning the environmental conditions favourable to the growth of dry rot fungus. Research done by Schmidt is reliable which is due to the fact that he has used internal transcript spacer (ITS) sequencing to identify the fungus investigated. In his article he overturned a number of accepted scientific knowledge relating to dry rot fungus. According to Schmidt the minimum wood moisture content for dry rot decay is 26% and the optimal is between 45 to 140%. Furthermore, the maximum moisture content for dry rot decay in wood is 240%. [11, p. 6] Bech-Anderssen stated that “dry rot has a special ability to transport water through its strand mycelium for up to 6 metres and can overgrow dry wood and moisten it” [3, p. 443]. This commonly accepted fact was overturned by Schmidt’s article in 2007 stating that “strands only carry a solution of nutrients, and they do not act as a conduit for water transportation”. However, mycelium can transport water and change the moisture content of wood, but this is possible only in already colonized areas. Schmidt also underlined in his article that “the erroneous opinion that the enzymatic decomposition of wood alone can produce enough water for the fungus to survive can be found even in recent publications”. [11, p. 8]

Dry rot mainly attacks softwood, but it can also penetrate some hardwoods [2, p. 110]. It is able to grow in temperatures between -2 to around 26 to 27°C, but the optimal temperature

is about 20 to 22°C [3, p. 443; 12, p. 141]. Dry rot can be killed in temperatures above 50°C in 4 hours and it also dies below -6°C. [11, p. 7; 12, p. 141] Hot air treatment is used in Denmark for the control of house rot fungi. It is supposed that lethal value in hot air treatment for house rot fungi is 60°C. [11, p. 8]

In more developed stages of decay the wood colonized by dry rot appears dry, from which dry rot derives its name. The lustre in the wood disappears in the early stages of dry rot (brown rot). Furthermore, when the dry rot infiltration in wood proceeds, the wood turns into anomalous brown in colour. [2, p. 110] Dry rot changes the appearance of wood into a cuboidal rot, with cubes up to 7 cm long [3, p. 443]. Filaments of hyphae are not usually visible on the wood surface, although under elevated moisture conditions a woolly covering of mycelium can be found [2, p. 110; 3, p. 443]. Mostly more than 2 mm thick fruiting bodies, white in the early stage and turning brown from the centre as it grows, are only formed where light is present to ensure dispersal of spores [3, p. 443]. To identify fungal growths there are four essential characteristics that can be used. These four characteristics are the appearance of mycelium, strands (Rhizomorphs), sporophores (fruiting bodies), and the type of decay in the wood. [5, p. 330] These characteristics of dry rot are presented and compared in the Table 1 for those of wet rot which contains major part of wood destroying fungi including white rot, some soft rots and all the brown rot species except dry rot [2, p. 109-110; 3, p. 442; 4, p. 80; 5, p. 331; 6, p. 427].

*Table 1. Main characteristics of dry rot decay in timber compared to those of wet rot [5, p. 331].*

<b>Characteristic</b>	<b>Dry Rot</b>	<b>Wet Rot</b>
Mycelium	-Damp conditions: Masses of tears on silky white surface, with bright lemon patches. -Drier conditions: Thin skin of silver grey in colour, with deep lilac tinges.	-High humidity: Yellow to brownish in colour
Decaying Wood	-Deep cuboidal cracking associated with differential drying shrinkage -Reduction in weight -Dull brown in colour -Resinous smell gone	-Cuboidal cracking on smaller scale -Thin skin of sound wood -Weight loss -Localised infection
Strands (Rhizomorphs)	-3-6 mm in diameter -Brittle when grey -Off white / dark grey in colour	-Thinner than dry rot -Flexible when dry -Creamy white in colour
Sporophores (Fruiting bodies)	-Tough, fleshy pancake or bracket-shaped, varying from a few cms to a metre across -Ridged centre: Yellow-ochre when young, darkening to rusty red when mature -Lilac/white edged -Distinct mushroom smell	-Not very common in buildings -Must smell, rather than mushroom smell associated with an active growth of dry rot

The dry rot is problematic because of its ability to move inside damp masonry or stone, behind plaster and in mortar joints [2, p. 110]. Dry rot contaminated wet masonry being contacted to timber in the absence of air movement is essential for the growth of dry rot in timber. Therefore, the decay due to dry rot is limited to the ends of timber members (e.g. beams) if even minimal air change occurs in the surroundings. After the structure is repaired, no timber member should be in contact with the damp contaminated masonry. If the new timber parts would be attached to the contaminated masonry, the masonry should be dried permanently so that the timber parts would not exceed moisture content of 16%. [6, p. 426]

### **Cellar fungus (*Coniophora puteana*)**

Cellar fungus is the most common wood decaying fungus in houses under temperate and subtropical conditions [1, p. 442]. However, the damage that cellar fungus causes is far less than dry rot. Cellar fungus does not have the ability to live and travel through masonry that dry rot has and therefore attacks are more localized in wood. [6, p. 427] It has the ability to attack and decay both hardwoods and softwoods, and it can spread to houses from forests [3, p. 442; 6, p. 427]. Optimal conditions in buildings for cellar fungus are typically found for example in cellars, floor partitions and where wood is placed on moist masonry [3, p. 442].

The optimum temperature for cellar fungus according to Schmidt is at 22.5 to 25°C and its lethal temperature on agar is 60°C for three hours [11, p. 7]. Furthermore, the minimum temperature is approximately 3°C and the optimum pH level is 5.7 to 6.3 [7, p. 74]. The optimal wood moisture content for the decaying process of the cellar fungus is between 36-210%, minimum being 22% maximum being 262% and minimum for colonization of wood being 18% [11, p. 7].

The mycelium of the fungus penetrates wood but in moist environments it is possible that the fungus generates yellow mycelium to the surface of wood or a strand mycelium that changes the colour to dark brown in early stage. [3, p.442]. Cellar fungus belongs to the wet rot species. Their fruiting bodies are seen a lot less in buildings than dry rot. It is hard to identify which wet rot is in question if the fruiting body is missing. [6, p.427] However, if the fruiting body of a cellar fungus is found they are yellowish brown, few millimetres thick and have a white perimeter. [3, p. 442]

When the wood is attacked it turns yellowish brown, but after a while it turns reddish brown. The rot is cuboidal with shallow perpendicular to grain and deeper parallel to grain cracks usually about 1 x 1 cm in size. However, if the air humidity is low the cubes of the rot are approximately 2 to 3 mm long and the disintegration occurs inside the wood leaving a thin wood surface. [3, p. 443]

### **2.1.2 White rot**

The bleaching of the wood due to white rot fungi is connected to the deterioration type subdivision of basidiomycota and higher forms of ascomycetes. In the attack of white rot, the wood appearance is not affected considerably before the final stages of decay. In the final stages the wood appears “as a spongy or fibrous mass with white pockets or streaks, separated by areas where the wood remains strong”, Harris describes. White rot does not cause cuboidal cracking to wood like brown rot. White rot quickly affects the surface toughness of the wood, which has a negative effect on the strength properties in that area. White rot mainly attacks hardwood, but it can also deteriorate softwood, especially in situations where it is located close to the ground. [2, p. 110-111]

In the deterioration process white rot breaks down lignin and cellulose, whereas brown rot has no influence on lignin [2, p. 111; 3, p. 444]. Cellulose is left untouched in the form of fibrous whitish material [3, p. 444].

The most common white rot species are *Donkporia expansa*, *Pleurotus ostreatus*, *Asterostroma*, and *Phellinus contiguus* [5, p. 331]. *Donkporia expansa* prefers moist conditions, hardwoods (particularly oak) and colonizes especially beam ends that are built inside external permeable masonry walls. The mycelium of *Donkporia experansa* is yellow to red-brown. [4, p. 81] It is able to hollow out large cross section beams without being visualised from outside [6, p. 427].

### 2.1.3 Soft rot

Soft rot type of deterioration is related to the subdivision of Ascomycota and Deuteromycota fungi, which has a softening effect on wood [2, p.111; 7, p.77]. In the deterioration process it superficially softens the wood. However, planing or sanding can be simply used to remove the deteriorated soft parts easily. The only strength loss due to soft rot relates to the loss of surface toughness which can be reduced 15 to 30%. Wood colonized by soft rot turns the surface of the wood into varying colours such as shades of black orange and green (Figure 1). Soft rot deteriorated wood turns checked and brittle from the surface layers when it dries out. However, the wood layers under the rotten parts remain unaltered with no change in their properties. Soft rot appears in wood with high moisture content such as wood in contact with moist soil and wood in water contact. [2, p. 111-112]



*Figure 1. Appearance of soft rot [13, p. 3].*

### 2.1.4 Typical structural timber parts degraded due to fungal growth

If the environmental conditions favour fungal growth (mentioned above) in timber structure, it is in danger of fungal contamination. There are many reasons which can lead to moisture levels favourable to fungal growth in wood. Moisture in buildings contribute from factors such as condensation, penetrating damp, rising damp, building defects, construction moisture and building disasters [5, p.331]. However, these reasons can be prevented with proper design, construction and maintenance. Typical fungal growth areas for structural timber are e.g. structures in contact or within small distance from external walls, roof truss structures

under or near damaged or untight roofing material, structures exposed to weather and structures near or in contact with soil [14, p. 497].

## **2.2 Deterioration assessment methods for historic load-bearing timber members**

New “Principles for the Conservation of Wooden Built Heritage” were adopted as an ICOMOS doctrinal text on 15<sup>th</sup> December 2017 [15, p. 1]. These principles among other things describe the practice how the condition of wooden built heritage should be inspected. The text instructs that “the diagnosis must be based on documentary evidence, physical inspection and analysis and, if necessary, measurements of physical condition using non-destructive (NDT), and if necessary on laboratory testing”. However, the text “does not preclude carrying out minor interventions and emergency measures where these are necessary”. The adopted principles also state that if the inspection cannot be carried out sufficiently without structural openings these temporary openings are possible, “but only after full recording has been carried out” from the structure. [16, p. 2]

It is important that the actual mechanical properties of the material in the existing timber structure being inspected is evaluated in the first stage to estimate the safety of the structure. Destructive testing methods are only methods that can give genuine strength properties of a timber member. However, destructive methods are usually not approved in the assessment of historic buildings or even in other timber structures. [17, p. 236] The true condition of historical timber member can be hard to define, which can lead to errors in repair works. Common methods for analysing the condition of historic timber structures that can be used according to the values of ICOMOS are presented below.

There are many non-destructive timber testing methods that can be applied on site. Each on-site timber structure assessment should be started with visual inspection. Visual inspection is limited to the surfaces of materials that can even sometimes be out of reach and the results are bound to the experience of the surveyor. Therefore, it is advisable to use an experienced surveyor or even a group of specialists when performing visual inspections to historic buildings. Endoscopy can be used to detect structures that are hidden behind other structures impossible to observe with naked eye. Endoscope can be used when a minimum of 5 to 20 mm hole in diameter is drilled or already exist in the structure that is blocking the view. The endoscope is then inserted through the existing or drilled hole to investigate the structures hidden. [18, p. 54, 66]

Tapping (sounding) is the sound that comes when a blunt object is tapped against timber with an obtuse object such as a hammer. The inner conditions of timber are evaluated with a reference sound that arises from the tapping. The sound differences that can be sensed in members with tapping are also evaluated as the density of the wood varies with the frequency of the sound that arises. With this analysing method decay, fungi or insect damages can be estimated in a rough scale. Surveyor’s experience is important when using tapping as an assessment method because the estimation of the sound is highly dependent on the experience. [18, p. 56]

Measuring the environmental conditions (relative humidity and temperature) and the timber moisture content can reveal if the conditions favour fungal growth in timber members. If the relative humidity of the environment does not exceed 80%, the moisture content of the hygroscopic timber member should be under 20%. [19] Furthermore, if it exceeds moisture

content of 20% it means that the timber member is absorbing moisture from some unfavourable source. Figure 2 shows the correlation between the environmental conditions and moisture content in timber. Measuring wood moisture content with oven dry method is not applicable for in-situ investigations due to its destructive nature. Therefore, non-destructive resistance method is used. Resistance method is based on the electrical current which is low in wood and high in water. The higher the moisture content in wood the lower the resistance. [18, p. 62-63]

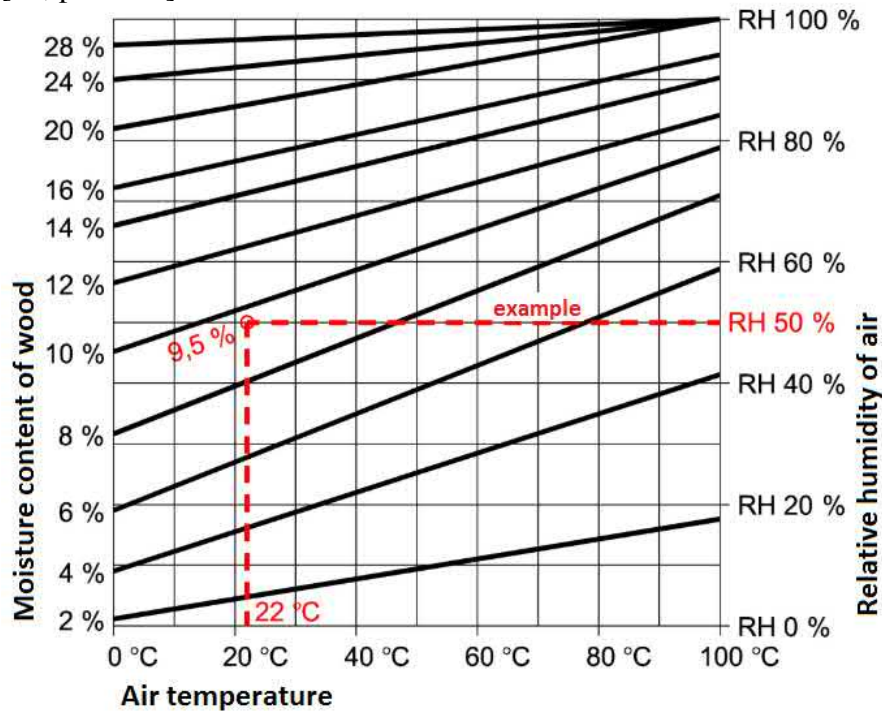


Figure 2. The correlation of air temperature and relative humidity to moisture content in wood [16].

Infrared thermography (IRT) is used to visualize the surface temperature of the structure without contact. The method is based on the infrared radiation that is emitted by the structures. In the assessment of timber structures, it is currently used to detect large scale decayed areas, high moisture content, concealed timber, voids, structural defects, hidden connections or insect attacks. [20, p. 242; 21, p. 38] These issues can be assumed if homogenous material has substantial temperature differences shown by IRT in same environmental conditions (Figure 3). The bigger the temperature differences in homogenous material the larger defects can be indicated. [21, p. 38] There are ongoing investigations on how IRT could be used to reliably estimate the density of timber [20, p. 242].



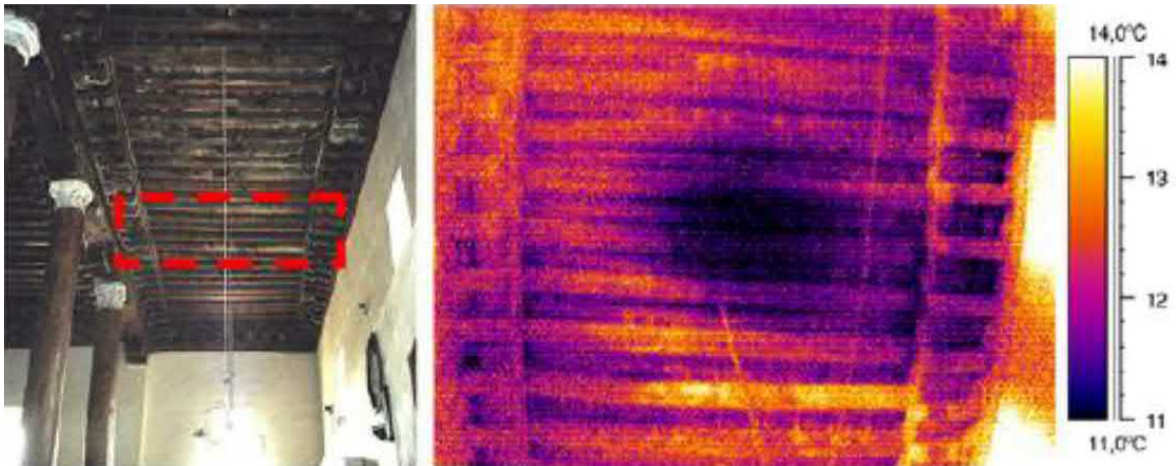


Figure 3. The IRT image from the timber ceiling showing the damp areas with lower temperature [21, p. 39].

Penetration resistance assessment is used to identify the compression strength of the outer layer (20 mm) of the timber member. Penetration depth measurement tool commonly used is Pilodyn shown in Figure 4 which shoots a striker pin needle to the wood with defined spring force that is released. Penetration resistance method can be used to measure the density of the timber without using the common destructive method presented for e.g. in EN 384. This method cannot be applied to frozen or very dry timber members. This method is low-destructive as it leaves a hole of approximately 2.5 mm in diameter. [18, p.68-69]



Figure 4. Pilodyn tool and its use for historic timber structures [22, p. 41].

Drill resistance testing method analyses the resistance of the timber member. It can detect the depth and scale of decay due to fungi or insects within penetration area. Resistograph (Figure 5) or Siebert can be used in the drill resistance method. When the wood is decayed it gives no resistance and the results show flat line. However, the points and the amount of the drillings should be chosen carefully because if there is a void caused by a crack, misleading interpretations for e.g. on fungal or insect attacks can be made relating to the structural capacity of the timber member. The method is semi-destructive as the diameter of the point is from 1.5 to 3 mm. [18, p.72-73]





*Figure 5. Resistograph in use.*

In core drilling small circular cores of about 5 mm in diameter are drilled from the wood and analyzed in the laboratory. Core drilling is a semi-destructive method that can be used to establish properties such as density, moisture content, compressive strength and modulus of elasticity. [18, p. 75; 21, p. 43] In laboratory testing the cores are loaded mainly parallel to grain because the strength properties along the fibres are generally more determining in failures of timber members than perpendicular to fibres. The properties of whole structural members are possible to estimate with correlation from a number of specimens taken. [21, p. 43] Furthermore, the type of fungi and insect attack including age and origin of the wood can be detected from samples in the laboratory. The extraction of cores does not compromise the strength of the timber member. Although the holes that are left vary in size (depending on the drilling head that is used) they are still generally smaller than most knots. [18, p. 75, 104]

There are four different stress wave assessment methods that can be applied to historic timber structures. In the stress wave method sound waves are used to find out the mechanical properties or detect voids and decay from inside the timber member. Thus, the fastest way for a sound wave to move is the shortest way, and if it takes longer time than with reference sound wood values, the condition or the grade of the timber member can be evaluated. Beside the common calculated velocity of sound waves, the frequency spectrum analysis is also used. [18, p. 82] These stress wave methods are all sensitive to characteristics of a timber member, such as ring orientation, geometry, preservative treatment, moisture content, temperature and mechanical stresses in member which have to be taken into account when using these methods. Furthermore, attention should be given to the bond ability of coupling agents, frequency response and the sensitivity of converters, the use of the hammer (impact duration and energy) and to other possible measurement conditions. [18, p.86]

X-ray can be used to scan 2D (two-dimensional) images from the timber structure. Thus, the given images and density data received from X-ray shows the average density and not the density in specific depth points which makes the evaluation of possible defects of cracks

quite hard. Analysing the scale of deterioration from X-ray timber image can be hard because of superimposed sound wood over decayed parts. [18, p. 90-91]

All these methods that are shortly presented above can be used for analysing the deterioration rate of historic timber members. There are also other suitable assessment methods for historic timber structures available, such as mapping of cracks and pull-out resistance tests, which do not differ significantly from the ones presented. One must have a cogent reason why other than non-destructive testing methods should be used for timber structures with historic value. Structural safety is one of these cogent reasons that must be investigated thoroughly. Efficient repair or strengthening solutions can only be proposed when the structural behaviour and condition of the structure is analyzed in detail [23, p. 1].

## **2.3 Intervention materials**

There are different intervention materials that are used to repair deteriorated timber members, including timber, steel, adhesives and fibre reinforced polymers. However, caution must be used when choosing the material for repairing historic timber structures. Material that is used should be traditional or compatible, and present-day materials should be used only if it is proven to be efficient over a long period of time. Materials that are used to repair deteriorated timber members are presented in this chapter.

### **2.3.1 Timber**

It is common to find timber repairs from historic buildings as it has been and still is the most used material for the repair of timber structures. When using timber in repairs of timber structures, the durability can be well predicted even in fluctuating environmental conditions. Thus, different physical behaviour of materials that can cause degradation are avoided when using timber. All-timber connections (connections made entirely of timber) are also possible in most cases due to the modern and traditional knowledge. The reliability for traditional timber material used in connections has been obtained during centuries of use, which is an advantage compared to many other materials. When comparing timber to modern materials, many timber structures have sustained many centuries with proper maintenance, but many modern materials have not even been used for many decades. All in all, timber is an authentic and reversible material that is a natural solution for repairing timber structures. Timber that is used in the repair of historic timber buildings has to be carefully selected to sustain the performance of the structure. The new timber part should meet the characteristics of the historic timber member to prevent incompatibilities that can result from different species, quality, moisture content or physical properties. [22, p. 52-53]

### **2.3.2 Steel**

Metals have been used in historic timber structures in interventions or as an original material. The physical and mechanical properties of metals have been used to improve the performance of timber structures and simplify the complex carpentry details in connections increasingly since the industrial revolution in the 19<sup>th</sup> century. Applications such as bolts, nails, ties and straps have been widely used in connections. In general, the timber connection was designed with metal application or it was improved with metal after the detection of functional problems in the timber connection. Some techniques that have been used are still applicable for interventions, but others are proven to be ineffective. [22, p. 54]

The mechanical properties of steel make it a suitable repair material for timber structures. However, environmental conditions and the resistance to fire have to be taken into account

when using steel in interventions. Problems such as condensation can occur on the interface of timber and steel element causing the decay of the surrounding timber affecting the durability of the connection. In worst case scenario, the deterioration cannot be seen if it occurs inside the timber member. Stainless steel should be used to avoid corrosion, which makes using steel more expensive option. Steel quickly loses its strength under high temperatures, which can be a major threat to the structural safety in fire situations as steel is often used in essential load-bearing parts in structures. [22, p. 55] Fairly new innovations have been developed where metals are used in timber connections to retain the structural integrity in fire situations. Steel is applicable repair material for historic timber structures when these presented issues are taken into account.

### 2.3.3 Fibre-reinforced polymer

Fibre-reinforced polymers (FRP) are heterogeneous and anisotropic composite materials with linear elastic behaviour until failure. FRP is made of polymeric matrix (commonly consist of epoxy resin but polyester or vinylester resins are also used) and reinforcing fibres made of glass, carbon or aramid varying in size and shape (thickness of laminates is generally some tenths of millimetre). Table 2 presents the properties of fibres used in FRP which can be compared to steel and polymeric resin. [24, p. 7-8, 18] As can be seen from Table 2, the density of FRP is much lower than the density of steel, which makes FRP easier to handle on site. The thermal conductivity of Glass FRP is approximately 80 times lower when compared to steel [57, p. 2].

Table 2. Comparison between the typical properties of fibres, matrix (resin) and steel [24, p. 8].

	Young's modulus $E$ [GPa]	Tensile strength $\sigma_T$ [MPa]	Strain at failure $\epsilon_T$ [%]	Coefficient of thermal expansion $\alpha$ [ $10^{-6} \text{ }^\circ\text{C}^{-1}$ ]	Density $\rho$ [g/cm <sup>3</sup> ]
E-glass	70 – 80	2000 – 3500	3.5 – 4.5	5 – 5.4	2.5 – 2.6
S-glass	85 – 90	3500 – 4800	4.5 – 5.5	1.6 – 2.9	2.46 – 2.49
Carbon (high modulus)	390 – 760	2400 – 3400	0.5 – 0.8	-1.45	1.85 – 1.9
Carbon (high strength)	240 – 280	4100 – 5100	1.6 – 1.73	-0.6 – -0.9	1.75
Aramid	62 – 180	3600 – 3800	1.9 – 5.5	-2	1.44 – 1.47
Polymeric matrix	2.7 – 3.6	40 – 82	1.4 – 5.2	30 – 54	1.10 – 1.25
Steel	206	250 – 400 (yield) 350 – 600 (failure)	20 – 30	10.4	7.8

FRP can be applied in the form of for e.g. plates, sheets, rods or stripes. Nails, bolts, screws or adhesive can be used to connect the FRP to timber. The chosen connection type has its own effect “on the connection behaviour and in particular on the transfer of stresses, which influences the stiffness of the composite element and the exploitation of the single materials”. Adhesive bonding is the most common type of connection in FRP strengthening of timber members. The practice has shown that FRP can be used in repairing and strengthening of timber members under bending, tension and shear including trusses, beams and frames. They are used to connect different elements or between prosthesis and original element. Also bridging, crack opening prevention and local rupture confinement are possible to prevent or limit defects. When using FRP in strengthening of joints, the risk due to tensile stresses perpendicular to the fibres reduces and the ultimate behaviour of the connection and under

cyclic load improves. Stiffening of timber floors with the use of FRP is proven an effective measure against in plane actions. [25, p. 5-6]

The elastic behaviour until failure of the FRP composites should be carefully taken into account in design. This is due to the brittle failure type common to timber, which is caused by natural defects such as excessive fibre inclination and knots. The brittle failure can be avoided by installing the strengthening to the tension zone in members subjected to bending, causing higher strength in tension zone and higher strains in compression zone. This changes the failure of the member to localized plasticization instead of failure of the tension zone. [25, p. 8]

The strengthening fibre should be carefully chosen for the application because they have different kind of properties. Glass fibres have high ultimate strain and low elastic modulus, which makes them more suitable for timber strains, reducing the danger of premature collapse and debonding phenomena. Aramidic fibres are less sensitive to impulsive loads, whereas carbon fibres are more resistant to environmental conditions and creep phenomena. [25, p. 12]

Different behaviour of FRP and timber in fire situations and in varying temperature and humidity conditions have to be taken into account in design. The durability of the adhesive bond has to be taken into account, as the adhesive can only be considered compatible when it adapts to the shrinking and swelling of timber in varying environmental conditions. Used FRPs have to be designed (chemical resistance and adhesive compatibility) for the environmental conditions that they are subjected to during the service life which, in case of historic structures, is very long. [25, p. 5-7]

The two-component epoxy adhesives that are commonly used for bonding FRP have glass transition temperatures under 100°C. The fire behaviour of FRP can be improved with sufficient timber covering. [26, p. 109] Fire exposure tests have been performed under mechanical loads on glulam beams without and with three different types of FRP laminates bonded either between two bottom laminations or externally. The internally reinforced beams showed an average of 44% higher fire resistance with no difference on the type of FRP laminates used. [27, p. 5, 7] One-hour fire rating can be achieved in fire test protocols for a timber member that is reinforced with FRP directly exposed to the fire on the tension side of the beam. The tests have been carried out on two different FRP reinforcements which showed no perceptible differences in fire performance. [28, p. 7]

Using FRP to increase the compression strength in timber members is not adequate in long term effectiveness due to the thermo-hygrometric variations that affect the bulking and shrinkage movements that can compromise the “confinement effect”. These reasons prevent the use of FRP wrapping based strengthening methods in timber structures. Traditional timber truss joints are not recommended to be strengthened with bonding FRP plates, because this would restrict the displacement of members under loading and change the normal behaviour of the truss. The type of FRP as a component has to be carefully chosen in the design process as there are elements which have fibres oriented in the same plane and elements with fibres disposed in different directions. These different kinds of fibre orientation have an effect on the stresses that they can withstand. [25, p. 6-7]

### 2.3.4 Adhesives

Adhesives are divided to structural, semi-structural and non-structural adhesives. Only structural adhesives can be used in load-bearing timber structures. [29, p. 221] Structural adhesives are divided into groups based on their service environment as shown in Table 3 [30, p. 176]. The most common structural adhesives that are used for wood bonding are formaldehyde adhesives [29, p. 249; 4, p.119]. Epoxy adhesives are structural adhesives that are not generally used for wood bonding, instead they are used to bond wood with other materials [29, p. 261]. Adhesives are quite seldom used in situ repair works due to the restrictive conditions that must be fulfilled to ensure a functional joint.

*Table 3. Classification of adhesive types to service environments [30, p. 176].*

Service environment of structural adhesive	Adhesive type
Fully exterior (withstands long-term water soaking and drying)	Phenol formaldehyde Resorcinol formaldehyde Phenol-resorcinol formaldehyde Emulsion polymer isocyanate Melamine formaldehyde
Limited exterior (withstands short-term water soaking)	Melamine-urea formaldehyde Isocyanate/pMDI Epoxy
Interior (withstands short-term high humidity)	Urea formaldehyde Casein

#### **Formaldehyde adhesives**

Urea formaldehyde and phenol-formaldehyde are the most common types of adhesives used in bonding timber structures. In softwoods and medium-density hardwoods connections that are made correctly, the failure occurs in the timber behind the glue line. Thus, the adhesive should be stronger than the timber connected. [4, p. 120] This assumption can be used for timber members with specific gravity up to 0.70 to 0.80 [30, p. 163]. When using metal fasteners and glue in the same connection, the strength of these have to be taken into account individually, because the metal fasteners start to carry loads after the stiff glue line fails. [4, p. 120-121] Different requirements for the use of formaldehyde adhesives are presented below.

Moisture content of the timber should be between 6 to 14% to achieve optimum bond strength [30, p. 163]. If the moisture content of the timber is higher than 20% the risk for inadequate bond increases. The timber members being bonded should have moisture content within the same range not differing more than 3%. Furthermore, the equilibrium moisture content of timber member should be within 5%. Different formaldehyde adhesive compounds have their own temperature requirements during the curing of adhesive, for example minimum of 20°C for resorcinol formaldehyde glues. Manufacturers must provide adequate information on the use of their products. [4, p. 121]

The roughness of the surface has influence on the bonding strength, that is, the smoother the surface the better bond. For example, bonding strength of sawn wood is worse than planed wood which increases wetting and penetration of adhesive into the wood due to more efficient contact. [30, p. 159] One of the main prerequisites for good bonding strength is the ability of adhesive drop to form a low contact angle with the surface (this process is called wetting). [30, p. 159] Furthermore, the surfaces should be “close fit” and the planing of the surfaces should be done maximum of 24 hours before the gluing. “Close fit” means that the maximum glue line thickness is about 1 mm. The contact pressure in gluing should be according to the manufacturer’s instructions but generally they vary between 0.7 to 1.2 N/mm<sup>2</sup>. [4, p. 121-122]

These requirements described should be taken into account when planning the use of formaldehyde adhesives in situ repair works. Furthermore, using adhesives for wood bonding in historic timber structures would be quite questionable if there are other more traditional options that are applicable.

### **Epoxy resins**

Epoxy will be presented because it has been used to repair historic timber structures since 1970s [31, p. 7]. However, it has not been used in Finland for the repair of historic timber structures, but it is used to repair glulam beams for example in the repair of glulam beams in Lakeustalo located in Oulu [32]. Epoxy can bond to variety of surfaces such as wood, plastics, concrete, ceramics and metals, which makes it widely used [29, p. 261]. Furthermore, it has good environmental resistance and it does not require high pressure during bonding and curing. Also, the bond-line thickness variation is not as critical as with formaldehyde adhesives. [29, p. 261, 33, p. 1] Epoxy adhesive families are suitable for in situ use because they can be produced to cure in different ambient conditions. [33, p. 1] There are also issues that have to be taken into account when using epoxy resins in timber repairs. These issues are characterized in this chapter.

Cleary [31] has focused “on the compatibility of historic structural timber members and epoxy repairs by the means of a reviewing and analysing the state of the art of epoxy and wood durability and structural functional performance over the past couple of decades as a means to reconsider epoxy use in the preservation of historic structural timber members” in his master’s thesis “Considering the Use of Epoxies in the Repair of Historic Structural Timber” in 2014 [31, 2]. He did not recommend the use of epoxy in the repair of load-bearing timber structures due to the knowledge gained from current research and marketed products in the US. However, he suggested that when there is no possibility of the wood to get wet, epoxy could be used, but, as said, only in dry environments. [31, p. 68] His findings among other research related to the issue are presented in this chapter.

Many studies have shown that structural epoxy adhesives have excellent initial joint strength in normal climate conditions, as they are normally used in service classes 1 and 2 (EN 1995-1:2004), which is one possible reason for the lack of concern relating to their service durability. [33, p. 2] Primarily epoxy has been used in historic timber structures as a gap-filling adhesive and prosthetic [31, p. 7]. Epoxy resins are more expensive than most wood adhesives, which has an effect on the use of epoxy in wood bonding. Furthermore, their durability is limited in some cases. [29, p. 261]. It is also possible to use epoxy as a consolidant for structural timber members [31, p. 41; 34, p. 1]

Two-component epoxy adhesive consist of epoxy that is the resin and a hardener that cross-links the epoxy. The most common hardeners are amines, but anything that reacts with the epoxy groups can be used as hardeners. [29, p. 261] DGEBA (Diglycidyl Ether of Bisphenol A) type resin is used in wood conservation. Moreover, it is the most common epoxy resin type from which 75% of other resin types are derived from [29, p. 261; 31, p. 38].

The wood surface factors affecting the bond when using epoxy are similar to those when using formaldehyde adhesives. These factors are surface roughness, wettability, surface uniformity, non-fluctuating operating conditions, free from extractives/contaminants, adhesive compatibility and surface soundness. Moreover, when using epoxy as an adhesive to bond structural timber, the curing and service conditions of the product, including temperature and moisture in surrounding environment must be carefully taken into account. [31, p. 52; 22, p. 62]. Thus, for example insufficient hardening can be provoked when curing at low temperatures, inferior to 15°C [22, p. 62]. Tests conducted by Cruz and Custódio (published at 2006) on structural epoxy adhesives that have low glass transition temperatures emphasize that surrounding environmental temperatures higher than 45°C may have critical effect on the structural safety of the joint [35, p. 9]. However, thermal activation (post-curing at 80°C for four hours) with the use of additives can increase this critical temperature (Figure 6). Variations in moisture content during service life causes stresses in the glue line [31, p.52]. Wheeler and Hutchinson revealed in their tests (published in 1997) that timber with moisture content up to 22% can be bonded with epoxy adhesive without weakening the bond strength or changing the layer of failure in the structural joint [36, p. 13]. Hankinson's formula can be used to approximate the bond strength when wood is bonded in an angle greater than parallel [31, p. 65].

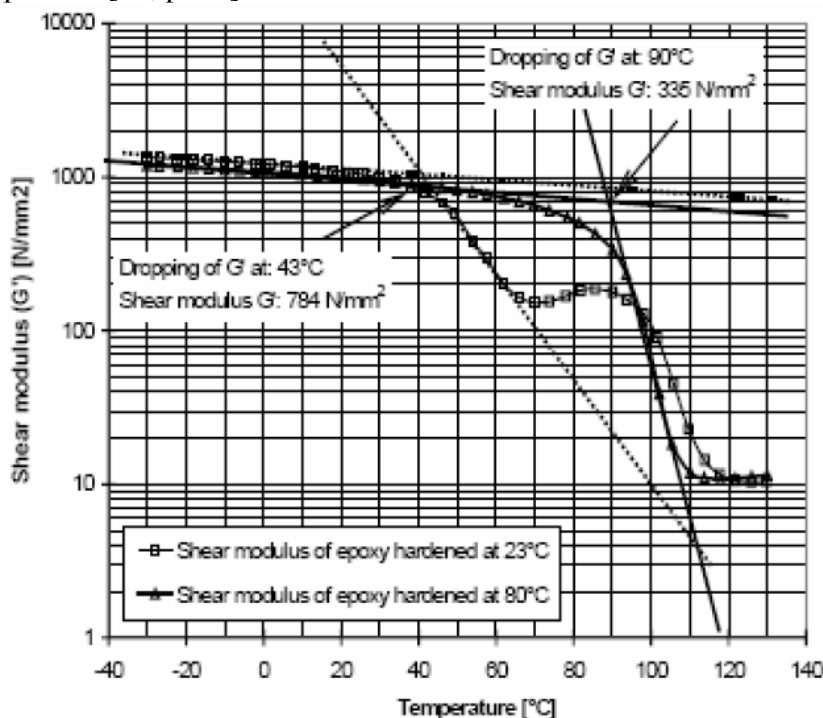


Figure 6. The effect of the hardening temperature on the shear modulus in different service temperatures [22, p. 62].

Experimental tests have been conducted on four commercial two-component structural epoxy adhesives to obtain information on the service durability and what kind of effect does the moisture and other environmental conditions during mixing, curing and postcuring have

on the viscoelastic properties of adhesive. They discovered that the type of mixing method (hand or machine) has only a small effect on the glass transition temperatures of epoxies. One main finding from their weathering tests was that the curing periods are longer for complete reaction than mentioned in the manufacturer's product data sheets. This is especially under variable conditions in situ where under-curing or a slow progression of cure can take place which can both cause shorter life span of the structure. To achieve wanted results in variable conditions (in situ) the post-cure of cured adhesive should be performed in temperature above glass transition temperature. [33, p. 1, 11, 16]

Custódio et al. also found out that all the tested structural adhesives are subjected to strength loss with the increase of temperature above 50°C. Furthermore, the used epoxy adhesive should be carefully selected to guarantee the structural integrity of the bond in withstanding environmental conditions such as high temperatures. Information on how the mechanical properties alter with temperature change should be provided by the commercial product data sheets, the manufacturer or it should be investigated with experimental methods in order to find out whether it can be used for the purpose intended. In addition, the temperature-induced creep has to be taken into account when approving adhesive to structural use as the tested commercial adhesives have shown totally different viscoelastic responses during normal service temperatures. The maximum service temperature should be significantly lower than the glass transition temperature of chosen adhesive to guarantee the performance of the bond during the whole service life. [33, p. 15]

## **2.4 Intervention methods**

There can be numerous intervention approaches for existing structures but in this thesis they are divided into six different categories that are presented in Table 4. These intervention approaches are: abstention, mitigation, reconstitution, substitution, circumvention and acceleration. [2, p. 39] Which approach to choose depends on the situation. However, in structures with historical value acceleration is unlikely to be used as an intervention approach.



*Table 4. Shows the definition and the degree of invasiveness for intervention approaches. The repair methods that are presented in this thesis are also listed according to the intervention approach.*

Intervention approach	Definition	Repair methods that are presented in this thesis	Degree of invasiveness
Abstention	Investigated structure is left as it is without any intervention.		0
Mitigation	Attenuating the environmental conditions that support the deterioration mechanism in the structure.		1
Reconstitution	Deteriorated structural part is being removed and replaced with the same material in same size in the same location.	Replacement, timber prosthesis	2
Substitution	Material in the structure is being replaced with another material to decrease the influence on the deterioration rate.	Timber prosthesis, gap-filling adhesive, consolidation, partial substitution with steel	3
Circumvention	New structural system is applied, and the functional ability of the existing material is ignored.	Circumvention	4
Acceleration	Dismantlement or demolition of the structure totally or partially.		5

ICOMOS has included 16 clauses considering guidelines for interventions subjected to wooden built heritage in “Principles for the Conservation of Wooden Built Heritage” [16, p. 2-4]. These or similar guidelines should be followed carefully when choosing a repair method for a specific structure. Clause number 11 from the “Principles for the Conservation of Wooden Built Heritage” sums up some important aspects that has to be taken into account when planning the intervention:

*“11 Interventions should preferably:*

- a be the minimum necessary to ensure the physical and structural stability and the long-term survival of the structure or site as well as its cultural significance;*
- b follow traditional practices;*
- c be reversible, if technically possible;*
- d not prejudice or impede future conservation work should this become necessary;*
- e not hinder the possibility of later access to evidence exposed and incorporated in the construction;*
- f take environmental conditions into account.”*

Choosing the appropriate material and repair method can be a hard decision which have to be evaluated with caution. However, these guidelines should not limit the structural repair proposals that can be applied as the repaired structure itself is the restrictive covenant. However, the aim is that the structural engineer or other specialists must find a repair solution that pleases all the affecting participants. Repair methods that can be applied in situations where the timber members are rotten from their ends in historical timber structures are presented in the following sections. These presented repair methods are replacement, timber

prosthesis, gap-filling adhesive, consolidation, partial substitution with steel and circumvention.

### **2.4.1 Replacement**

Original members in structures should be preserved as much as possible, replacement of an entire member should be only advisable when other less invasive methods are not applicable [16, p.3]. Situations where the entire timber member is deteriorated the replacement of the whole member is adequate. In addition, if the timber member is decayed or collapsed due to imperfections in the member, these imperfections should be corrected in the new design of the member in order to prevent premature failure [22, p. 63].

There are some general guidelines that should be followed when replacing a timber member in a structure that relate to the quality and integration of the new timber member to the old structure. Same species of wood in adequate grade should be used, and the wood should have similar natural characteristics and moisture content with the historical parts. If the original construction technology and craftsmanship in connection technology is supposed to be the most suitable, they should be used instead of using the secondary materials (e.g. nails). One should be able to identify the new member from the original structure. However, aesthetical values of the historic structure should not be affected by the new member. It is also advised that the new member should be marked so that it can be identified later. [22, p. 63-64]

The visibility of the member can have an effect on the degree of authenticity. More visible members to the audience are more detailed in order to retain the authenticity of the structure. Thus, members that are not generally seen can be less detailed, such as members substituting the structural role of the original member in a roof truss. However, they are still made in a manner that respect the original structure. [22, p. 64]

### **2.4.2 Timber prosthesis**

There are situations where entire timber members are replaced due to rotting, but it has been studied that the replacement of one end in timber member covers the majority of timber repairs. [4, p. 110]. Usually timber elements that are close to the supports of roof frames and floor beams are places where prosthesis interventions are used, as shown in Figure 7 and 10 [22, p. 66]. For example, timber beam-ends that are supported from masonry walls are critical points for deterioration due to fungal attacks [37, p. 6]. The decayed timber part that is being removed can be replaced with all-timber prosthesis (prosthesis made entirely of timber) or with the help or use of other materials.

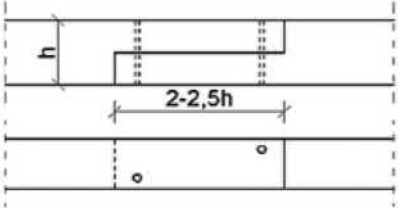
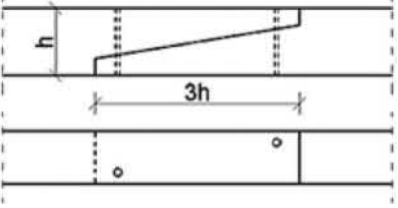
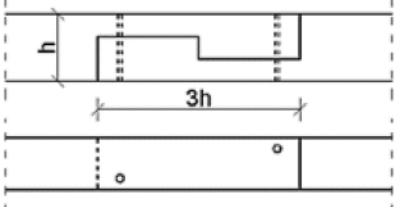
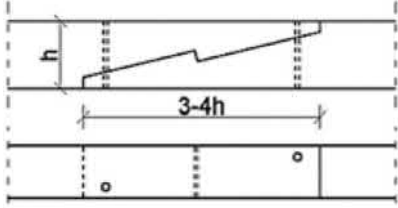
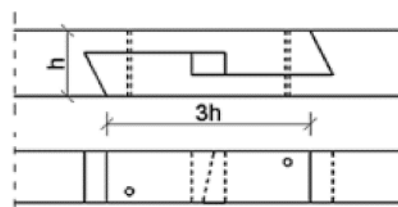
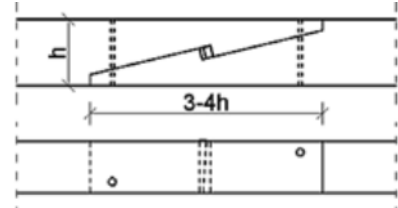


*Figure 7. Removed floor joist end replaced by timber supported from masonry wall in Prague year 2007 [22, p. 69].*

If the deterioration of a wooden member has taken more than a hundred years, replacing the deteriorated part to a new wooden part is a potential repair method, even though the mitigation of environmental conditions would not be possible [2, p. 42]. However, if the mitigation of negative environmental conditions is possible in the respect of the historic structure these measures would be welcome.

There are different kinds of connections that can be used when a deteriorated part of a timber member is removed and a new timber piece is attached to the remaining timber piece. If the timber member is visible, it is usually aligned with the original member. The connections can be made entirely from wood or by using metal fasteners or adhesives as connectors. The original unjointed timber member is stronger than a scarf jointed timber member made entirely of wood, which has to be taken into account in design. [4, p. 110-114] Although all-timber connections in prosthesis are not used in Finland for simple supported beams in bending due to the lack of design guidelines, they have been successfully used in recent restorations with modern carpentry techniques in Prague [22, p. 69]. Methods for designing and performing carpentry scarf joints have been certified by the Ministry of Culture of the Czech Republic in 2016 and they are presented in the paper “Lapped Scarf Joints for Repairs of Historical Structures” [38, p. 2-3]. These methods could also be applied in Finland if all-timber connections are desired in prosthesis where bending and simultaneously compression/tension occurs in simple supported beam. The type of connection applied between the new and old timber piece depends on the stresses that are acting in the member. [4, p. 110-114] Table 5 shows some examples of traditional connections that can be applied when joining timber members lengthwise in different situations.

Table 5. Examples on connections that can be applied in lengthwise joining of timber members. Adapted from source: [39, p. 64].

Type of joint	Schematic	Applications, notes
Half lap splice joint		For ground beams on the supporting masonry wall; pegging is essential; does not transfer tension.
Beveled lap splice joint		Applied as with the half lap splice joint to purlin plates; pegging is essential; somewhat more resistant to lateral forces than half lap splice joint.
Tabled lap splice joint		For ground beams placed on a supporting masonry wall or in other cases strengthening with internal bolts or stirrups; may transfer tensile stresses
Hooked scarf joint with nibs		Applied as with the tabled lap splice joint; more resistant to lateral forces; with additional fittings can transfer flexural loads
Wedged tabled splice joint		e.g. between posts in a timber-frame wall, pegging is needed only to counteract sideways shifts; good flexural performance for short spans.
Key locked hooked scarf joint with nibs		Application and behaviour as with the tabled splice joint; more resistant to lateral forces; with appropriate fittings, it can carry flexural loads also for longer spans

If the visual appearance of the repair is not important or if alignment is not possible for example lack of space, single or double lap joints can be used where a piece of wood is attached to the side or both sides of the wood with steel connectors. Single or double lap joints do not require as much craftsmanship skills compared to for example several scarf joints presented in the Table 5.

When higher strength and stiffness are required from the connection of two timber pieces, metal fasteners are used. Steel connectors can withstand larger shear stresses than timber dowels with respect to diameter. In addition, bolts with washers can bear tensile forces if needed. [4, p. 114] Using stainless steel can solve the problem of corrosion, which is a major reason for failures in metal fasteners in timber structures. [37, p. 8-9] As mentioned before, steel is vulnerable to high temperatures, and protective details against fire have to be designed when using steel connectors. [22, p. 68]. Figure 8 shows an example how dowel fasteners with washers can be used in connections for timber prosthesis in historic timber structures.



Figure 8. The use of metal fasteners in timber end replacements in Buštehrad Castle, Czech Republic [22, p. 68].

Traditionally screws, bolts and dowels have been loaded perpendicular to the fastener axis as shown in Figure 8 [40, p.1; 41, p. 16]. However, the design guidelines for inclined self-tapping screws that can be used in timber-to-timber connections were presented in 2002 [40, p. 1]. These inclined self-tapping screws are drilled in an angle of 30 to 60°. Five times higher stiffness and two times higher strength can be achieved using inclined screws compared to the traditional screw connections. [41, p. 16] Using inclined self-tapping screws in repairs of timber members can guarantee a service life of 100 years. If the structure remains dry and the maximum utilization rate of the design is 70%, longer service life close to 200 years can be predicted. [32] Self-tapping screws leave holes only to one side of timber member, which can be an advantage when using these screws in historic timber structures with visual requirements.

As different materials have different physical behaviour in varying environmental conditions, using all-timber connections has the advantage of avoiding these incompatibilities that can cause degradation of materials. Experimental tests have been made to halved timber joints in bending in Czech Republic which show that their connection stiffness can be as high as in bolted joints although having a lower ultimate strength. [22, p. 70]

### **Glued-in steel and FRP rods**

Timber prosthesis can be connected also with steel or FRP rods/plates bonded together with adhesive. The advantages considering the use of Carbon FRP instead of steel is the light weight. However, steel is cheaper and there are number of downsides that makes the use of FRP very questionable in historic and heritage timber structures. [22, p. 60] Glued-in steel screws are also an option to transfer loads between timber members [42, p. 3]. Glued-in steel screws are connected to the wood through its threads and through glue line mainly in the



smooth area of the screw. The use of steel and FRP rods/plates or steel screws is only achievable in service class 2 and 3 with adhesives that are classified to type I according to EN 301. In service class 1, type II adhesives can be also applied. [43, p. 7] Suitable adhesives for this process are epoxy, polyurethane or resorcinol formaldehydes that fulfil the requirements for structural bonding between wood and steel/FRP [42, p. 6]. However, epoxy adhesives have lower prerequisites for environmental conditions, which makes them more preferable to be used. As mentioned before, the maximum service temperature should be significantly lower than the glass transition temperature of chosen adhesive to guarantee the performance of the bond during the whole service life [33, p. 15]. Glued in rods/screws can be installed parallel, perpendicular and on an angle to grain [42, p. 3]. Glued-in rods/screws are used in new engineered timber products in Finland. For example, glued in rods are used to reinforce new glulam beams and glued in screws to distribute loads from glulam members. [32, 42, p. 3-4] There is no experience of repairing massive or sawn timber members with glued in rods/screws in Finland [32, 46].

Experimental tests have been conducted on FRP profile (plates and rods) connections in sawn timber cut with varying angle and the adjacent timber members having glued or unglued surfaces (Figure 9). Plates in 45° joints with no bonding between the timber elements showed the highest strength results in the tests. [22, p. 71]

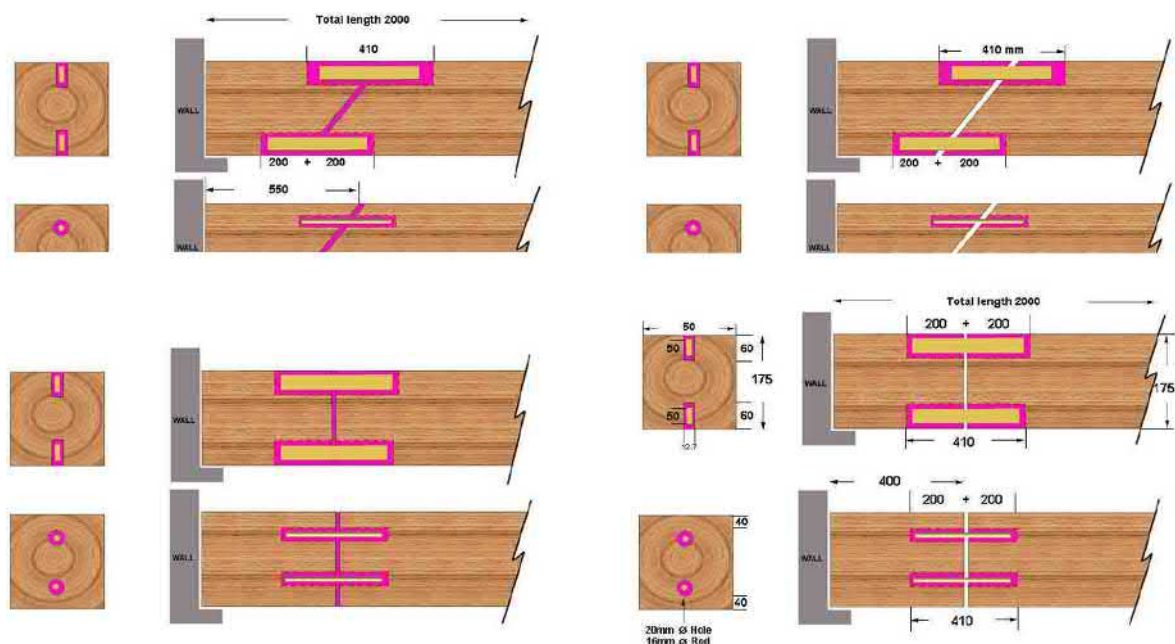


Figure 9. The schematic pictures from the connections that were loaded in the experimental tests conducted by Cruz et al. [44, p. 6]

### 2.4.3 Gap-filling adhesive

Epoxy is used as a gap-filling adhesive in timber repairs. Generally, when using epoxy as a gap-filling adhesive, embedded steel or FRP rods/plates are needed to provide sufficient load transfer between the timber and the gap-filling epoxy [37, p. 10; 31, p. 56]. Reinforcements enable the adhesive bond at the wood interface to be mediocre and still sufficient. High viscosity of epoxy is important to guarantee sufficient mechanical strength and maintain shape during curing. Figure 10 shows a typical beam end epoxy repair system with reinforcing bars installed to holes drilled into the end grain of sound wood. [31, p. 56-57]

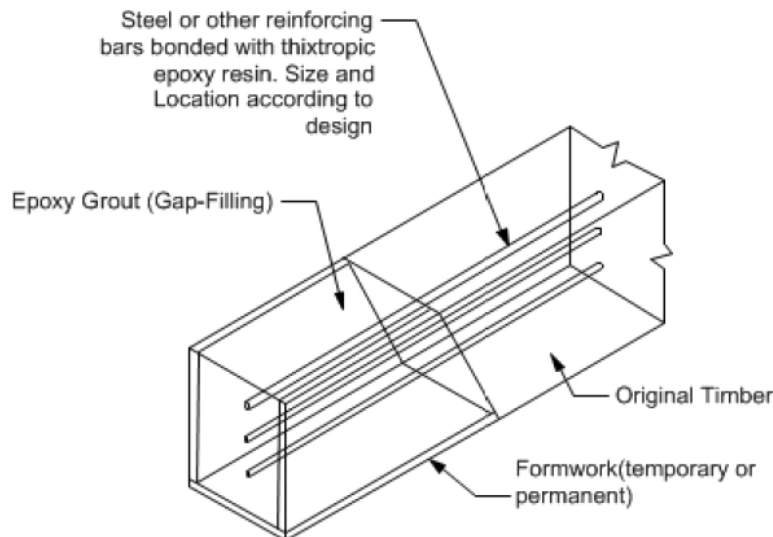


Figure 10. Typical beam end repair with epoxy as gap-filling and embedded reinforcement for transferring the structural load from sound wood to the epoxy [31, p. 56].

Stumes investigated the efficiency of wood epoxy reinforcement systems in 1975 [45, p. 34]. He found that specific epoxies with tensile reinforcements can resist higher stresses than most species of wood. In addition, epoxy with embedded reinforcements can transfer the loads from wood that has lost its structural capacity. Allowable stresses method can be applied in design procedure of load transfer from wood to epoxy and reinforcements. The unfortunate finding was that epoxy quickly loses its strength under elevated temperatures not much higher than normal room temperature. It is possible to protect epoxy with wood cover as a thermal insulator against heat. [45, p. 34] However, fire exposure tests have been made to beams with short epoxy replacement in the end of the beam connected with steel bars to the timber beam. The tests showed that one-hour fire resistance can be achieved. The steel bars had a minimum cover of 60 mm to the surface. [26, p. 109]

Broughton and Hutchinson [31] have studied the effect of wood moisture content on the bonded-in reinforcement rods. They found that timber members, specifically white oak, with moisture content above 30% (saturated wood), showed 60 to 65% reduced pull-out strength compared to dry wood specimen. The increased moisture content also relocates the failure point in the structure. As in dry specimen the failure occurs in the adhesive close to the interface of rod/adhesive and in saturated specimen the wood/adhesive interface becomes dominant for the failure to occur. [31, p. 57-58]

The temperature-induced creep mentioned before should especially be taken into account when using epoxy adhesive as gap-filling. This is because in gap-filling the epoxy performs also as a structural prosthetic, which can cause safety issues due to deformations. [31, p. 66-67]

Although these kinds of repair methods are not used for historic timber structures in Finland [32; 44] they are used for example in Portugal. Thus, the research on these epoxy repair methods are mainly done in Portugal. Even though the research shows that there are issues that can cause problems in the structure, gap-filling methods are used. Figure 11 shows an epoxy gap-filling repair plan for a connection of a rafter and tie beam in a Portuguese library that dates back to early 17<sup>th</sup> century [47, p. 1975].





Some of these Cleary's hypotheses from his master's thesis above are not based on experimental research but on reviewing and analysing, which should be taken into account when making conclusions. Experimental research that would take these presented long-term issues into account would be valuable for the possible use of epoxy consolidation in the repair of timber structures. With information available nowadays, using epoxy consolidation in historic timber structures would be quite imprudent.

#### 2.4.5 Partial substitution with steel

Splice plates are plates that are installed to each side of a timber member. The connection can be designed with screws, nails, bolts or bolts with connectors. Different shape of sections can be used, such as angles or U-shaped, if additional strength is required. Different section shapes are viable when using splice plates to support beam ends in situations where the end of beam is rotten and cut away. This is applicable where the mitigation of environmental conditions favourable to fungal growth is not possible. [4, p. 117] Different examples of splice profiles that can be used to strengthen the existing beam, work as a connector for timber pieces or work as a substitute for timber in the support are shown in the Figure 12 [22, p. 79].

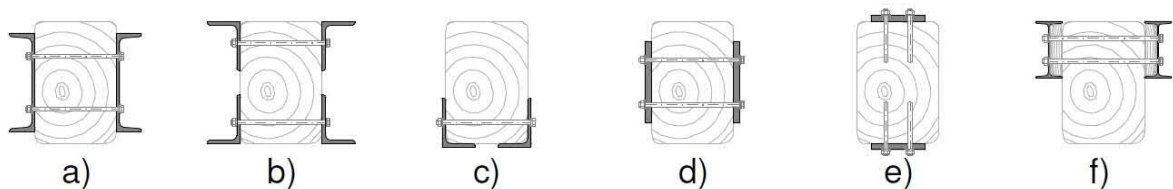


Figure 12. Different shapes of steel splice profiles [22, p. 79].

Timber beams deteriorated from their ends can be repaired using a steel flitch plate that is inserted along the beam length. T-shaped plates can be used on the top or on the bottom (Figure 13) side of the beam depending on the situation. In a simple supported beam, the steel profile in the support has to transfer only shear forces. [37, p. 9]



Figure 13. Deteriorated timber beam ends repaired with flitch plates [37, p. 10].

Experimental tests have been conducted on timber beams with splice steel profiles in their ends to find out whether it would be an adequate repair method for floor beams with decayed ends. In these tests, steel profiles were attached on the upper section and partly inserted to the timber beam (Figure 14). The steel profiles were connected with screws. 30 timber beams, from which 10 were from a 120-year-old building, with attached steel profiles were tested in bending to obtain stiffness and load carrying capacities. The research concluded that steel parts with limited length approximately from 10 to 20% of the entire length of the

timber member can be used to solve problems affected by the timber decaying support conditions. [48, p. 37]



Figure 14. Failure occurred in steel profile during the bending test [48, p. 44].

#### 2.4.6 Circumvention

As mentioned before, the circumvention approach does not directly affect the deteriorated member. Instead new load-bearing parts/structures are added, which provide extra support. These new parts/structures can even change the load paths of the structure in order to decrease the structural load affecting the deteriorated member. Circumvention approach is possible when conservation bodies or local authorities do not authorize retrofitting interventions due to for example decorative paintings or carvings in the structures with historical value that have to be left untouched. However, it is important when circumvention approach is used that the deterioration mechanism is not active anymore. The active deterioration might destroy the decorative paintings that are to be conserved and cause safety issues due to possible failure of deteriorated timber member from its own weight.

There are many different applications that can be used in the circumvention approach depending on the situation. Figure 15 shows one example where additional steel trusses are installed to provide extra support for the roof trusses. However, using circumvention approach needs to be evaluated carefully in historic timber structures, because it changes the authenticity of the structure.



*Figure 15. Additional steel roof trusses are installed to increase the load-bearing capacity of the timber roof structures [49, p. 5].*

### 3 Louhisaari manor

Herman Fleming, a nobleman constructed Louhisaari manor (Figure 16) on his family estate located in western Finland, Askainen (Masku) in the 1650s [1, p. 13]. He chose to build his manor in Askainen because he already had a palace in Stockholm next to the royal castle. The palace was constructed by his father Klas Fleming (1592-1644) from 1641 to 1642 [1, p. 13; 50]. Louhisaari is a unique entity in the history of Finnish architecture and arts. Although the architect who designed the entity of Louhisaari is not known, the layout of Louhisaari manor is similar to a manor that is located in Södermanland in Sweden, which was designed by an architect Jean de La Vallée who worked for various noblemen in the mid-17<sup>th</sup> century. This uniformity in the layouts shows the cohesion in architecture of Louhisaari manor and Swedish manors from the same era. Many of the experienced craftsmen who built and decorated Louhisaari manor came from Sweden and had previously worked in recognized projects. [1, p. 13-14, 18]



Figure 16. Louhisaari manor. The longer side shown in the figure is facing the sea (southwest).

Louhisaari manor has high hipped shingle roof with curving slopes near the eaves. All the sides of the roof have gables with hatches and dormers in two rows. The load-bearing roof structures are known to be original. The Church of Askainen built in 1653 and the Old Church of Uusikaupunki built in 1629 are the only buildings in Finland known to have similar load-bearing roof structures as Louhisaari manor. However, these kinds of roof trusses are more common in Sweden, of which Skokloster castle (built between 1654 and 1676) shows a good example. It has one of the biggest wooden roof structures in historic buildings. The preserving of Louhisaari manors original roof structures makes it very valuable in the North European scale. [1, p. 101-102]

#### 3.1 Structural system

Previous research on Louhisaari manor's roof structures has been made in 2017 by university students and their advising lecturers. Their outcomes are presented in the book "Ruotsin

Suurvalta-ajan Vesikattorakenteet Suomessa” (“Roof Structures in Finland During the Swedish Empire”) [1]. A way to mark the structural timber members in the roof was created by the architects working with Louhisaari manor in the beginning of 2019. These markings are used in this thesis in order to unify and ease current and forthcoming work related to roof structures in Louhisaari manor. The markings of rafters and leaning trestles are presented in the Figure 17. The observations in situ were performed between February and April 2019 to verify the previous research results made in 2017 and to obtain new information on the structures.

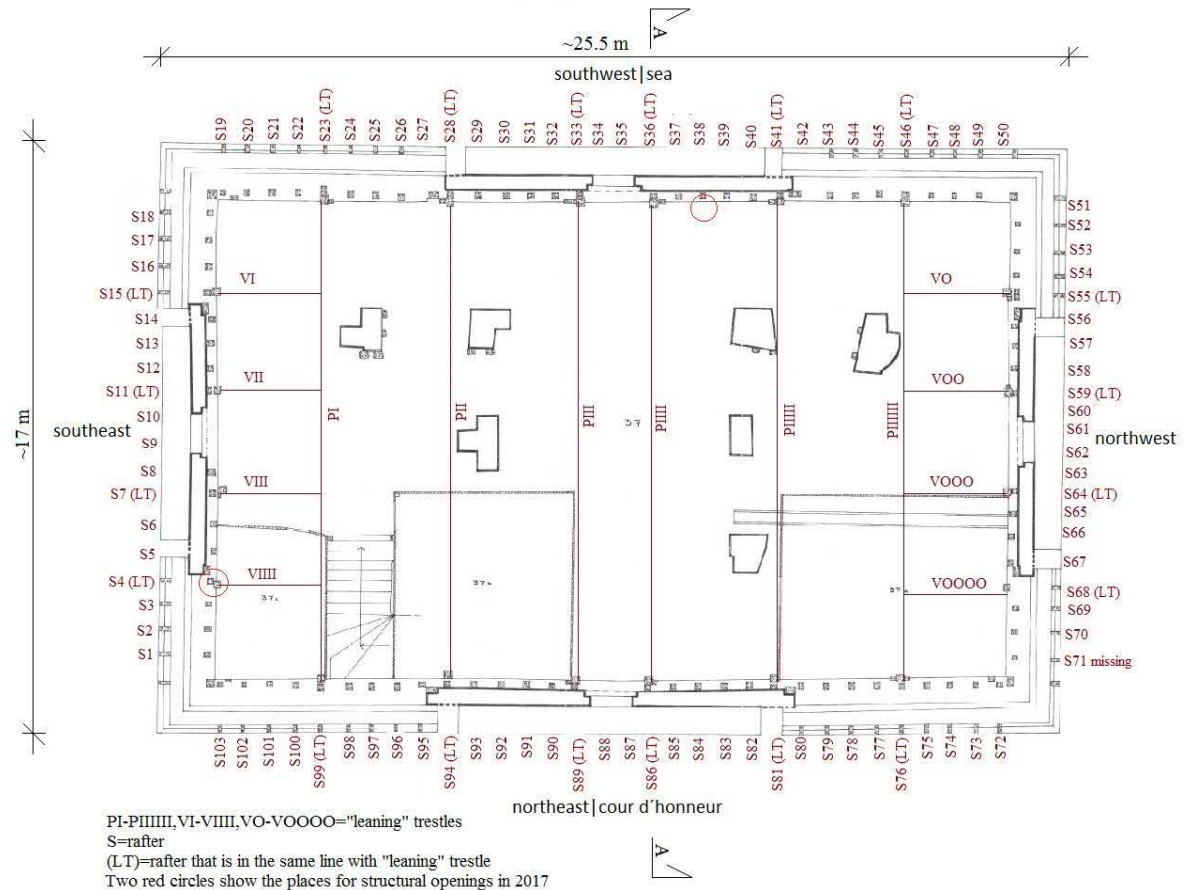


Figure 17. The markings that are used for the leaning trestles and rafters in the floor plan drawing of the attic.

The previous inspections indicate that the load-bearing roof structure would be as shown in Figure 18 in the longer side of the roof. [1, p. 127] The assumption is that tie beam connects to the rafter and to the post of the leaning trestle inside the load-bearing masonry wall.



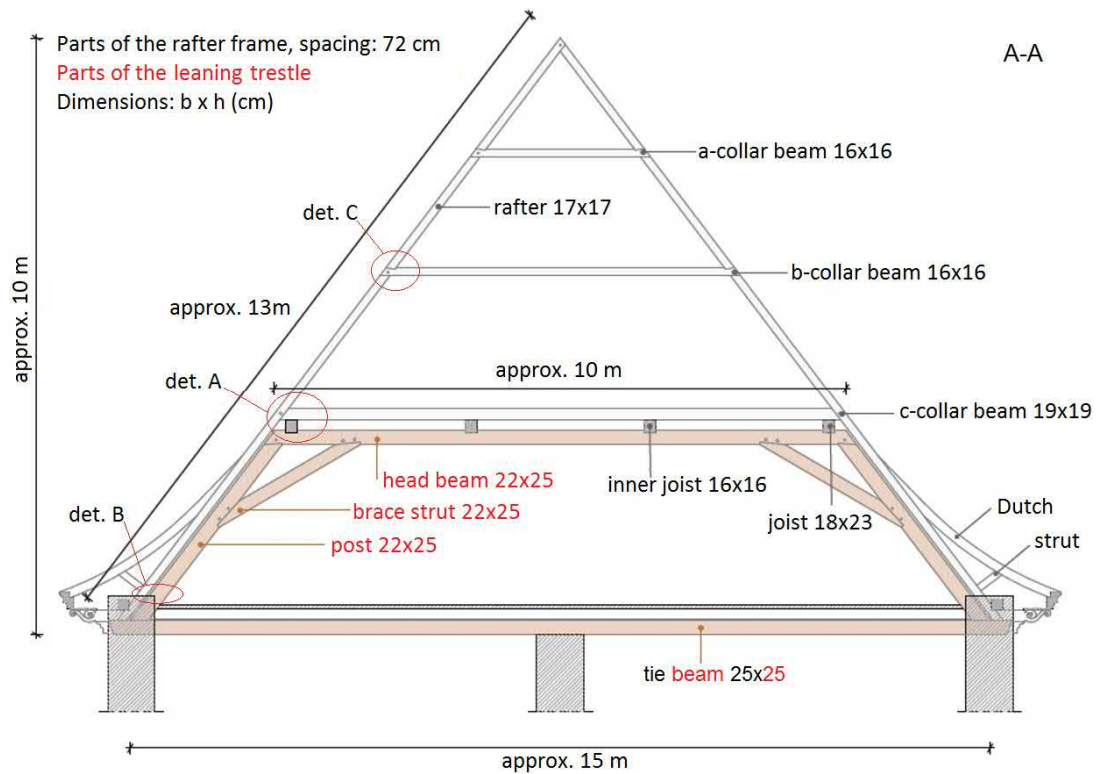


Figure 18. The load-bearing roof structures with relevant mean dimensions of members in the longer side of the building. Figure is adapted from the original figure. [1, p. 103]

The timber corbels that support the eave structures are also supported from inside the masonry wall, as shown in Figure 19. [1, p. 127] Echo is given to these previous observations and assumptions made in 2017 during the observations on site in 2019. However, Figure 20 shows that the batten under the corbel is made of timber, and during the observations in 2019 it was found that it is made of masonry.

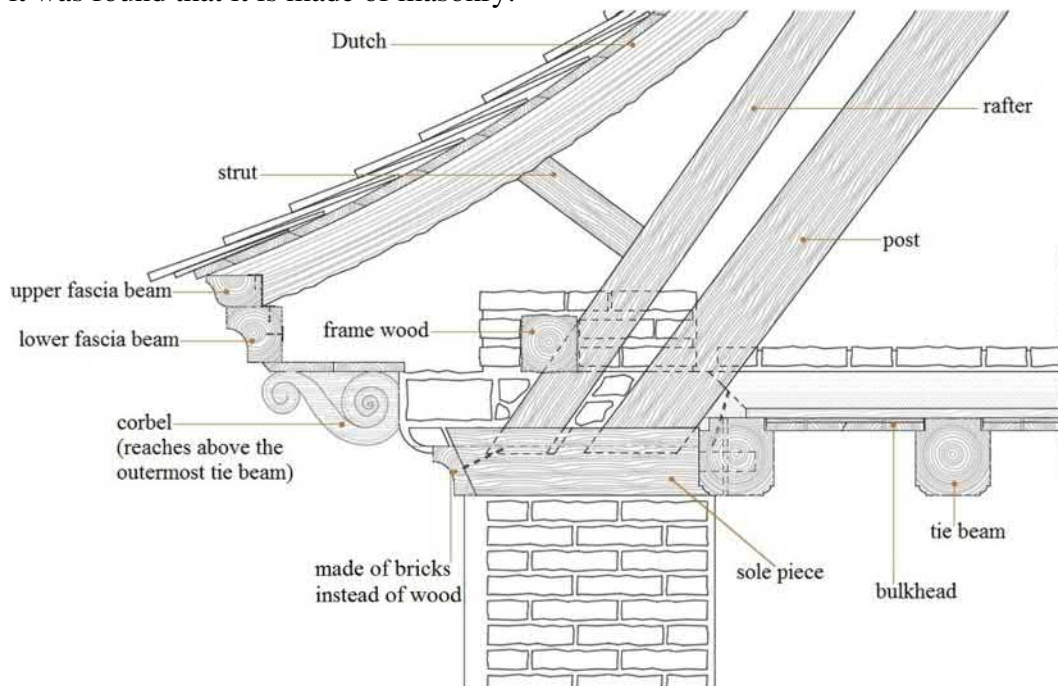


Figure 19. Elevation from the eave structure in the shorter side of the roof. Adapted from the original figure. [1, p. 104] The previous inspection assumed that the batten is made of timber, but it was found that the whole façade is made of bricks.

### 3.1.1 The leaning trestles



Figure 20. Leaning trestle spanning across between the long external walls.

Six leaning trestles support the roof structures along the shorter span of the roof (Figure 20). Leaning trestles are placed about 3.6 meters from centre to centre and 2 meters near the centroid of the roof structure. The leaning trestle consist of head beam, brace strut, post and tie beam, which are all made of pine. On the shorter side, the leaning trestles are placed about 3 meters from the centre to the centre, and they are supported by the head beam of the outermost leaning trestle that spans across between the long external walls, as shown in Figure 21. The leaning trestles are stiffened with cross bracings with cross section of 15 x 15 cm. The stiffening cross bracing is missing at the location of gable on each side of the roof.



Figure 21. The outermost leaning trestle which spans across between the long external walls is supporting the leaning trestles on the shorter side. Cross bracings can be seen between leaning trestles. The cross bracings are missing where the gables are located. One of the collar beams have been cut due to previous lead through.

Mortise and tenon joints with timber dowels are used in the connections between members in leaning trestles and cross bracings connected to the posts. The head beam and the cross bracings are connected to the post with one dowel and the brace strut contains two dowels in its joints. Doweled mortise and tenon joints are used in the connection of head beams in the shorter side to the outermost head beam in the longer side. It was assumed in the previous investigations that the connection between the sole piece and the post would be similar on the shorter side [1, p. 124]. The outermost joists that lie above the head beams are notched to the head beams (Figure 22), which beside the cross bracings also stiffen the leaning trestles in longitudinal direction in the longer side of the roof.

If the leaning trestle would not include brace struts, it would collapse due to the low rotational stiffness of the connections between the timber members. The all-timber connections are tight, but they are not tight enough to withstand the racking forces produced by the wind loads. This makes the connections between timber members hinges. [61, p. 104-105]

### 3.1.2 The rafter frames

The rafter frame consists of three collar beams (compressive struts), two rafters and a tie beam (tension chord). Some of the collar beams have been cut or notched due to chimneys or other structures that are or have been in the way of collar beams, as can be seen from Figure 22. Rafter frames on the longer side of the roof have approximately 2.5 cm gap between the posts of the leaning trestles but two rafters are leaning on the leaning trestle from the highest point of the posts, which can have an effect on the load paths of the structure in these regions. The rafters on the shorter side have much bigger gaps between the posts of the leaning trestles. The rafters are notched to the frame wood that lies longitudinally inside the masonry wall above the corbels. However, the function of the frame wood is not known. It is possible that the frame wood has given support or longitudinal stiffening to the rafters during construction phase.

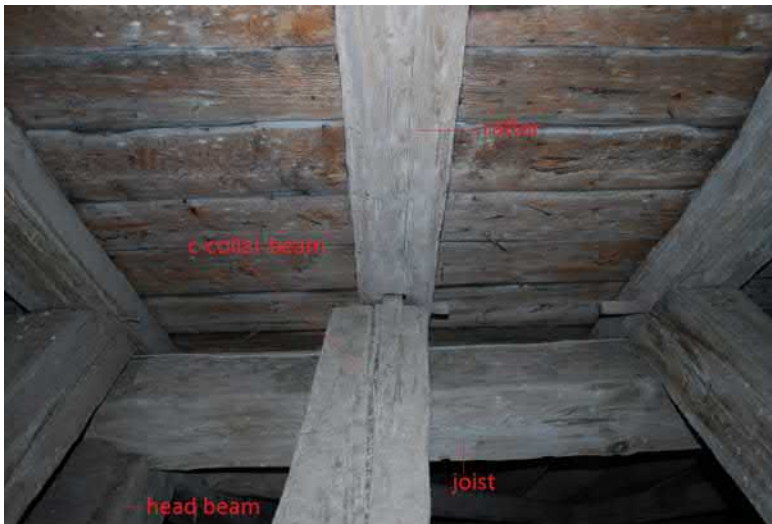


Figure 22. Notched joist lying above the head beam. C-collar beam and the rafter is connected with doweled mortise and tenon joint. See detail A in figure 18.

The lowest collar beam lies above the joists and is connected to the rafters with doweled mortise and tenon joint (Figure 22). The higher collar beams are connected to the rafters with timber doweled half lapped dovetail joints. The connection between rafters in the ridge of the roof is timber doweled half lapped joint. The Dutch that are connected to the rafters



with nails and are supported by brace strut, eave structure and also in some areas additional support at the edge of masonry wall, are made of naturally curved timber, which causes the curving of the roof before the eaves.

The connection between the rafter and the tie beam is unknown, as it is hidden inside the masonry wall, but assumptions have been made that it would be similar as the joint between the lowest collar beam and the rafter. This kind of assumption is based on the connection between the tie beam and the rafter (Figure 23) in Skokloster castle. [1, p. 114]



Figure 23. The rafter connecting to the tie beam in the Skokloster castle [60, p.39].

### 3.1.3 Eave structures

The eave structures have not been investigated closely from outside. It has been evaluated that the corbels that support the eave structure have a cross section of 10" x 10" and are approximately 160 cm in length, reaching above and connected with nail to the outermost tie beam in the shorter side of the roof. [1, p. 127] The facade between and under the corbels is made of plastered bricks.

### 3.1.4 Third floor ceiling

The ceiling between the third floor and non-heated attic is supported by the tie beams that are notched from the upper corners of the cross section. Bulkhead boards are laying in the notches. Tarred timber boarding is installed perpendicular above the tie beams. The structural layers in the ceiling can be seen from Figure 24.

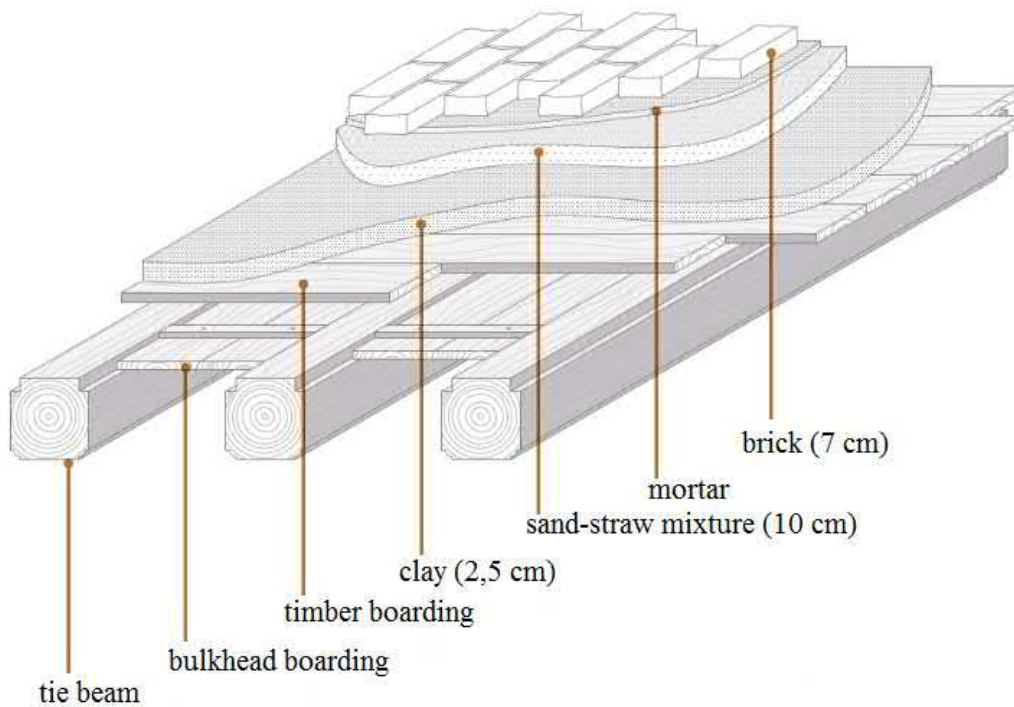


Figure 24. The structural layer of fire bottom between the attic and the third floor [1, p. 135].

The tie beams and the bulkhead boards have decorative paintings, some of which are heavily restored and others more in their original appearance. Decorative paintings that are known to be original are located in the banqueting hall in the northern corner of Louhisaari manor. These original paintings shown in Figure 25 have been painted around the year 1660 and have high art historic value. [1, p. 16-17]



Figure 25. The ceiling of banqueting hall with original decorative paintings painted on the tie beams and bulkhead boards.

Due to the long span of approximately 10 meters of tie beams in the banqueting hall, three additional steel beams (Figure 26) with hangers attached to the tie beams have been installed in the 1960s above the floor of the attic for additional support [1, p. 109].



Figure 26. Two from the three steel beam pairs that were installed for additional support of tie beams in 1960.

## 3.2 Structural analysis

The aim of the structural analysis was to obtain the normal forces that are acting in the timber parts that are embedded inside the masonry wall where the timber members are known to be mainly rotten. These normal forces are essential for the adequate design phase of the chosen repair method.

The structural performance of the undamaged timber members located inside the masonry wall is calculated in ULS with the existing design guidelines. This is performed in order to find out whether these structural parts would be adequate with the existing design guidelines. Approximations on the load-bearing adequacy of the rotten timber members inside the masonry wall can be made according to the results received from the structural performance analysis.

The roof truss system is analyzed on the longer side of the roof where the tie beams are acting. The shorter side of the roof is not included in these calculations. The structural analysis was performed with finite element models in Robot Structural Analysis 2016 software. The reliability of the finite element model created on the software was proven with calculations by hand. The structural calculations can be found from the Appendix A.

### 3.2.1 Structural system

The initial information for the structural system was obtained from field studies on site and from dimensional drawings. Some of the measures from the dimensional drawings were verified on site and the measures were coherent.

The load-bearing division for one leaning trestle is 3.6 meters in parts of the roof where the structural members are analyzed. And one division of two leaning trestles contains five rafter frames with the division of 72 cm. According to the analysis, one leaning trestle carries the loads that are applied to and from these five rafter frames through c-collar beam. It was estimated that the loads that are applied to and from the rafter frame below the c-collar beam are transferred to the masonry wall through rafters and have no effect on the leaning trestle.

### 3.2.2 Loads

Typically, the design age applied for new buildings is 50 years and for monumental buildings or structures 100 years. However, this historic building with original load-bearing structures has stood for more than 350 years. The service life for load definition used in the design was chosen to be 250 years as it is ideal that this building would maintain its structure as long as

possible. This chosen service life has an effect on the magnitude of the wind load [51, p. 137].

The loads for the structures are based on EN standards and Finnish national annexes. Loads that are acting in the roof structures are wind, snow and self weight. The roof of the manor is quite steep and according to the measurement drawing its angle is approximately 53°. High roof angle has an effect on the governing load combination because the snow load decreases as the angle of the roof increases. If the angle of the roof is higher than 60°, the snow load can be excluded from the calculations [52, p. 102]. The curving of the eaves increases the snow load factor. In the calculations the curved part of the roof was calculated with mean value of 33.4°. The wind loads were calculated with the surface pressure method, which is suitable for designing structural members in the roof [51, p. 143]. The loads that affect the structures are presented in the Table 6.

*Table 6. The basic values of loads affecting in the roof structures. Wind load, snow load and the load from the roofing materials are presented with the division of one rafter frame (72 cm).*

		Basic load value (kN/m)
Wind load	Upwind face	0.5
	Downwind face	-0.21
Snow load	Linear part (53°)	0.31
	Curved part (33°)	1.19
Self weight	Roofing materials	0.41
	Rafter	0.14
	C-collar beam	0.18
	A/B-collar beam	0.13
	Outermost joist	0.21
	Inner joist	0.13
	Tie beam	0.31
	Head beam/post/brace strut	0.28

The normal forces acting in the timber members located inside the masonry wall were calculated with four different ultimate limit state load combinations, which are shown in the Table 7. The highest normal forces acting in the timber members inside the masonry wall are obtained with the chosen load combinations. These load combinations in the Table 7 are the most governing ones when evaluating the structural performance of individual timber members inside the masonry wall. This is because as the duration of the affecting load decreases, for example from self weight to snow or from the snow to wind, the load-bearing capacity of the structural member increases. This is because timber can sustain higher loads for short periods of time. [52, p. 49]

*Table 7. Load combinations that were used to calculate the normal forces in the timber members embedded in masonry. The factors that were used in different load combinations for basic load values are also shown.*

Load combination (ULS)	1. $1.15 \cdot \text{Self weight} + 1.5 \cdot \text{Wind (governing)} + 1.05 \cdot \text{Snow}$
	2. $1.15 \cdot \text{Self weight} + 1.5 \cdot \text{Snow (governing)} + 0.9 \cdot \text{Wind}$
	3. $1.15 \cdot \text{Self weight} + 1.5 \cdot \text{Snow}$
	4. $1.35 \cdot \text{Self weight}$



### 3.2.3 Supports

The roof structures are supported from inside the rigid exterior masonry walls that are approximately 80 cm in width. The other support in the calculations is modelled as a hinge (upwind side) and the other as a roller (downwind side). Rafters and posts are connected to the tie beams in the support inside the masonry wall.

### 3.2.4 Internal forces

To obtain the forces that are acting in the connection of the post of the leaning trestle and the tie beam, two separate free body diagrams were analyzed. The first step was to obtain the loads that are distributed from the rafter frame to the leaning trestle through c-collar beam. These forces were calculated from the free body diagram shown in the Figure 27. The support reactions that were received from the free body diagram shown in the Figure 27 were multiplied with 5, which is the amount of rafter frames that the leaning trestle has to bear through c-collar beams. The vertical support reactions were then applied as external forces to the leaning trestle. It was calculated that the horizontal support reaction was also entirely distributed to the leaning trestle through friction between the head beam and the joists in every load combination. The frictional coefficient that was used prior to sliding between head beam and joists was 0.63 [59, p. 25]. The structural system was simplified and only the outermost joists transfer loads from rafter frame to the leaning trestle. Finite element analysis showed that the inner joists transfer only minimal amount of the loads to the leaning trestle.

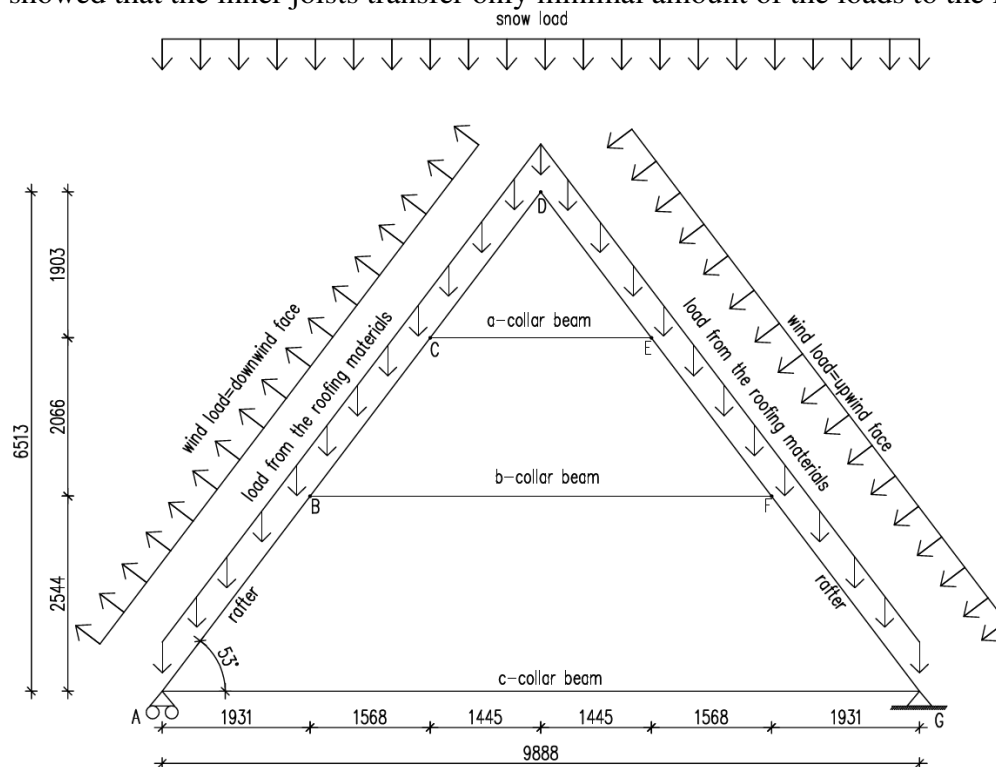


Figure 27. Free body diagram that was used to obtain the loads that one leaning trestle has to bear.

The internal forces acting in the connection of the post of the leaning trestle and the tie beam were obtained from the leaning trestle free body diagram shown in the Figure 28 which was solved in Robot Structural Analysis 2016 software. The highest external load combination  $F_1$ ,  $F_2$  and  $F_3$  that the leaning trestle has to bear result from load combination 1. (Table 7). The magnitudes of the loads are  $F_1=54.6$  kN,  $F_2=44.9$  kN and  $F_3=34.6$  kN. Figure 29 shows

the normal force diagram received from leaning trestle FBD (free body diagram) with load combination 1.

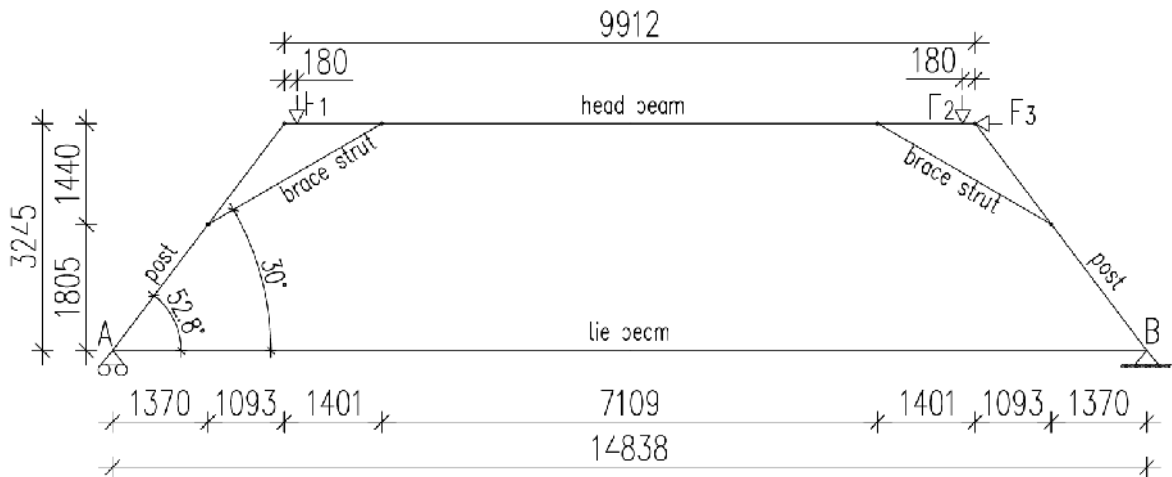


Figure 28. Normal forces acting in the connection of the post and tie beam were calculated from this free body diagram.

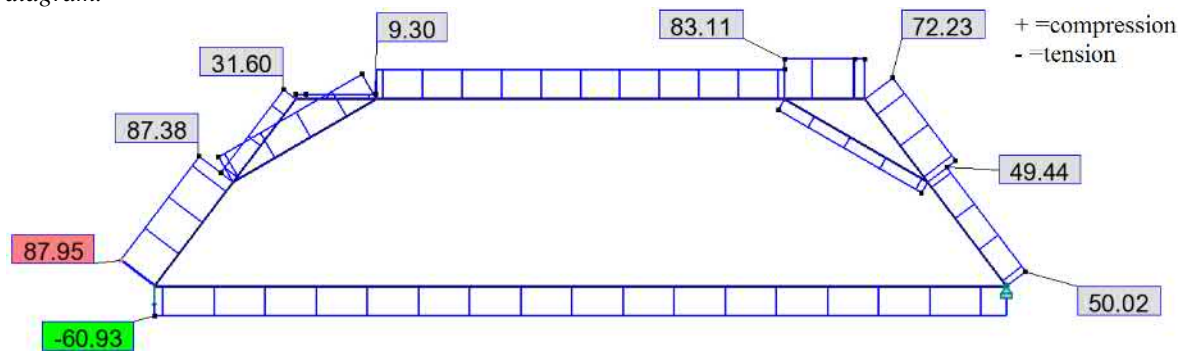


Figure 29. Normal forces [kN] acting in leaning trestle according to finite element model made with Robot Structural Analysis 2016 software. Load combination 1 (Table 7) was applied to obtain these normal forces.

The normal forces that are acting in the connection of the rafter and the tie beam were calculated in a situation where the leaning trestle (which would normally carry the forces of rafter frame through c-collar beam) would have lost its load-bearing capacity and the load paths would be rearranged. This was implemented to obtain the highest possible normal forces in the connection of tie beam and rafter. It was calculated that the joists would not have enough capacity to distribute the loads to adjacent leaning trestles and the rafter frame would have to bear all the loads that are applied to it. The free body diagram that was calculated to obtain the loads acting in the connection of rafter and the tie beam is shown in Figure 30. The curved part in the eaves of the roof was simplified to a mean value. The uplift below the corbels due to wind was not included in the calculations because it is carried by the corbels and the forces acting in the corbels were not included in the calculations. In addition, the forces acting in the corbels has no effect on the internal forces acting in the connection of rafter and tie beam. Figure 31 shows the normal force diagram that was received from the rafter frame FBD with load combination 1 (table 7).

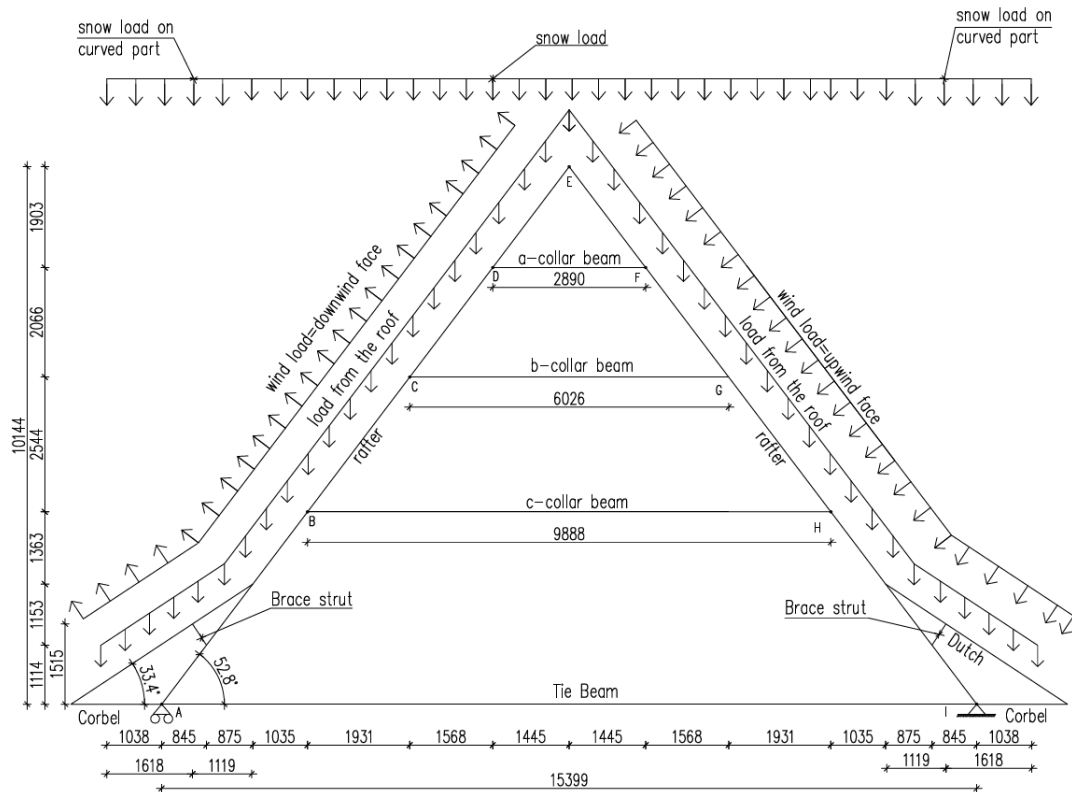


Figure 30. Rafter frame FBD. The normal forces acting in the connection of the tie beam and the rafter were calculated from this FBD in a situation where the leaning trestle would not carry any loads through c-collar beam.

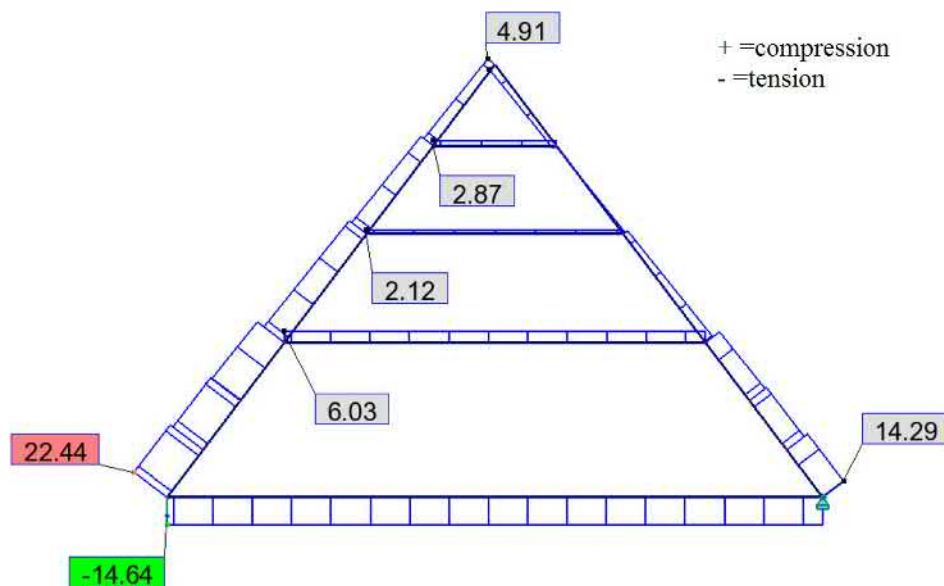


Figure 31. Local extreme normal forces [kN] acting in the rafters, tie beam and collar beams according to rafter frame finite element model analyzed with Robot Structural Analysis 2016 software. Load combination 1 (Table 7) was applied to obtain these normal forces.

The normal forces received from the analysis are shown in the Table 8. The forces that were received from the leaning trestle FBD are intended to be used when designing the repair of the rotten structures. It would also be recommended to use the values obtained from the rafter frame FBD in the repair design process even though lower forces could be also implemented if the load-bearing capacity of the leaning trestle can be guaranteed.

Table 8. The normal forces that are acting in the connections inside the masonry wall with different load combinations. Only higher compression forces are presented.

Load combination (ULS)	FBD = leaning trestle		FBD = rafter frame	
	Tie beam (tension) (kN)	Post (compression) (kN)	Rafter (compression) (kN)	Tie beam (tension) (kN)
SW+W(g)+S	60.9	88	22.4	14.6
SW+S(g)+W	55.1	82.1	22.2	13.4
SW+S	42.2	66.7	18.6	9.9
SW	38.6	60.1	13.6	7.7

Explanations:

SW self weight

W wind

S snow

(g) governing variable load

### 3.2.5 Structural performance

The structural performance of the cross sections in the members embedded to the masonry wall was evaluated with the obtained normal forces in ULS with the existing design guidelines used in Finland.

Table 9 shows the utilization rates that were obtained in timber members (tie beam, post and rafter) with the strength class of C24 that are embedded in the masonry wall. The utilization rates were calculated as if the timber members would have been new, meaning that the load history or other characteristics that have changed due to the long age of the timber members in the structure were not included. The governing design condition is compression at an angle to grain in the connection. The details of the connections between timber members inside the masonry wall are not known, which is why the structural capacity of the connection in detail is not evaluated. Buckling and lateral buckling was not included in the structural performance analysis as these are more related to the analyzing of entire members and the buckling/lateral buckling would not occur in the timber parts that are embedded into the masonry wall.

Table 9. Utilization rates with different load combinations in different cross sections and design criteria. Utilization rates were calculated with the higher tie beam tension values shown in Table 8. The lower values in the rightmost column in Table 8 were not included as their utilization rate values would be insignificant.

Load combination (ULS)	$k_{mod}$	Post		Rafter	
		Tie beam (tension parallel to grain)	(compression parallel to grain)	(compression at an angle to grain in the connection between tie beam)	(compression at an angle to grain in the connection between tie beam)
SW+W(g)+S	1.1	8%	9%	66%	32%
SW+S(g)+W	1.1	7%	8%	61%	32%
SW+S	0.8	8%	9%	68%	36%
SW	0.6	9%	11%	82%	35%



Table 9 shows that the self weight is governing when calculating the structural performance of the post and tie beam with the normal forces received from the FBD of the leaning trestle. When calculating the structural performance of the rafter frame, the governing load combination is self weight and snow, which is due to the higher snow load in the curved part of the roof. Value of  $k_{mod}$  has a significant effect on the governing load combination when calculating the structural performance. The results show that the cross sections of timber members embedded in the masonry wall are adequate with the structural design guidelines that exist. If the leaning trestle would have lost its load-bearing capacity the rafter frames would be able to bear the loads in the parts of the timber members that are embedded into the masonry wall (rafters and tie beams). However, the function of the leaning trestle is to stiffen the structure and restrict excessive deformations and bending moments occurring in the rafter frames, which was also identified from the finite element analysis. If the leaning trestles would not exist in the structure, the rafter frames would collapse.

Utilization rates can be used to approximate the structural performance of the embedded timber members. As the rotting of timber members embedded to masonry wall continues, they slowly lose their load-bearing capacity. When the rot has decayed more from the cross section of individual timber member than the utilization rate enables, the load-bearing capacity of the member exceeds and the member cannot bear the loads that are applied to it. Depending on the member that has lost its load-bearing capacity, the load paths are rearranged through other members which still have sufficient load-bearing capacity. If the load-bearing capacity of the post is exceeded the load paths are rearranged so that the rafter frames have to bear all these forces. However, if one of these rafters has also lost its load-bearing capacity, the loads are transferred to the adjacent rafters through timber boarding, which stiffens the roof structure. This rearranging of load paths continues as the rotting of members increase. This accumulation of loads and rotting of members will lead to deformations in structures and possible collapsing of members. Eventually the entire roof structure will lose its stability.

According to the investigations the major part of the timber members embedded into the masonry wall are rotten. This includes the connections between the timber members inside the masonry wall. It can be assumed that some of these connections have lost their functioning due to rot, and the masonry wall has to bear horizontal forces that the rafters and posts are not able to transfer to tie beams. In the long term, the amount of connections that are not able to transfer the horizontal loads to tie beams increase due to rotting. This accumulation of horizontal forces that the masonry wall has to bear can cause cracks in the joints of bricks and inflict the masonry wall to lean slightly into the direction of horizontal forces. These kinds of defects were not detected during the investigations on site.

## 4 Investigations

The difficulty for the assessment with many existing non- or semi-destructing testing methods is the fact that the timber members that should be investigated are partly not tangible as they are inside the load-bearing walls. This narrows down the possibilities for assessment methods as it is possible that the hypothetical fungal decay in timber members inside the masonry wall has not spread to reach the parts that are tangible. The investigations that were performed on site are visual inspections, infrared thermography and resistance drillings. The rot report based on these investigations can be found in the Appendix B.

Infrared thermography imaging was chosen as one assessment method to localise possible leaking points in/near the tie beams in immediate contact with the outer masonry wall on third floor. It was also estimated that it could be possible to locate possible damp areas in the tie beams that could indicate biotic decay in the timber members. If significant leakage is detected in tie beams penetrating the masonry wall due to excessive moisture in timber members, it increases conductivity and the IRT can show decreased temperatures in these areas. If timber contains excessive moisture, conditions favourable to fungal growth can occur.

Resistance drilling was chosen for the timber assessment method because it is actually the only existing assessment method being found that can give sufficiently reliable results from the conditions of timber members embedded in masonry wall without structural openings.

### 4.1 Visual inspections

Two structural openings (places marked with a circle in the Figure 37) have been made in the attic during previous inspections to points which had already been damaged due to water leakage and seemed to have been opened earlier also [1, p. 119]. Structural openings show rotten wood inside the masonry wall as can be seen from Figure 32.



Figure 32. Structural openings that have been made in the attic. The left one is in the southeast and the right in the southwest side of the roof.

Visual inspection was performed on the third floor and in the attic; mainly on the structural parts that are penetrating the masonry wall. However, the corbels that are supporting the eave structures were only partly investigated due to lack of space. The structural timber members on the upper parts of the roof structure were also observed, but in a less detailed manner. The visual inspection of the higher parts of the roof was partly limited because of danger of falling.

Assisting instruments such as a blunt hammer and a knife were used during the visual inspection in the attic when needed. Knife was used to verify the stage of decay and hammer to discover hidden rot with tapping method.

The connections between structural timber members are mainly made of timber, but nails and other exceptions with metal have also been used. Flat iron bars have been used in some connections as can be seen in Figure 33.



*Figure 33. Rafter S86 on the left and S94 on the right are for unspecified reason connected to the posts of the leaning trestles with flat metal bar. See detail B in Figure 18.*

Almost all the connections between timber members in the roof structures are in relatively good condition. Only one connection was found that had lost its structural capacity due to failure. This failure had occurred in a timber dowel in the connection between the b-collar beam and rafter shown in Figure 34.



*Figure 34. Connection that has lost its structural capacity. Original markings can be seen on the side of the rafter. Also, one collar beam is entirely missing from its place which can be due to obstacles in between the rafter pairs. See detail C in Figure 18.*



Visual inspection showed that the timber structures in the attic had damages due to brown-rot fungi. However, the fungal growth has not been active during the inspections. Thus, the environmental conditions were not favourable to fungal growth during the inspection (winter frosts). Fruiting bodies were not found during the inspections. The rot had reached its final stages in many parts and the wood was crumbling to dust where it occurred. Rotten parts exist mainly on the southeast and southwest (sea) side of the roof close to the dormers but also on the other sides. The timber members were rotten in parts that were penetrating to the masonry wall (rafters and posts of leaning trestles) as shown in Figure 35, but also cross bracings attaching to the masonry were found rotten. In addition, one rotten rafter that is penetrating to the masonry wall has already been repaired in previous interventions in the 1960s which can be seen in Figure 36. Only one rotten timber member was found on higher parts of the roof which was in a rafter near the connection of b-collar beam. The visual inspection of the roof structures in the higher parts was partly limited.



*Figure 35. Rotten rafter S29 penetrating to the masonry wall.*



*Figure 36. Previous repair intervention on the end of the rafter S43.*

Visual rot was found only in one tie beam that is the outermost tie beam in the storage room under the attic. The tie beams, which are painted and located on the heated rooms on the third floor, showed no signs of rot when investigated visually. The tie beams corresponding to the leaning trestles were tapped with knuckles. Tie beam end in the southwest side that is connecting to the leaning trestle PIIIIII sounded clearly hollow. Stains of previous water leakages were perceived in some parts of the tie beam ends and on the wall paintings on the southwest side near the tie beam that sounded hollow. This indicates that the water that has leaked through the roof has reached the third floor in some parts. Figure 37 shows the mapping of rotten timber members near the floor level of the attic based on visual inspections.

PI-PIIIII, VI-VIII, VO-VOOOO = Leaning trestle

S = Rafter

(LT) = Rafter which is in the same line with the leaning trestle

Circle = Structural opening

■ = rot

■ = out of reach

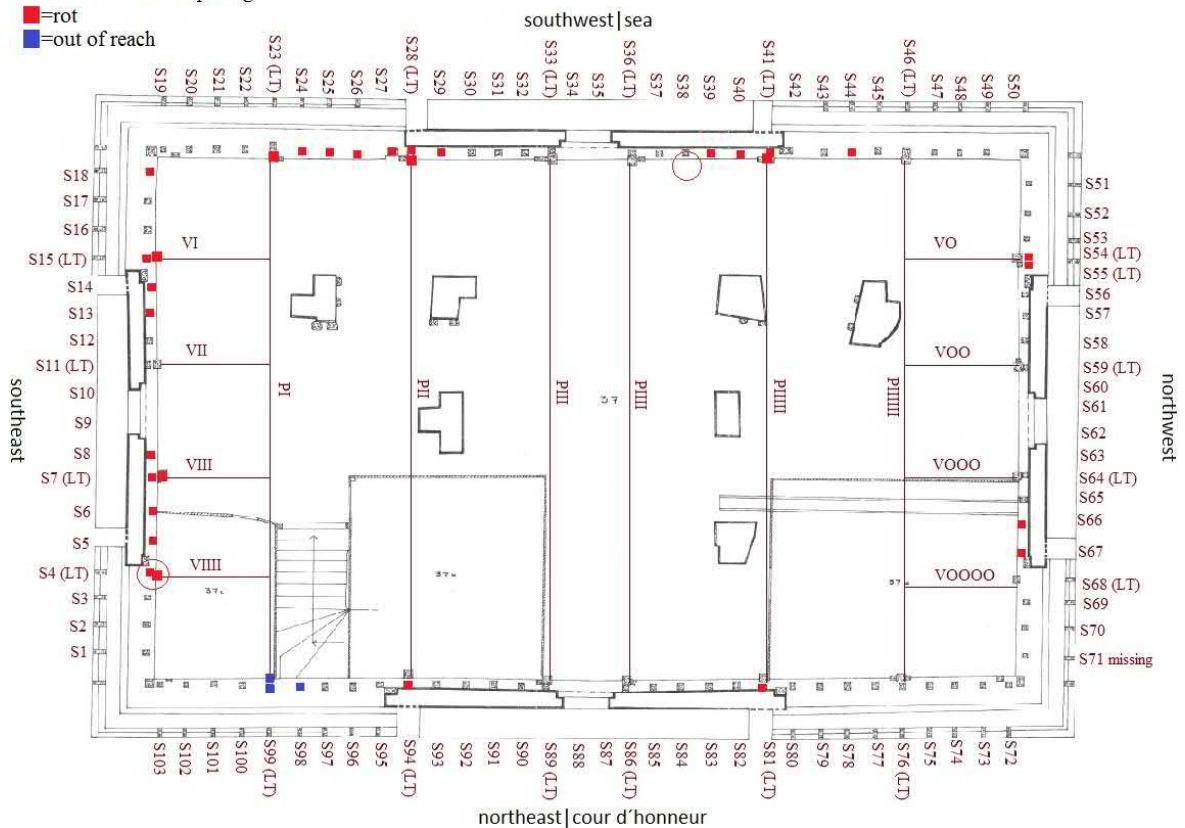


Figure 37. The mapping of rotten timber members in the attic near the floor level based on the visual inspection is shown in the figure with red markings.

The strength class of existing timber members was roughly evaluated with SFS 5878 INSTA 142 [58], which is used for visual grading of new structural timber members. The strength grade value C24 that was evaluated for the existing timber members does not take into account the load history of timber members or other characteristics of timber that might have altered due to the long age of timber members in the structure. Strength grade C24 was used in the structural calculations. The evaluation of strength class was based on visual evaluation through pictures taken from the roof structures. The evaluation of the strength class included the relative amount of knots in the cross section and the rate of growth. The slope of grain was not evaluated because the interpretation from pictures was not sufficient enough. However, large slopes in grains connected to gurdy grain were not identified. The possible defects that are located inside the timber members could not be included in the evaluation as the

evaluation was done through pictures. These defects are the depth of fissures and possible ring shakes. The table 10 shows that the load-bearing timber members could fulfill the requirements for C30 based on the division of annual growth rings, but the relative amount of knots in the cross section could only fulfill the requirements for C24.

*Table 10. Shows the results based on the investigations and the allowable amount of knots and the division of annual growth rings for C24 and C30 strength requirements according to SFS 5878 insta 142.*

Characteristic	Requirements for strength classes		Results from investigation	Structure fullfills
	C30	C24		
Knots	Maximum of 1/5 from the side of member	Maximum of 2/5 from the side of member	Approximately maximum of 2/7 from the side of member	C24
Division of annual growth rings	Maximum of 4 mm	Maximum of 6 mm	Approximately 0.5 to 1.5 mm	C30

## 4.2 Resistance drillings

Resistance drillings were performed by arborist Teppo Suoranta on the 30<sup>th</sup> of March in 2019 with Resistograph (IML RESI PD400). The maximum drilling depth with the used Resistograph was 40 cm and the diameter of the drilling needle was 3mm and the shaft was 1.5 mm. The resistographs propagation speed can be from 50 cm/min up to 200 cm/min and the maximum rotation speed can be 5000 rpm. [54] Resistograph (IML RESI PD400) measures the drilling resistance and the feed force. The drilling resistance curve (black line) in the Resistograph profile includes shaft friction which is caused by the wood shavings that clamp the shaft. The deeper the drill bit penetrates, the more friction is in the shaft. However, mainly drilling hardwood has an influence on the shaft friction, and drilling softwood has only a minimal influence. The feed force curve (green area) in the Resistograph profile measures the force that is needed to push the drill bit into the wood which is only minimally affected by the shaft friction. This makes feed force more liable in identification of early state wood degradation. [50, 56, p. 2]

The drillings were performed approximately in an angle of 45° in relation to perpendicular to the timber member with approximately +/-10° error margin. Figure 40 shows the basic principle of how the resistance drilling was performed on the tie beams. The penetration depth depends on number of issues that have to be taken into account. For example, the drill bit is automatically pulled back if it meets timber with significantly high or low resistance. This kind of high resistance can be for instance a knot, and low resistance for instance extremely rotten wood. In addition, the Resistographs timber contacting surface has a detector that has to be pressed inward during the drilling or the drill bit will be automatically pulled back. Sometimes this detector was released due to the challenging position in which the drilling was performed. When one of these errors occurred during the drilling the structural member was redrilled to achieve more proper results. [54]

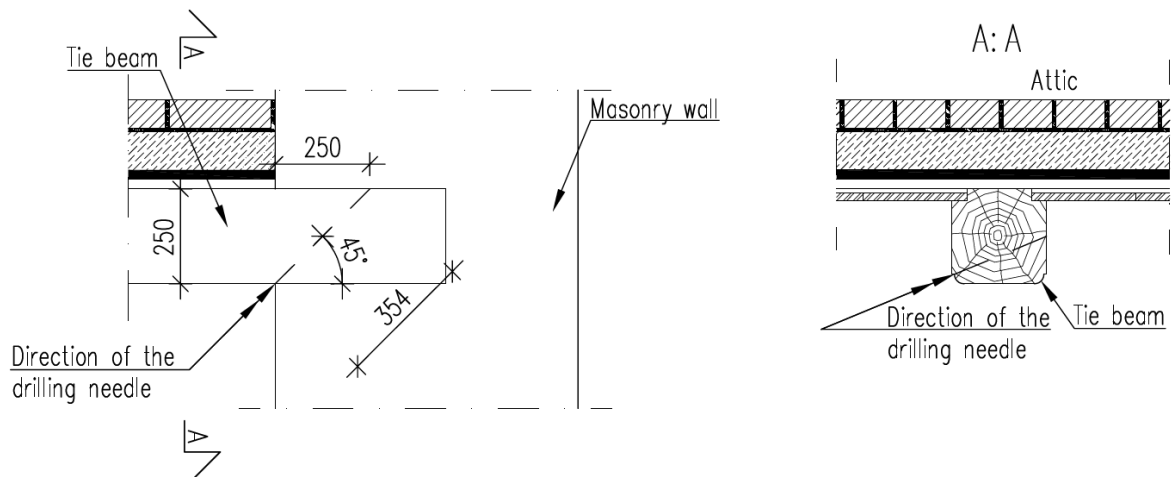


Figure 38. Schematic drawing how the resistance drilling was performed to the tie beams in the third floor. The post and the rafter connect to the tie beam inside the masonry wall even though it is not presented in this figure.

The small diameter of the Resistographs drilling shaft (1.5 mm) makes it flexible, and the flexibility can make the drilling needle to follow possible cracks inside the timber, which can falsely show decreased density of the timber. High propagation speed of the drill and blunt drill bit can cause this effect to take place. A propagation speed of 100 cm/min was used and the drill bit was changed if it was damaged to prevent this unwanted event from occurring. This potential error was also evaluated during the resistance drillings and if doubt arose the drilling was performed again to verify the results received from the drilling. [54] However, it was found after the results were received from the drillings that a couple of the results were not as explicit as was intended.

The used rotation speed was 2500 rpm, which is suitable for this kind of work. If the rotation speed is too high, the drill bit can bounce when it dashes into solid wood after going through a crack. This can affect the direction of the drill bit after entering into a crack. [54]

The tie beam ends that are located in the banqueting hall were not included in the resistance drillings, but all the other tie beam ends on the ceiling of third floor were. A total of 53 tie beam ends were investigated and 11 were left untouched. This gave an extensive result on the condition of the tie beams inside the masonry wall. The ends of tie beams in the banqueting hall were excluded from the investigations because they are covered with paintings that are known to be original which makes them unique. Figure 41 shows how the resistance drillings were performed on the tie beam ends.





*Figure 39. Resistance drillings taking place with Resistograph on the tie beam end in the third floor of Louhisääri manor.*

Posts of leaning trestles were drilled from the attic except four posts (PI-PIII) from the north-east and one post (PI) from the southwest side. The Figure 42 shows how the drillings were performed on posts of leaning trestles.



*Figure 40. Resistance drilling performed to the post of the leaning trestle (PIIII) on the southwest side of the roof. The figure also shows that birch bark has been used to protect the embedded parts of the post from moisture.*

Examples on the Resistograph profiles received from resistance drillings are shown in Figure 43, 44 and 45. Figure 43 shows that timber with higher density can occur between the rotten parts. The Resistograph profile in Figure 43 shows that the tie beam end is rotten, but the visual inspection showed no sign of decay in the tie beam or in the rafter or post to which the tie beam connects inside the masonry wall. However, the resistance drilling profile of the post that is connecting this rotten tie beam A36-86L, showed a small amount of rot/decreased density. This result points out that the visual inspection does not show the true stage



of decay in the structures. The highest peaks in the Resistograph profile (Figure 44) represent the latewood and the lowest peaks earlywood. However, the rate of growth could not be evaluated from the Resistograph profiles as the resistance drillings were not implemented perpendicular to tangential plain of timber members. Some of the resistance drilling profiles are not explicit and the condition of timber member can be argued. Figure 45 shows an example of an unclear resistance drilling profile where the two drops in drilling resistance curve and force feed curve indicate either rot or shrinkage cracks in the timber member. This Resistograph profile (Figure 45) was evaluated to be without defects as it is highly possible that the drops in this profile are cracks. The fact that there are no other defects in this particular profile (Figure 45) than these two drops makes it more likely that the drops in the profile are cracks.

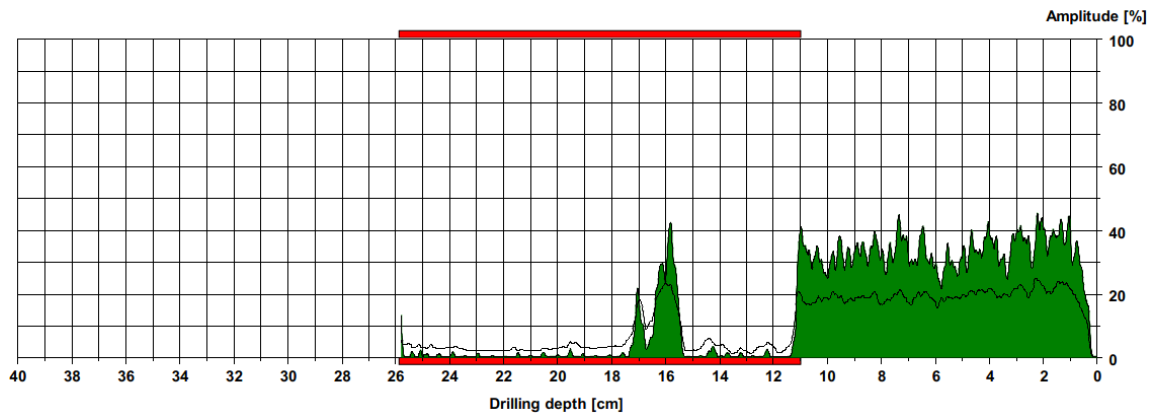


Figure 41. Resistograph profile from tie beam end A36-86L shows clearly that the timber is rotten which can be seen in the drop of resistance drill curve (black) and force feed curve (green area) when the drilling depth reaches 11 cm.

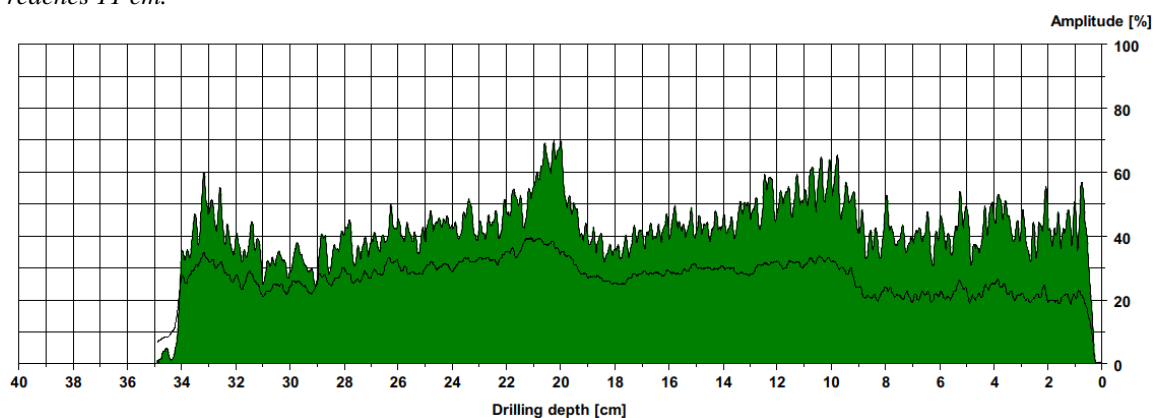


Figure 42. Resistograph profile from the tie beam end A44-78 L shows good quality timber.

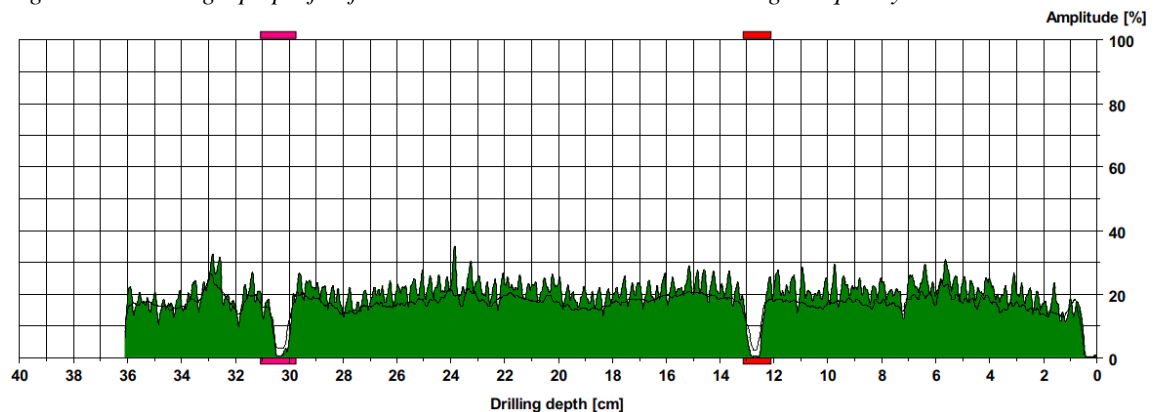


Figure 43. Resistograph profile from the tie beam end A33-89 K shows that the condition of timber can be argued in some drillings.

Resistance drilling outcomes verified that the rot problem lies extensively in timber members that are embedded into the masonry wall. Based on the evaluation of the resistance drilling diagrams, clear signs of rot/extremely soft wood was found from 61% of the tie beam ends that were resistance drilled. According to the results of resistance drillings, there is no significant difference in the rate of rot between the side that is facing the sea and the northeast side. This finding is not coherent with the visual inspections which showed that the side facing the sea is more heavily damaged due to rot than the northeast side. When comparing visual inspection and resistance drillings, it can be generalized with one exception (rafter S44) that the tie beams are rotten inside the masonry wall where the corresponding rafters were found rotten during the visual inspection. However, the resistance drillings show more wider rot problems in tie beam parts inside the masonry walls than the visual inspection in the attic indicated. Figure 46 shows the condition of the tie beam ends on the third floor according to the resistance drillings.

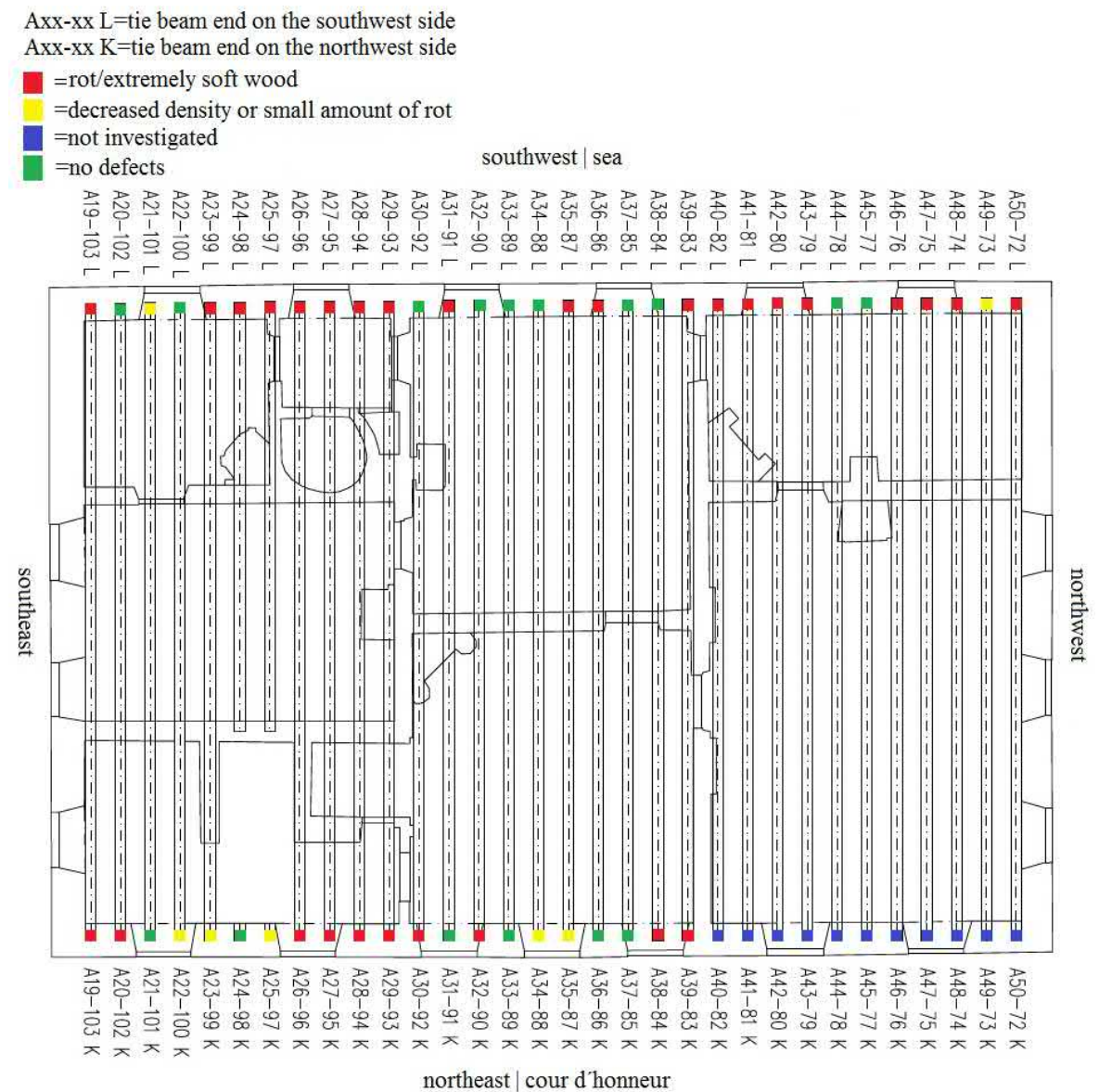


Figure 44. Condition of tie beams ends in the third floor are marked according the resistance drillings.

Clear signs of rot/extremely soft wood were found on two-thirds of the posts that were resistance drilled. Figure 47 shows the condition of posts in the floor plan of the attic according to the resistance drillings.

PI-PIIIIII, VI-VIII, VO-VOOOO = Leaning trestle

S = Rafter

■ =rot/extremely soft wood

■ =decreased density or small amount of rot

■ =not investigated

■ =no defects

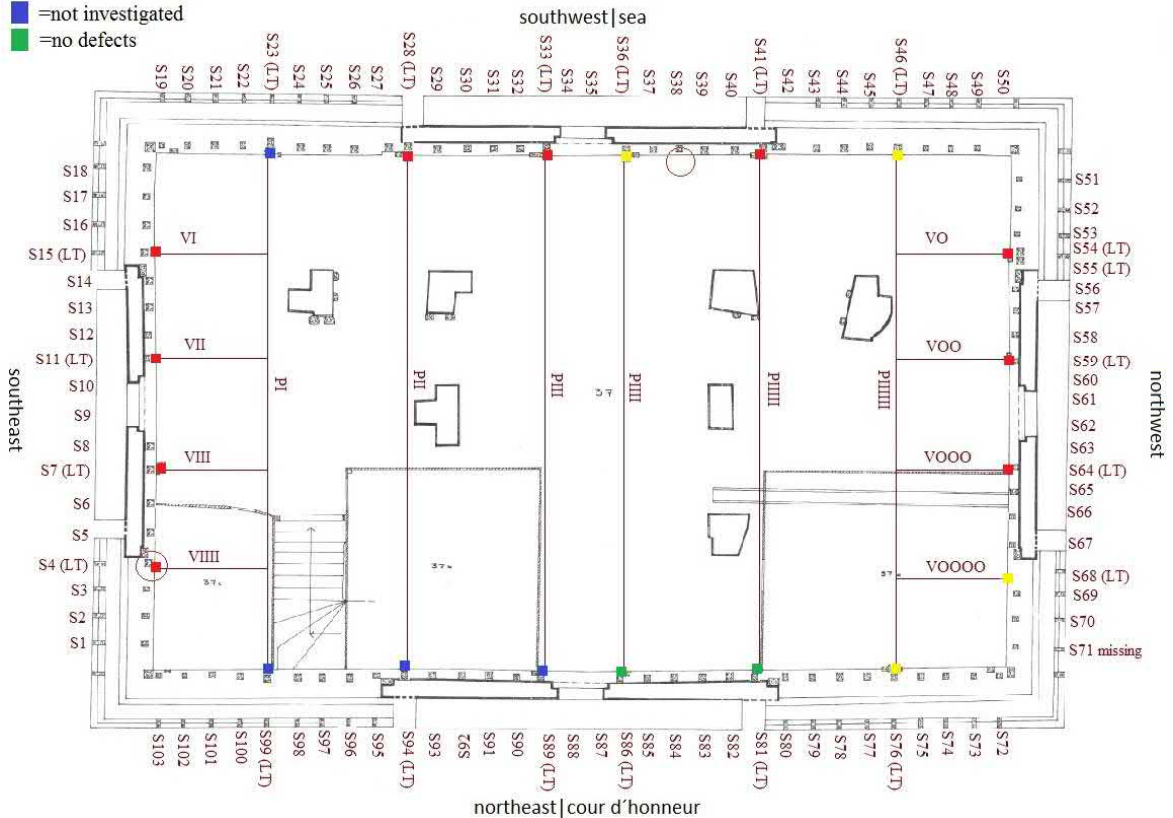


Figure 45. Shows the condition of the posts according to the resistance drillings.

### 4.3 Infrared thermography imaging

All the ends of tie beams on the third floor were scanned with infrared thermography device Flir E4. During the infrared thermography imaging, the inside temperature of the third floor was +10°C and the outside temperature was -5°C. This gives temperature difference of 15°C which is adequate for reliable results for infrared thermography scanning [53, p. 49].

The IRT scanning did not indicate any abnormal leaking of cold in the structure. The only spot that showed abnormal leaking of cold (Figure 38) was in a spot that had structural opening in the attic. In addition, the tie beam which clearly sounded hollow (Figure 39) when tapped which indicates to rot, showed no indication of abnormal leaking which indicates that there was no excessive moisture in the structure. However, this is only speculation and the results are approximate. Moisture measurements could identify if timber contains excessive moisture.

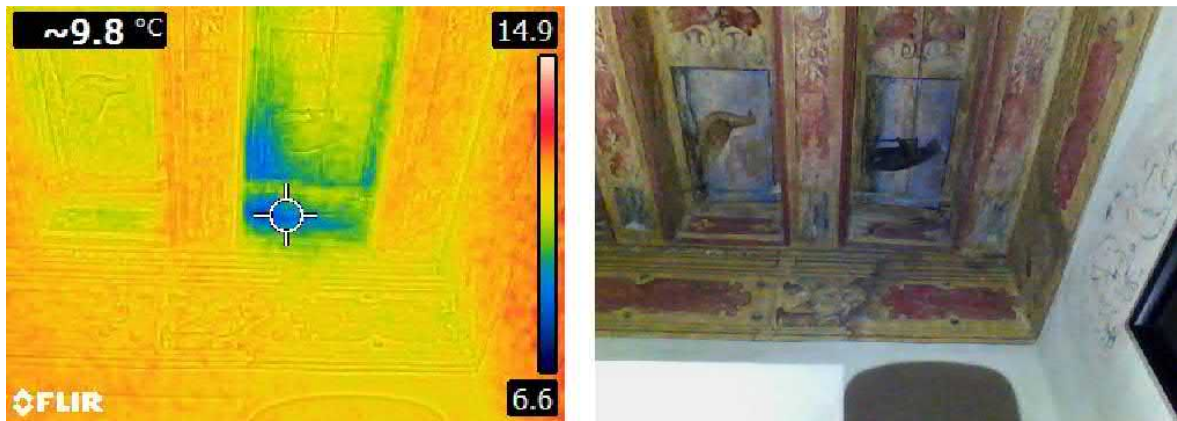


Figure 46. The leaking of cold can be seen in the IRT -image of a spot in the attic where a structural opening has been made.

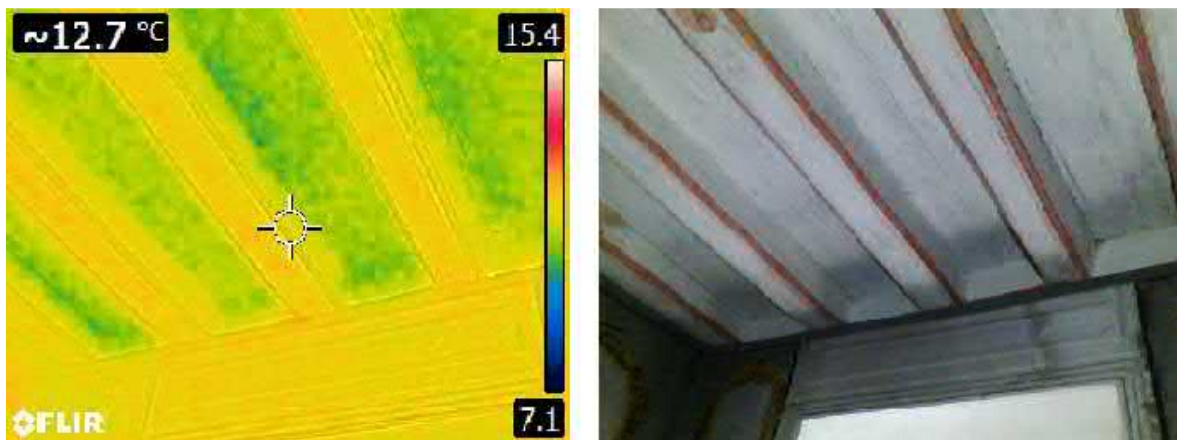


Figure 47. The second tie beam from the left sounded hollow when tapped close to the masonry wall which indicates rot in the beam. However, the infrared thermography showed no increase of cold leaking from outside.

#### 4.4 Discussion

The investigation of the timber structures was essential as the results from the visual inspection and resistance drillings show clearly that rot is a major concern in the load-bearing timber members that are penetrating to the masonry wall. Leaking roof especially from the notches has caused the conditions favorable to fungal growth, which can be analyzed from the results of visual inspection as the rotten timber members were mainly close to the dormers. When combining the visual inspection and resistance drillings from the northeast side, the results indicate that the exposure conditions inside the masonry wall would be favorable to fungal growth even without the leaking of the roof. This is because the visual inspection did not show as extensive rot growth rate as resistance drillings on the northeast side.

The rot problem has been dominating the timber structures penetrating the masonry for some time, which can be estimated on the intervention that has been implemented to one rafter frame in the 1960s. However, the stage of decay in the timber members in relation to time is impossible to estimate. It can be assumed that if the roof structures penetrating the masonry wall from the attic would have been in similar condition in the 1960s as they are now based on the visual inspection, probably more invasive interventions would have been implemented then.



It is hard to tell with these investigations if the rot is active in the timber members that are embedded in the masonry wall. However, it is known that rot is a major concern in timber structures that are embedded to masonry. This leads to an assumption that it is likely that the rot is active in the embedded timber parts at least some periods of the year when the prevailing conditions are favorable for fungal growth.

As the problem of decay lies inside the masonry walls where the tie beam connects to the post and the rafter, it is probable that some of these connections are not working like they should. It is possible that the load-bearing walls might have to bear some of the horizontal forces that the tie beam is not able to bear due to the rotting of its cross section. This causes shear stresses in the load-bearing masonry wall, which can cause deformation or cracks in it. However, these kinds of deformations or cracks were not found on the masonry wall during the visual investigations.

The results from the resistance drillings show that major a part of the members that were drilled are rotten. In addition, one drilling shows only 3 mm in diameter maximum of approximately 250 mm parallel to grain timber member sections. This is a relatively small sample from a timber member with for example cross section size of 250 x 250 mm penetrating approximately 40 cm into the masonry wall. So even when the drilling data shows normal quality of wood, it is possible that the drill bit did not reach to the rotten parts.

Based on the results, it is highly recommendable that extensive structural openings are implemented to all the parts that are embedded into the masonry wall during the repair of the structures. This is the only solution how the condition of timber members inside the masonry wall can be properly analyzed. When these kinds of extensive repairs are implemented, it is beneficial that all the critically rotten parts are repaired now to prevent other possibly more invasive repair interventions in the future.

The results that were received from the investigations can be used to roughly approximate the magnitude of repair that the structures require. Resistance drillings gave valuable information about the condition of timber members embedded into the masonry wall. Without the implementation of resistance drillings, the magnitude of the future repairs would seem far less invasive than they truly are.

Based on the results received from the resistance drillings and visual inspection it was suggested that a structural opening should be implemented on the longer side of the roof to a place where the structural timber members are not so severely rotten according to the investigations. The permission for the structural opening was received from the National Board of Antiquities and Historical Monuments and it will be implemented during autumn 2019 or spring 2020. If the timber members connecting inside the masonry wall will be found rotten even though the results from resistance drillings and visual inspection did not show high indications of rot, an assumption can be made that all the timber members connecting inside the masonry wall are rotten. If the structural opening shows that the quality of timber is normal, less invasive structural repairs can be predicted to the structures. The structural opening will also show valuable information on how the timber members are connected to each other inside the masonry wall.

## **5 Intervention method for the rotten timber structures**

This chapter discusses the intervention method that could be applied in order to repair the rotten timber members that are embedded into the masonry walls from their ends. These timber members are tie beams, rafters and posts.

### **5.1 Boundary conditions**

The boundary conditions restrict the use of any available intervention method. Some of the boundary conditions are not as restricting as others. It can also be a matter of one's opinion which of the boundary conditions are more determining.

The force that is acting in the timber member to be repaired is the governing boundary condition when choosing the intervention method. The safety of the structure can only be guaranteed when the design method fulfills the prevailing forces in the members. Only the detailed design phase can show whether the intended intervention method can fulfill the prevailing forces. The detailed design process is not included in this thesis.

The durability of the intervention method should also be evaluated carefully as the existing timber structures are more than 350 years old. The used intervention method should guarantee similar service life as the original structures have survived. However, the environmental conditions change rapidly due to climate change when comparing to the previous 350 years, which complicates the evaluation of the intervention methods durability.

Valuable paintings on the surfaces of tie beams exclude interventions that would damage the tie beam surfaces. Especially the tie beams located in the banqueting hall should be left untouched as they are known to be original with high artistic value.

The guiding boundary conditions for the repair of historic timber structures are presented in the "Principles for the Conservation of Wooden Built Heritage". The intervention method should be evaluated based on these principles in order to universally accept the method that is applied.

### **5.2 Analysis of intervention methods**

Table 11 shows the summary of the evaluation of different intervention methods in relation to the boundary conditions. Replacement of timber members is not included in the analysis, as only relatively small parts of timber members need to be repaired. However, if it occurs during the repairs that the rot has spread to much wider areas than expected, replacement of the entire member has to be considered. The consolidation with epoxy resin is also not included in the possible intervention methods to be used because no information was found that this intervention method would have been applied to repair load-bearing timber members. Only experimental tests with epoxy consolidation have been implemented, which do not fulfill the criteria in this thesis to be analyzed as a possible intervention method.

Table 11. Summary of the analysis of possible intervention methods to be used in the repair of Louhisaari manor's rotten timber members that are embedded into the masonry wall.

	Follows traditional practices	Paintings in tie beams can be preserved entirely	Experience in historic timber structures in Finland	Takes prevailing cultural values into account	Maintains the original function of the structure	Durability	Reversibility	Degree of intervention
Timber prosthesis with all-timber/metal fastener connections	+	+	+	+	+	+	+	+
Glued-in steel and FRP rods	-	+	-	-	+	0	-	+
Gap-filling adhesive	-	+	-	-	+	-	-	+
Partial substitution with steel	-	+	+	0	+	0	+	+
Circumvention	-	+	+	0	-	+	-	-

Explanations:

- + Fulfills the boundary conditions
- 0 Unclear
- Does not fulfill the boundary condition

### 5.2.1 Timber prosthesis with all-timber/metal fastener connections

Using timber prosthesis with all-timber/metal fastener connections could fulfill all the boundary conditions that have been issued. This intervention method is justifiable as it follows traditional practices. Timber prosthesis with all-timber/metal fastener connections is reversible and enables minimal intervention to achieve structural safety. The long-term durability of the structure would also be ensured with this intervention method as the original embedded timber structures have partly given service life longer than 350 years. This intervention method would also give value to the cultural significance of the manor.

It might even be possible to use all-timber connections in prosthesis of posts and rafters as shown in the Figure 48. This depends on the magnitude of the bending stress in relation to normal stress acting in the connection between the prosthesis and old timber member [38, p. 24]. All-timber connections would have the advantage of avoiding incompatibilities that can cause degradation of materials. However, it would be also justifiable to use metal in the connections between the prosthesis and the old timber member because metal has been used also in some parts of the original structure between timber members.



Figure 48. Timber prosthesis with all-timber connections used similarly as could be applied to rafters and posts in Louhisaari manor. This intervention method has been used in a building located in Prague. [22, p. 69]

The preserving of paintings on the surfaces of tie beams might be achieved with the use of inclined self-tapping screws. This would require that additional timber member would be connected to the tie beam from above (attic) with inclined self-tapping screws. [32] The posts and rafters would connect to this new timber member with traditional timber connections in the support (masonry wall). However, the possibility to use this kind of design method should be carefully evaluated in the detailed design phase as it is possible that the connection between post and the new timber member would be partly located outside the support (masonry wall) due to the height of the new member. This would cause bending stresses unable to bear by the screw connection and/or the member. The thermal conductivity should be evaluated in the detailed design, as the dew point could be build up in the end of the glued-in steel screw as the temperature difference during winter can be more than 30°C between the third floor and the attic. If self-tapping FRP screws would be available, condensation would not be a problem due to the lower thermal conductivity of FRP compared to steel. The service life of this kind of repair method could sustain for up to 200 years if the utilization rates of screws would not be higher than 70% [32].

### 5.2.2 Glued-in steel and FRP rods

Using glued-in steel or FRP rods would not fulfill all the boundary conditions of the intervention method as the long-term durability cannot be guaranteed. Also, the future interventions might have to be more invasive in situations where this intervention method would have to be repaired again due to possible lack of durability. This intervention method would not follow traditional practices or be technically reversible as the glued in rods would have to be cut away with part of the original timber members. The preserving of paintings in the surfaces of tie beams might be achieved with the use of additional timber member connected to the tie beam with glued-in screws/rods similarly as with non-glued inclined self-tapping screws. However, this is not advisable in historic timber structures if the connection can be



implemented with screws without using glue. Glued-in steel screws or rods have not been used in the repair of historic timber structures in Finland instead this method is mainly used in new engineered timber products such as glulam beams [46, 32].

### **5.2.3 Gap-filling adhesive**

Gap-filling epoxy resin intervention method with steel or FRP rods is one of the methods that could be applied in order to preserve the valuable paintings on the surfaces of tie beams. However, the durability of this kind of intervention method is questionable as it has only been used and developed from the 1970s, and if this intervention method would fail, future interventions would have to be more invasive and the valuable paintings would inevitably be damaged in these interventions. No information has been found that gap-filling epoxy intervention method would have been applied in Finland, even though it is used in historic timber structures in some other European countries. The unfamiliarity and uncertain long-term durability of gap-filling epoxy method makes it very questionable to be used in a valuable historic timber structure.

### **5.2.4 Partial substitution with steel**

In order to preserve the valuable paintings on the surfaces of tie beams, it might be possible to use a special kind of steel flitch profile attached to the upper surface of the tie beam end connected with self-tapping inclined screws. Using steel flitch profile instead of timber prosthesis on the top side of the tie beam end would have higher possibility to avoid the additional bending moment, as it depends on the height of the member above the tie beam in which the rafter and the post are connected to. However, this issue should be analyzed in detail in the design phase. High thermal conductivity of steel has to be taken into account, as it can cause condensation during winter frosts. This condensation can cause environmental conditions beneficial for fungal growth in the long term and have an effect on the durability of the repaired structure. This condensation problem should be also investigated in a detailed analysis. Other option to connect this special steel flitch profile into the tie beam is to use steel dowels. However, this method would create small holes on the sides of tie beams and the original paintings would inevitably be damaged. These small dowel holes could be conserved so that the dowel ends would be hidden under the surfaces of tie beams.

### **5.2.5 Circumvention**

If the aim is to preserve the valuable paintings on the surfaces of tie beams, circumvention approach could be applied to replace the structural function of the tie beams. This could be done with additional steel ties that could be installed between the rafter and post pairs. However, the tie beams carry the weights of the third-floor ceiling which causes shear forces near the support. It is possible that these shear forces are close to critical load-bearing capacity in the rotten tie beam ends. This structural capacity of tie beams should be evaluated when using circumvention approach, and if needed similar types of hangers should be designed, as has been implemented in the 1960s. However, if this method would be used, it should be guaranteed that the deterioration mechanism in the ends of tie beams is not active to prevent further damages.

Circumvention approach is not authentic, and the degree of intervention is high. The reversibility of the intervention method is questionable as it depends on many different detailed design choices that are made during the design phase.

### **5.3 Recommendation for the intervention method**

The decision about which intervention method is applied should be based on careful evaluation by all of the parties involved. The chosen intervention method should fulfill the values related to historic structures and the structural and physical requirements for the design. These following recommendations are based on my evaluation and do not give direct answers in all situations.

Based on the analysis I would recommend using the timber prosthesis intervention method, which could be applied for the rotten rafters and posts penetrating to the masonry wall from the attic. The connections could be made either from all-timber, if the detailed design requirements would allow it, or by using metal connectors.

For the repair of rotten tie beam ends I would recommend attaching additional timber member above the tie beam end with inclined self-tapping screws that would reach the sound timber in tie beam. Rafter and post would connect to this additional timber member in the support (masonry wall) with traditional timber connections in order to distribute the forces through the additional timber member to the tie beam. If using additional timber member would not fulfill the detailed design phase, my recommendation for the repair would be to use a special steel flitch profile connected to the tie beam end with inclined self-tapping screws. Or if small holes to the decorative paintings on the sides of tie beams would be accepted the connection between the tie beam and special steel flitch profile could be made with steel dowels. The dowel holes would be conserved after the installation so that the surface of the tie beams would seem untouched. The special steel flitch plate would connect to the rafter and post in the support (masonry wall) by using metal connectors. Both of these repair recommendations could be applied in order to preserve the decorative paintings on the surfaces of tie beams.

If neither of these recommendations would fulfill the design requirements, the other options to be used in order to entirely preserve the valuable paintings on the surfaces of the tie beams would be gap-filling adhesive, glued-in steel rod/screw or circumvention methods. The long-term durability of the gap-filling adhesive intervention method is questionable, and it does not represent the values that prevail in the conservation of historic structures. In addition, it is not a method that has been used in Finland, which makes it questionable. Epoxy glued-in rods/screws instead of inclined self-tapping screws could be applied if the load-bearing design requirements would not be fulfilled with self-tapping screws. However, the durability of glued-in rods/screws is questionable, and its use is not suggested without careful evaluation. In circumvention method new structural elements with modern technique would be installed to the old structures, which would change the function and the aesthetics of the structures in the attic, which is questionable. However, circumvention method has already been used when the manor was repaired in the 1960s, which makes this technique more acceptable.

### **5.4 Additional measures**

In order to enhance drying and minimize the decay due to fungal growth in structures embedded into the masonry wall, air circulation should be improved. This could be promoted through air circulation gaps in the masonry wall and by protecting the surfaces vulnerable to moisture with for instance birch bark, which has been traditionally used. It is also advisable to leave free space between the structures that have been repaired and the masonry wall, in

order to improve the durability of the repair and circulation of air. Figure 49 shows an example of a repair where free space has been left to improve air circulation, and the timber surface has been protected with birch bark.



*Figure 49. Repair of a tie beam end in 2010 in the catholic church located in Helsinki. The rotten end of the tie beam supported by masonry wall was replaced with a new timber piece and the connection between members was implemented with steel plates and bolts. Birch bark was installed to the surfaces of timber member, and air gaps surrounding the member were left to improve the durability of the structure. [55]*

The roof should be inspected, and possible defects should be repaired in order to prevent the roof from leaking. Only continuous and active maintenance of the building can guarantee the long-term survival of the structures and prevent new damages from arising.

## 6 Conclusions

The structural system of the roof was analyzed, and it was recognized that the leaning trestles bear the loads applied to and from the rafters through c-collar beams. The normal forces acting in the connections of the tie beams and the posts were solved in order to find out what kind of load-bearing requirements the design of the repair works has. Structural analysis showed that the leaning trestles have to bear the highest normal forces in the roof structure. The normal forces acting in the connection of the rafter and the tie beam were also calculated in a situation where the leaning trestle would have lost its load-bearing capacity due to rot, in order to figure out the highest forces that can occur in the connection.

The structural performance calculations with the received normal forces showed that the cross sections of the undamaged existing timber members embedded into the masonry wall would fulfill the structural design requirements in ULS. However, the load history and other characteristics that might have altered in the existing timber members during time were not taken into account. The governing load combination, with the normal forces that were received, was self weight for the leaning trestle and self weight with snow for the rafter frame. This was due to the effect of the load duration factor  $k_{mod}$ . It was found that the rafter frames were capable of bearing the normal forces even if the leaning trestles would not be in the structure. However, it was discovered that the function of the leaning trestles is to stiffen the roof structure and restrict the excessive deformations and bending moments occurring in the rafter frame. If the leaning trestles would not exist in the structure, the rafter frames would collapse.

Most general types of wood-destroying fungi are presented in this thesis, as well as the conditions that have to prevail in order for the fungi to thrive. Fungal growth in untreated timber requires a source of infection (fungal spores), oxygen, adequate temperature (approximately 20-25°C) and adequate moisture content in timber (28 to 30%). The only way to prevent the fungal growth in timber structures is to minimize the amount of moisture accumulation. When the maintenance of the structures is neglected, the conditions favorable to fungal growth are more likely to emerge, for example due to a leaking of the roof. However, certain structural solutions in historic timber structures, such as timber members embedded into masonry, can inflict fungal growth in the long term. It was found that both of these reasons have inflicted the fungal growth in Louhisaari manor's roof truss structures.

The visual inspections in the attic of Louhisaari manor showed that wood destroying fungi has severely decayed the timber members (rafters and posts) that penetrate to the outer masonry wall. Semi-destructive resistance drillings were implemented to discover the rate of rot in the members that are embedded into the outer masonry wall from the third floor (tie beams) and from the attic (posts). This method was used because it is the only assessment method that can give sufficiently reliable results from the parts of timber members that are not tangible. Structural openings would have been another option to figure out the conditions of timber members inside the masonry wall, but this would not have been advisable due to its destructiveness in this stage of condition survey.

The implementation of resistance drillings gave valuable information on the conditions of structurally essential timber members (tie beams and posts). Results from the resistance drillings showed that more than 60% of the tie beams and posts that were resistance drilled have clear signs of rot or are extremely soft.

It must be underlined that the stage of decay can be even wider than the results show, because the resistance drillings show the condition of the timber member maximally into the depth of 25 cm parallel to grain inside the masonry wall. And it is possible that the timber members are rotten in deeper stages inside the masonry wall although showing good quality of wood in the Resistograph profile. This being realized, based on the results received from the resistance drillings and visual inspection a new structural opening will be implemented to the longer side of the roof will during autumn 2019 or spring 2020. The results received from the opening can be compared to the results from the resistance drillings, which can give valuable information on the condition of timber members in general. If the structural opening is implemented to a place which showed no results of rot in the resistance drilling profile and the timber members in the structural opening are rotten, an assumption can be made that all the timber members connecting inside the masonry wall can be rotten. If the structural opening shows that the quality of timber is normal, less invasive structural repairs can be predicted to the structures. The structural opening will also show valuable information on how the timber members are connected to each other inside the masonry wall.

Based on the results received from the investigations, the repair of the structural roof members is essential to guarantee the safety and the survival of the valuable roof structures. The only way to ensure that all the rotten timber members are repaired is to implement structural openings during the restoration process to all the places where the rafters, posts and tie beams are embedded into the outer masonry wall. If these structural openings are not performed during the repair process hidden and in worst situation active rot can remain in the structures.

This possible decaying process hidden in the structures will eventually lead to repair interventions more invasive than they would be now. If the structures are investigated properly and all the necessary repairs are implemented in this next repair process the future interventions to the roof structures will be more minor.

In Finland, all-timber connections have not been used in prosthesis intervention methods where bending occurs in simple supported timber member due to the lack of design guidelines. It was found that these all-timber design guidelines for simultaneously bending and compression/tension for beams have been developed in Czech Republic in 2016. These design guidelines could also be used in the structural design procedures in Finland. These guidelines have their limitations that have to be taken into account and they are not suitable in all situations. However, these guidelines could be studied, and the possibility to use them for the repair of rotten timber members in Louhisaari manor could be evaluated.

The feasibility of possible intervention methods that could be applied for the rotten timber members in Louhisaari manor were evaluated based on the boundary conditions based on the values presented in the “Principles for the Conservation of Wooden Built Heritage” and specific characteristics of Louhisaari manor. It was discovered that timber prosthesis with all-timber or metal fastener connections could be applied as an intervention method for the rotten rafters and the posts.

In order to preserve the valuable decorative paintings on the surfaces of tie beams additional timber member or special steel flitch profile attached above the tie beam end could be applied. The post and the rafter would connect to this additional timber member in the support (masonry wall) with traditional timber connections or with metal fasteners if special steel flitch profile would be applied. The detailed design phase shows which of these methods is more applicable. In addition, the decision which repair method to use should be discussed by all the parties involved in the project.

## Bibliography

- [1] Huttunen, Marko & Eerikäinen Laura & Laine, Laura & Saarinen, Pauliina & Savolainen, Panu & Senaatti-kiinteistöt & Museovirasto. 2018. Ruotsin Suurvalta-ajan Vesikattorakenteet Suomessa. Helsinki. ISBN 978-952-7239-29-1.
- [2] Harris, Samuel Y. 2001. Building Pathology: deterioration, diagnostics, and intervention. United States of America: John Wiley & Sons. ISBN 0-471-33172-4.
- [3] Bech Andersen, Jorgen. 2004. The structure of wood and biological decay. Drdäcký Milos. 2004. European Research on Cultural Heritage, State-of-the-Art Studies 2. Czech Republic: Tiskárna Glos Semily. ISBN 80-86246-23-X.
- [4] Ross, Peter. 2002. Appraisal and repair of timber structures. Great Britain: MPG Books. ISBN 0-7277-2051-1.
- [5] Singh, Jagit. 2001. Degradation of Cultural Heritage in Surrounding Environment. Drdäcký Milos. 2004. European Research on Cultural Heritage, State-of-the-Art Studies, Volume 2. Czech Republic: Tiskárna Glos Semily. ISBN 80-86246-23-X.
- [6] Brennan, Thomas & Brennan, Damien. 2006. Common Defects Found in the Built Environment throughout Ireland and their Relationship with Similar Problems Found throughout Europe. Drdäcký Milos. 2006. European Research on Cultural Heritage, State-of-the-Art Studies, Volume 4. Czech Republic: Tiskárna Glos Semily. ISBN 08-86246-25-6.
- [7] Reinprecht, Ladislav. 2016. Wood deterioration, protection, and maintenance. John Wiley & Sons, Ltd. ISBN: 9781119106500.
- [8] Nisula, Linda. 2018. Wood Extractives in Conifers, A Study of Stemwood and Knots of Industrially Important Species. Åbo Akademi University Press. ISBN 978-951-765-891-1.
- [9] Yang, Guangyu & Jaakkola, Pirjo. 2011. Wood chemistry and isolation of extractives from wood. Literature study for BIOTULI project. Saimaa university of Applied Sciences. Cited 28.1.2019. Available: [http://biotuli-hanke.fi/files/download/Biotuli\\_YangJaakkola2011.pdf](http://biotuli-hanke.fi/files/download/Biotuli_YangJaakkola2011.pdf)
- [10] Pitkäranta, Miia. 2016. Rakennuksen kosteus- sisäilmatekninen kuntotutkimus (Building moisture and indoor air quality assessment). Hansaprint, Turenki. Ympäristöministeriö. Pages 234. ISBN 978-952-11-4625-1
- [11] Olaf Schmidt. 2007. Indoor Wood-decay basidiomycetes: Damage, causal fungi, physiology, identification and characterization, prevention and control. Mycological Progress. 2007.
- [12] Watkinson, Sarah & Eastwood, Daniel. 2012. *Serpula lacrymans*, Wood and Buildings. Advances in Applied Microbiology. Volume 78. ISBN 978-0-12-394805-2.
- [13] Kisternaya, Margarita & Kozlov, Valery. 2015. Wood science approach for the preservation of historic timber structures.



- [14] Reinprecht, Ladislav. 2004. Biodegradation and Treatment of Ancient Wood in Slovakia. Drdáký Milos. 2004. European Research on Cultural Heritage, State-of-the-Art Studies 2. Czech Republic: Tiskárna Glos Semily. ISBN 80-86246-23-X.
- [15] Press release: 18 December 2017. ICOMOS Principles for the Conservation of Wooden Built Heritage. 2017. Cited 30.1.2019. Available: <http://www.icomos-uk.org/uploads/sidebar/PDF/Press%20release%20-%20new%20IWC%20Principles%202017.pdf>
- [16] ICOMOS. 2017. Principles for the Conservation of Wooden Built Heritage. Cited: 30.1.2019. Available: [https://www.icomos.org/images/DOCUMENTS/General\\_Assemblies/19th\\_Delhi\\_2017/Working\\_Documents-First\\_Batch-August\\_2017/GA2017\\_6-3-4\\_WoodPrinciples\\_EN\\_final20170730.pdf](https://www.icomos.org/images/DOCUMENTS/General_Assemblies/19th_Delhi_2017/Working_Documents-First_Batch-August_2017/GA2017_6-3-4_WoodPrinciples_EN_final20170730.pdf)
- [17] Branco, Jorge M. & Tomasi, Roberto. 2014. Analysis and Strengthening of Timber Floors and Roofs. Aníbal Costa. João Miranda Guedes. Humberto Varum. Structural Rehabilitation of Old Buildings. ISBN 978-3-642-3986-1 (eBook)
- [18] Dietsch, Philipp & Köhler, Jochen. 2010. Assessment of Timber Structures. Shaker Verlag. ISBN 978-3-8322-9513-4.
- [19] Homepage of Puuinfo: Kosteusteknisiä ominaisuuksia (Moisture technical properties of wood). Cited: 5.2.2019. Available: <https://www.puuinfo.fi/puutieto/puu-materiaalina/kosteusteknisi%C3%A4-ominaisuuksia>
- [20] López, Gamaliel & Basterra, Luis-Alfonso & Luis Acuña. 2018. Infrared thermography for wood density estimation. Infrared Physics & Technology. 2018. Volume 89.
- [21] Magina, Miguel Jorge. 2013. Historic Timber Roof Structures. Dissertation. New University of Lisbon. Cited 4.3.2019. Available: <http://citeseerx.ist.psu.edu/viewdoc/download?doi=10.1.1.926.2984&rep=rep1&type=pdf>
- [22] Pinto, Luis. 2008. Inventory of Repair and Strengthening Methods - Timber. Master's thesis. Polytechnic University of Catalonia. Advanced Master's in Structural Analysis of Monuments and Historical Construction (SAMHC). Spain.
- [23] Morales Conde, María Jesús & Rodríguez Liñán, Carmen & Rubio de Hita, Paloma. 2014. Use of ultrasound as a non-destructive evaluation technique for sustainable interventions on wooden structures. Building and Environment. Volume 82 (2014).
- [24] CNR-DT 200/2004. 2004. Guide for the Externally Bonded FRP Systems for Strengthening Existing Structures – Materials, RC and PC structures, masonry structures.
- [25] CNR-DT 201/2005. 2005. Guidelines for the Design and Construction of Externally Bonded FRP Systems for Strengthening Existing Structures - Timber Structures.
- [26] Schober, Kay-Uwe & Harte, Annette M. & Kliger, Robert & Jockwer, Robert & Xu, Qingfeng & Chen, Jian-Fei. 2015. FRP Reinforcement of Timber Construction and Building Materials. Structures.

- [27] Martin, Zeoni A. & Tingley, Dan A. 2000. Fire resistance of FRP reinforced glulam beams. Proceedings of World Conference on Timber Engineering. Canada.
- [28] Williamson, Thomas G. & Yeah, Borjen. 2006. Fire Performance of FRP Reinforced Glulam. Proceedings of 9th World Conference on Timber Engineering. Portland, U.S.A.
- [29] Rowell, Roger M. 2005. Handbook of Wood Chemistry and Wood Composites. United States. CRC Press. ISBN 0-8493-1688-3.
- [30] Stokke, Douglas D. & Wu, Qinlin & Han, Guanping. 2014. Wood and Natural Fiber Composites. United Kingdom. John Wiley & Sons, Ltd. ISBN 9780470710913.
- [31] Ryan Cleary. 2014. Considering the Use of Epoxies in the Repair of Historic Structural Timber. Master's thesis. University of Pennsylvania. Graduate Program in Historic Preservation. Philadelphia. Cited: 12.2.2019. Available: [https://repository.upenn.edu/hp\\_theses/568/](https://repository.upenn.edu/hp_theses/568/)
- [32] Asko Keronen. 2019. Licentiate of Technology. Structural engineer. Insinööritoimisto Asko Keronen. Nuottatie 8 H, 02230 Espoo, Finland.
- [33] Custódio, João & Broughton, James & Cruz, Helena. 2011. Rehabilitation of timber structures – Preparation and environmental service condition effects on the bulk performance of epoxy adhesives. Construction and Building Materials. Volume 25, Issue 8. 2011.
- [34] Andre, Neves & Henriques, Dulce Franco. 2014. Processes of Timber Conservation and Consolidation. Conference paper.
- [35] Cruz, Helena & Custódio João. 2006. Thermal performance of epoxy adhesives in timber structural repair. 9<sup>th</sup> world conference on timber engineering 2006. Volume 2.
- [36] Wheeler, Andrea S. & Hutchinson, Allan S. 1997. Resin repairs to timber structures. International Journal of Adhesion & Adhesives. Volume 18.
- [37] Corradi, Marco & Osofero, Adelaja Israel & Borri, Antonio. 2019. Repair and Reinforcement of Historical Timber Structures with Stainless Steel. Metals. Volume 9.
- [38] Kunecký, Jiri. & Fajman, Petr. & Sebera, Václav. & Hasníková, Hana. & Kuklík, Petr. & Tippner, Jan & Kloiber, Michal. 2016. Lapped Scarf Joints for Repairs of Historical Structures. Prague, Czech Republic. ISBN 978-80-86246-70-3.
- [39] Nowak, Thomas P. & Karolak, Anna. 2014. Historical carpentry joints. Journal of Heritage Conservation. Volume 40.
- [40] Bejtka, Ireneusz & Blaß, Hans Joachim. 2002. Joints With Inclined Screws. International Council for the Research and Innovation in Building and Construction. Working commission W18 – Timber Structures. CIB-W18/35-7-5.

- [41] Kevarinmäki, Ari. 2005. Puurakenteiden Uusia Liitostekniikoita. Rakenteiden mekaniikka, Vol. 38.
- [42] Ympäristöministeriö. 2013. Puurakenteiden vetorasitetut ja liimatut terästanko- ja ruuvi-liittimet. Cited 31.5.2019. Available: [https://www.ymparisto.fi/fi-FI/Maankaytto\\_ja\\_rakentaminen/Rakentamisen\\_ohjaus/Rakennustuotteiden\\_tuotehyvaksynta/Kansalliset\\_hyvaksyntamenettelyt/Varmennustodistus](https://www.ymparisto.fi/fi-FI/Maankaytto_ja_rakentaminen/Rakentamisen_ohjaus/Rakennustuotteiden_tuotehyvaksynta/Kansalliset_hyvaksyntamenettelyt/Varmennustodistus)
- [43] SFS-EN 301:2017. 2017. Adhesives, phenolic and aminoplastic, for load-bearing timber structures. Classification and performance requirements. Helsinki. Suomen Standardisoimisliitto SFS.
- [44] Cruz, Helena & Custódio, João. 2004. Execução e controlo de qualidade da reparação de estruturas de madeira com colas epoxídicas e FRPs. 1<sup>st</sup> Iberian Congress on Timber Construction University of Minho.
- [45] Stumes, Paul. 1975. Testing the Efficiency of Wood Epoxy Reinforcement Systems. Bulletin of the Association for Preservation Technology. Vol. 7.
- [46] Korhonen, Aapo. 2019. Liimakon Oy. Linturinteentie 30. 88900 Kuhmo.
- [47] Appleton, João & Appleton, Vasco & Aquino, Ana & Ferreira da Rocha, Margarida. 2012. Library roof – Santa Maria de Alcobaca Abbey, Alcobaca, Portugal. Structural Analysis of Historical Constructions. 2012. ISSN 0860-2395. ISBN 978-83-7125-216-7.
- [48] Gonzáles-Bravo & Maldonado-Ramos. 2011. Steel profiles for repairing deteriorated timber beam ends. Informes de la Construcción. Volume 63. ISSN 0020-08883.
- [49] Toker Beeson, Saadet. & Ozkan Yazgan, Esra. & Unay, Ali Ihsan. 2014. Strengthening of the Timber Roof of the Second Turkish National Assembly Building in Ankara. SAHC2014 - 9<sup>th</sup> international Conference on Structural Analysis of Historical Constructions.
- [50] History of Klas Fleming. Cited: 26.2.2019. Available: <https://historiesajten.se/visa-info.asp?id=17>
- [51] 2017. RIL 201-1-2017 Suunnitteluperusteet ja rakenteiden kuormat. Grano Oy. Suomen Rakennusinsinöörien Liitto RIL ry. ISBN 978-951-758-609-2.
- [52] 2017. RIL 205-1-2017 Puurakenteiden suunnitteluohje. Grano Oy. Suomen Rakennusinsinöörien Liitto RIL ry. ISBN 978-951-758-604-7.
- [53] Paloniitty, Sauli & Kauppinen, Timo. 2006. Rakennusten Lämpökuvaus. Rakennusteollisuuden Kustannus RTK Oy. ISBN 952-5472-44-2.
- [54] Suoranta, Teppo. 2019. Arborist/horticulturalist. Puiden hoito TS-ympäristöpalvelu Ky. Bonäsintie 400, 21710 Korppoo.
- [55] Haikala, Antti. 2019. HP Insinöörit Oy. Hämeentie 155 B 20, 00560 Helsinki.

- [56] Manufacturers brochure: Measured Variables of the IML-RESI PowerDrill, Drill Resistance and Feed Force Measurement. Cited: 26.6.2019. Available: [http://www.iml-na.com/fileadmin/user\\_upload/Measured\\_Variables\\_PD\\_USA.pdf](http://www.iml-na.com/fileadmin/user_upload/Measured_Variables_PD_USA.pdf)
- [57] FRP vs. Traditional Materials. Bedford Reinforced Plastics. 2017. Cited: 5.8.2019. Available: <https://bedfordreinforced.com/app/uploads/2017/08/BRP-FRP-vs-Traditional-Materials.pdf>
- [58] SFS 5878 INSTA 142. 2010. Sahatavaran visuaalisen lujuuslajittelun pohjoismaiset säännöt. Helsinki. Suomen standardoimisliitto SFS.
- [59] Thelin, Carl. 2006. Medieval Timber Roof Structures. Paper IV. Chalmers University of Technology. ISBN 91-7291-800-4.
- [60] Hallgren, Mattias. 2019. Carpenter. Hallgren Hantverk. Östbygatan 20 a, 53137 Lindköping, Sweden.
- [61] Yeomans, David. 2016. How Structures Work: Design and Behaviour from Bridges to Buildings. John Wiley & Sons. Ltd. ISBN 978-1-119-01227-6.

## **Appendixes**

Appendix A. Structural calculations. Pages 21

Appendix B. Rot report on Louhisaari manor's roof structures. Pages 41.

## Purpose of the structural calculations

The purpose of these calculations is to calculate the loads that are acting in the roof structures and to verify the reliability of the finite element models that were analysed with Robot Structural Analysis software.

The structural performance of the timber members embedded into masonry wall is also calculated in ULS with the existing standards and guidelines. This is performed in order to find out whether these parts would be adequate with the existing design guidelines. The results from structural performance analysis can also be used to roughly approximate whether the structural members that are rotten have capacity to bear the design requirements.

## A. Loads affecting on the rafter frame

### A.1. Permanent loads

Load resulting from roofing materials:

Average spacing between the rafter frames:  $k_R := 720 \text{ mm}$

Weight of timber:  $\rho_t := 5 \frac{\text{kN}}{\text{m}^3}$  (RIL 205-1-2017, p. 34)

Thickness of the shingles:  $t_s := 30 \text{ mm} \cdot 3 = 90 \text{ mm}$

Thickness of the roof boards:  $t_{rb} := 25 \text{ mm}$

Total load from the roofing materials:

$$g_{k.R} := \rho_t \cdot (t_{rb} + t_s) \cdot k_R = 0.41 \frac{\text{kN}}{\text{m}}$$

Self weight of the timber members:

C-collar beam:  
 $g_{c.collar.beam} := 190 \text{ mm} \cdot 190 \text{ mm} \cdot \rho_t = 0.18 \frac{\text{kN}}{\text{m}}$

Rafter:  
 $g_{rafter} := 170 \text{ mm} \cdot 170 \text{ mm} \cdot \rho_t = 0.14 \frac{\text{kN}}{\text{m}}$

A- and B-collar beam  
 $g_{a.b.collar.beam} := 160 \text{ mm} \cdot 160 \text{ mm} \cdot \rho_t = 0.13 \frac{\text{kN}}{\text{m}}$

Tie beam:  
 $g_{tb} := 250 \text{ mm} \cdot 250 \text{ mm} \cdot \rho_t = 0.31 \frac{\text{kN}}{\text{m}}$



Timber members in leaning trestle:

$$g_{LT} := 220 \text{ mm} \cdot 250 \text{ mm} \cdot \rho_t = 0.28 \frac{\text{kN}}{\text{m}}$$

Outermost joist:

$$g_{jo} := 180 \text{ mm} \cdot 230 \text{ mm} \cdot \rho_t = 0.21 \frac{\text{kN}}{\text{m}}$$

Inner joist:

$$g_{ji} := 160 \text{ mm} \cdot 160 \text{ mm} \cdot \rho_t = 0.13 \frac{\text{kN}}{\text{m}}$$

## A.2. Snow load (RIL 201-1-2017)

Snow load is being calculated according the eurocode 1 and national annex of Finland.

The value of snow load on the ground in the area of Masku:

$$s_k := 2.3 \frac{\text{kN}}{\text{m}^2} \quad (\text{RIL 205-1-2017, p. 208})$$

The inclination of the roof mainly defines the value of snow load, which in this case according to the measurement drawings is in the linear part of the roof:

$$\alpha := 53 \quad \text{if the inclination } \alpha \text{ would be } \leq 60 \text{ the snow load can be assumed as 0 in calculations.}$$

The form factor for roofs with inclination  $30 < \alpha < 60$ :

$$\mu_1 := 0.8 \cdot \frac{60 - \alpha}{30} = 0.19$$

The snow load in the linear part of the roof:

$$s_{snow} := s_k \cdot \mu_1 = 0.43 \frac{\text{kN}}{\text{m}^2}$$

Snow load for one rafter frame:

$$q_{s,R} := s_{snow} \cdot k_R = 0.31 \frac{\text{kN}}{\text{m}}$$

Snow load is larger on the curved eave structure as the inclination slowly decreases to  $13^\circ$  in the edge of the eave. The curved part is supported by the corbel and the rafter frame. However, the parts that have gables do not have curved eaves. The curved part is calculated with mean value.

The inclination on the edge of eave is approx.:

$$\alpha_2 := 13$$

The mean inclination on the curved part of roof:

$$\alpha_3 := \frac{\alpha + \alpha_2}{2} = 33$$

The form factor for roofs with inclination  $30 < \alpha < 60$ :

$$\mu_2 := 0.8 \cdot \frac{60 - \alpha_3}{30} = 0.72$$

The snow load in the curved part of the roof:

$$s_{snow,2} := s_k \cdot \mu_2 = 1.66 \frac{\text{kN}}{\text{m}^2}$$

Snow load with division of one rafter frame:

$$q_{s,2} := s_{snow,2} \cdot k_R = 1.19 \frac{\text{kN}}{\text{m}}$$

### A.3. Wind load (RIL 201-1-2017)

According to the Eurocode and Finnish national annex the fundamental value for basic wind velocity in Finland is:  $v_{b,0} := 21 \frac{m}{s}$ .

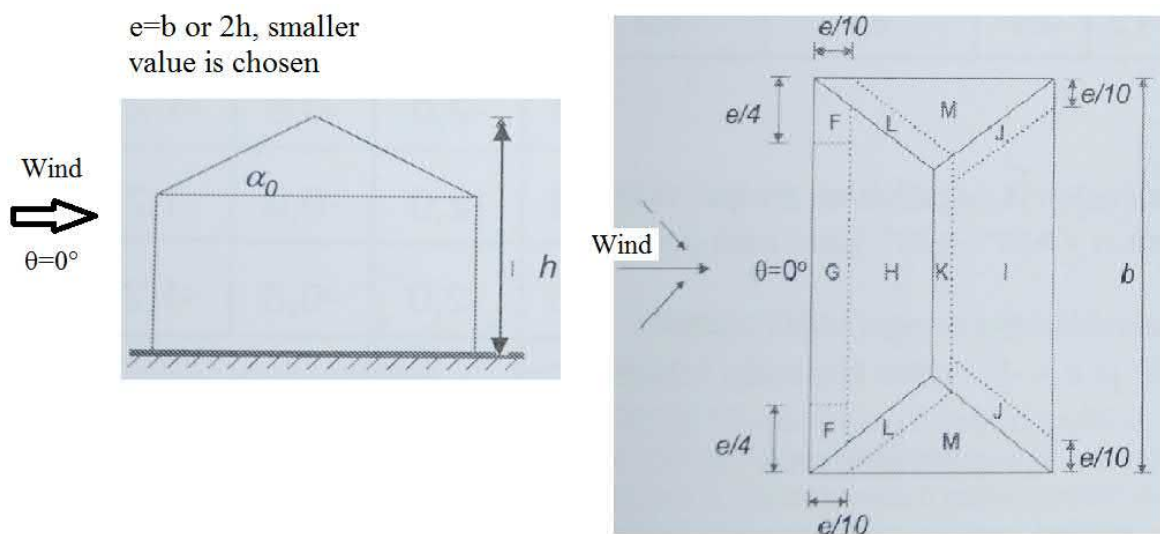
Louhisaari manors roof is subjected to terrain category 2 and the height from ground is approximately 25 m.

The service life for load definition is chosen to be 250 years which affects to the peak velocity pressure used in design.  $C_{prop}$  coefficient is applied according to RIL-201-1-2017.

$$\Rightarrow C_{prop} := 1.2$$

The peak velocity pressure for each rafter frame is obtained from table 4.2S (RIL201-1-2017):  $q_p := 0.82 \frac{kN}{m^2} \cdot k_R \cdot C_{prop} = 0.71 \frac{kN}{m}$

The manors roof is divided into sections according to RIL 201-1-2017 shown in the figure below. Different wind loads are affecting in different sections of roof.



$$b := 23690 \text{ mm} \quad \ll \quad h := 24600 \text{ mm}$$

$$\Rightarrow e := b = 23.69 \text{ m} \quad \frac{e}{10} = 2.37 \text{ m}$$

Only areas G, H, K and I are evaluated in these calculations because the roof structures being analysed are located in these areas. Area G and part of the area I is located on the curved part of the roof structure where the mean inclination is approximately  $33^\circ$ . However, this only has an effect on the windward. This effect is minimal as can be seen from RIL 201-1-2017, table 7.5. This minimal effect of curving eaves is not taken into account which makes the wind load values a bit conservative on the curved part of the roof structure. Due to this  $G=H$ .

Wind load pressures in different sections:

$$C_{pe.GH} := 0.7 \qquad w_{e.GH} := q_p \cdot C_{pe.GH} = 0.5 \frac{kN}{m}$$

$$C_{p.IK} := -0.3 \qquad w_{e.IK} := q_p \cdot C_{p.IK} = -0.21 \frac{kN}{m}$$

Structural factor  $c_s c_d$ :

$$c_s c_d := 1 \qquad \text{(RIL 201-1-2017, chapter 6.2)}$$

$$F_{w.GH} := c_s c_d \cdot w_{e.GH} = 0.5 \frac{kN}{m}$$

$$F_{w.IK} := c_s c_d \cdot w_{e.IK} = -0.21 \frac{kN}{m}$$

#### A.4. Load combinations (RIL 201-1-2017)

Ultimate limit state in STR.

Consequence class=2 =>  $K_{FI} := 1.0$

Factor for combination value of a variable action:

Snow load:  $\psi_{0.s} := 0.7$

Wind load:  $\psi_{0.w} := 0.6$

Governing wind load:

Wind loads in the windward:

Wind loads opposite to windward:

Area G and H:

Area I and K:

$$q_{w.d.GH1} := 1.5 \cdot K_{FI} \cdot F_{w.GH} = 0.74 \frac{kN}{m}$$

$$q_{w.d.IK1} := 1.5 \cdot K_{FI} \cdot F_{w.IK} = -0.32 \frac{kN}{m}$$

Snow load:

$$q_{s.d1} := 1.5 \cdot K_{FI} \cdot \psi_{0.s} \cdot q_{s.R} = 0.32 \frac{kN}{m}$$

Snow load of the curved part:

$$q_{s.d1.1} := 1.5 \cdot K_{FI} \cdot \psi_{0.s} \cdot q_{s.2} = 1.25 \frac{kN}{m}$$

Governing snow load:

Wind loads in the windward:

Area G and H:

$$q_{w.d.GH2} := 1.5 \cdot K_{FI} \cdot \psi_{0.w} \cdot F_{w.GH} = 0.45 \frac{kN}{m}$$

Wind loads opposite to windward:

Area I and K:

$$q_{w.d.IK2} := 1.5 \cdot K_{FI} \cdot \psi_{0.w} \cdot F_{w.IK} = -0.19 \frac{kN}{m}$$

Snow load:

$$q_{s.d2} := 1.5 \cdot K_{FI} \cdot q_{s.R} = 0.46 \frac{kN}{m}$$

Snow load of the curved part:

$$q_{s.d2.1} := 1.5 \cdot K_{FI} \cdot q_{s.2} = 1.79 \frac{kN}{m}$$

Self weights when live load is acting :

load of the roofing materials:

$$g_{k.R.d1} := 1.15 \cdot K_{FI} \cdot g_{k.R} = 0.48 \frac{kN}{m}$$

c-collar beam:

$$G_{c.collar.beam1} := 1.15 \cdot K_{FI} \cdot g_{c.collar.beam} = 0.21 \frac{kN}{m}$$

rafter:

$$G_{rafter1} := 1.15 \cdot K_{FI} \cdot g_{rafter} = 0.17 \frac{kN}{m}$$

a-collar beam:

$$G_{a.collar.beam1} := 1.15 \cdot K_{FI} \cdot g_{a.b.collar.beam} = 0.15 \frac{kN}{m}$$

b-collar beam:

$$G_{b.collar.beam1} := 1.15 \cdot K_{FI} \cdot g_{a.b.collar.beam} = 0.15 \frac{kN}{m}$$

outermost joist:

$$G_{jo1} := 1.15 \cdot K_{FI} \cdot g_{jo} = 0.24 \frac{kN}{m}$$

inner joist:

$$G_{ji1} := 1.15 \cdot K_{FI} \cdot g_{ji} = 0.15 \frac{kN}{m}$$

tie beam:

$$G_{tb1} := 1.15 \cdot K_{FI} \cdot g_{tb} = 0.36 \frac{kN}{m}$$

members in the leaning trestle:

$$G_{LT1} := 1.15 \cdot K_{FI} \cdot g_{LT} = 0.32 \frac{kN}{m}$$

Self weights when liveloads are not acting:

load of the roofing materials:

$$g_{k.R.d1.1} := 1.35 \cdot K_{FI} \cdot g_{k.R} = 0.56 \frac{kN}{m}$$

c-collar beam:

$$G_{c.collar.beam1.1} := 1.35 \cdot K_{FI} \cdot g_{c.collar.beam} = 0.24 \frac{kN}{m}$$

rafter:

$$G_{rafter1.1} := 1.35 \cdot K_{FI} \cdot g_{rafter} = 0.2 \frac{kN}{m}$$

a-collar beam:

$$G_{a.collar.beam1.1} := 1.35 \cdot K_{FI} \cdot g_{a.b.collar.beam} = 0.17 \frac{kN}{m}$$

b-collar beam:

$$G_{b.collar.beam1.1} := 1.35 \cdot K_{FI} \cdot g_{a.b.collar.beam} = 0.17 \frac{kN}{m}$$

outermost joist:	$G_{jo1.1} := 1.35 \cdot K_{FI} \cdot g_{jo} = 0.28 \frac{kN}{m}$
inner joist:	$G_{ji1.1} := 1.35 \cdot K_{FI} \cdot g_{ji} = 0.17 \frac{kN}{m}$
tie beam:	$G_{tb1.1} := 1.35 \cdot K_{FI} \cdot g_{tb} = 0.42 \frac{kN}{m}$
members in the leaning trestle:	$G_{LT1.1} := 1.35 \cdot K_{FI} \cdot g_{LT} = 0.37 \frac{kN}{m}$





Dimensions:

$$\begin{aligned} h_{tot} &:= 6.513 \text{ m} & h_1 &:= 2.544 \text{ m} & h_2 &:= 2.066 \text{ m} & h_3 &:= 1.903 \text{ m} \\ L_{tot} &:= 9.888 \text{ m} & L_1 &:= 1.931 \text{ m} & L_2 &:= 1.568 \text{ m} & L_3 &:= 1.445 \text{ m} \\ L_4 &:= L_3 & L_5 &:= L_2 & L_6 &:= L_1 & \alpha_1 &:= 53 \text{ deg} \end{aligned}$$

The support reactions are calculated:

Vertical support reaction A in parts:

$$A_{v1} := \frac{\left( q_{s.d2} + \frac{g_{k.R.d1} + G_{rafter1}}{\cos(\alpha_1)} + G_{c.collar.beam1} \right) \cdot \frac{(L_{tot})^2}{2}}{L_{tot}} = 8.6 \text{ kN}$$

$$A_{v2} := \frac{G_{b.collar.beam1} \cdot (L_{tot} - L_1 \cdot 2) \cdot \left( \frac{L_{tot}}{2} \right)}{L_{tot}} = 0.44 \text{ kN}$$

$$A_{v3} := \frac{G_{a.collar.beam1} \cdot L_3 \cdot 2 \cdot (L_4 + L_5 + L_6) + (q_{w.d.GH2} - q_{w.d.IK2}) \cdot \sin(\alpha_1) \cdot \left( \frac{h_{tot}}{2} \right) \cdot h_{tot}}{L_{tot}} = 1.58 \text{ kN}$$

$$A_{v4} := \frac{q_{w.d.GH2} \cdot \cos(\alpha_1) \cdot \left( \frac{L_{tot}}{2} \right) \cdot \frac{L_{tot}}{4} + q_{w.d.IK2} \cdot \cos(\alpha_1) \cdot \left( \frac{L_{tot}}{2} \right) \cdot \frac{3 \cdot L_{tot}}{4}}{L_{tot}} = -0.16 \text{ kN}$$

The total vertical support reaction in support A:

$$A_v := A_{v1} + A_{v2} + A_{v3} + A_{v4} = 10.46 \text{ kN}$$

Vertical support reaction G in parts:

$$G_{v1} := \left( q_{s.d2} + \frac{g_{k.R.d1} + G_{rafter1}}{\cos(\alpha_1)} + G_{c.collar.beam1} \right) \cdot L_{tot} - A_v = 6.73 \text{ kN}$$

$$G_{v2} := (q_{w.d.GH2} \cdot \cos(\alpha_1) + q_{w.d.IK2} \cdot \cos(\alpha_1)) \cdot \left( \frac{L_{tot}}{2} \right) = 1.26 \text{ kN}$$

$$G_{v3} := G_{b.collar.beam1} \cdot (L_{tot} - L_1 \cdot 2) + G_{a.collar.beam1} \cdot L_3 \cdot 2 = 1.31 \text{ kN}$$

Total vertical support reaction in support G:

$$G_v := G_{v1} + G_{v2} + G_{v3} = 9.3 \text{ kN}$$

Horizontal support reaction in support G:

$$G_h := (q_{w.d.GH2} - q_{w.d.IK2}) \cdot \sin(\alpha_1) \cdot \frac{h_{tot}}{\sin(\alpha_1)} = 4.15 \text{ kN}$$

To obtain the vertical loads  $F_1$  and  $F_2$  that the leaning trestle has to bear due to the structural system the vertical support reactions received are multiplied with 5, which is the number of rafter frames that the leaning trestle is supporting through the joists. The weights of the joists (2 outermost joists and 3 inner joists) are added here:

$$F_1 := A_v \cdot 5 + G_{jo1} \cdot 3.6 \text{ m} + G_{ji1} \cdot 3.6 \text{ m} \cdot \frac{3}{2} = 53.96 \text{ kN}$$

$$F_2 := G_v \cdot 5 + G_{jo1} \cdot 3.6 \text{ m} + G_{ji1} \cdot 3.6 \text{ m} \cdot \frac{3}{2} = 48.16 \text{ kN}$$

To obtain the horizontal force  $F_h$  that acts in the interface of the joists and head beam of the leaning trestle the horizontal support reaction in support G has to be multiplied with 5. However, the amount of horizontal force that is distributed to the head beam of the leaning trestle depends on the frictional coefficient between the surfaces as the joists are purely lying above the head beams with no visible connection.

$$F_h := G_h \cdot 5 = 20.76 \text{ kN}$$

The frictional coefficient for wood against wood when the grains of wood members are perpendicular to each other can vary between 0.63 to 0.81 prior to sliding and 0.27 to 0.59 during sliding. [Paper IV. p, 25-26. Carl Thelin. 2006. Medieval Timber Roof Structures. Chalmers Tekniska Högskola. ISBN 91-7291-800-4] The friction coefficient prior to sliding is chosen to be  $\mu_f := 0.63$  which favour the sliding of the joists/(rafter frame) above the head beam.

The maximum force that can be transported from the joists to the head beam through friction:

$$F_{max} := \mu_f \cdot (F_1 + F_2) = 64.34 \text{ kN} > F_h = 20.76 \text{ kN}$$

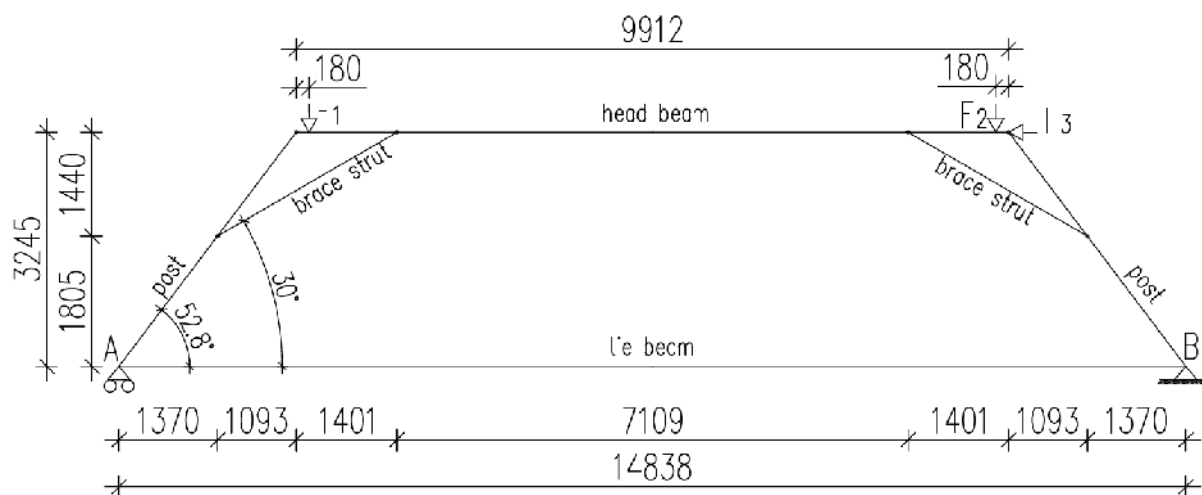
=> all the horizontal forces that are acting in the interface of joists and head beam is distributed to the head beam through friction:

$$\Rightarrow F_3 := F_h = 20.76 \text{ kN}$$

## B.2. Leaning trestle

To obtain the internal forces that are acting in the connection between the post of the leaning trestle and the tie beam the following free body diagram is solved. The forces  $F_1$ ,  $F_2$  and  $F_3$  are acting as external forces in the FBD of the leaning trestle. Internal forces that are solved are acting in parts of the structure that are inside the masonry wall where the rot is occurring in the structures.

Free body diagram of the leaning trestle:



Dimensions for the leaning trestle:

$$h_{tot} := 3.245 \text{ m} \quad h_1 := 1.805 \text{ m} \quad h_2 := 1.440 \text{ m} \quad L_{tot} := 14.838 \text{ m} \quad L_1 := 1.370 \text{ m}$$

$$L_2 := 1.093 \text{ m} \quad L_3 := 1.401 \text{ m} \quad L_4 := 7.109 \text{ m} \quad L_5 := 1.401 \text{ m} \quad L_6 := 1.093 \text{ m}$$

$$L_7 := 1.370 \text{ m} \quad L_8 := 9.912 \text{ m} \quad L_9 := 0.18 \text{ m} \quad \alpha_1 := 52.8 \text{ deg} \quad \alpha_2 := 30 \text{ deg}$$

Checking if the FBD is statically indeterminate:

$$\text{Amount of bars:} \quad s := 6$$

$$\text{Amount of hinges:} \quad k := 4$$

$$\text{Amount of support reactions:} \quad t := 3$$

$$n_s := s + t - 2 \cdot k = 1 < 0 \quad \Rightarrow \text{the structure is statically indeterminate.}$$

As the structure is statically indeterminate the FBD should be solved with using for example "force method" if calculated by hand. In order to rationalize the calculation process, it was chosen that the support reactions are calculated by hand but the internal forces are calculated with FEM software Robot Structural Analyses. The support reactions that are received from the FEM programme are compared to those received from the hand calculation in order to verify that the results are correct.

Calculating the support reactions of the leaning trestle. The reaction forces are calculated in parts.

$$A_{v1} := \frac{F_1 \cdot (L_{tot} - L_1 - L_2 - L_9) + F_2 \cdot (L_9 + L_6 + L_7)}{L_{tot}} = 52.93 \text{ kN}$$

$$A_{v2} := \frac{\frac{G_{LT1}}{\cos(\alpha_2)} \cdot \left( (L_2 + L_3) \cdot \left( \frac{L_2 + L_3}{2} + L_4 + L_5 + L_6 + L_7 \right) + (L_5 + L_6) \cdot \left( \frac{L_5 + L_6}{2} + L_7 \right) \right)}{L_{tot}} = 0.91 \text{ kN}$$

$$A_{v3} := \frac{\frac{G_{LT1}}{\cos(\alpha_1)} \cdot \left( (L_1 + L_2) \cdot \left( \frac{L_1 + L_2}{2} + L_{tot} - L_1 - L_2 \right) + \frac{(L_6 + L_7)^2}{2} \right)}{L_{tot}} = 1.29 \text{ kN}$$

$$A_{v4} := \frac{G_{tb1} \cdot \frac{(L_{tot})^2}{2} + G_{LT1} \cdot \left( L_8 \cdot \left( \frac{L_8}{2} + L_6 + L_7 \right) \right)}{L_{tot}} = 4.23 \text{ kN}$$

$$A_{v5} := \frac{F_3 \cdot h_{tot}}{L_{tot}} = 4.54 \text{ kN}$$

The total vertical support reaction in A:

$$A_v := A_{v1} + A_{v2} + A_{v3} + A_{v4} + A_{v5} = 63.9 \text{ kN}$$

Vertical support reaction B in parts:

$$B_{v1} := F_1 + F_2 + \frac{G_{LT1}}{\cos(\alpha_2)} \cdot (L_2 + L_3) \cdot 2 - A_v = 40.04 \text{ kN}$$

$$B_{v2} := G_{tb1} \cdot L_{tot} + G_{LT1} \cdot L_8 + \frac{G_{LT1}}{\cos(\alpha_1)} \cdot (L_1 + L_2) \cdot 2 = 11.04 \text{ kN}$$

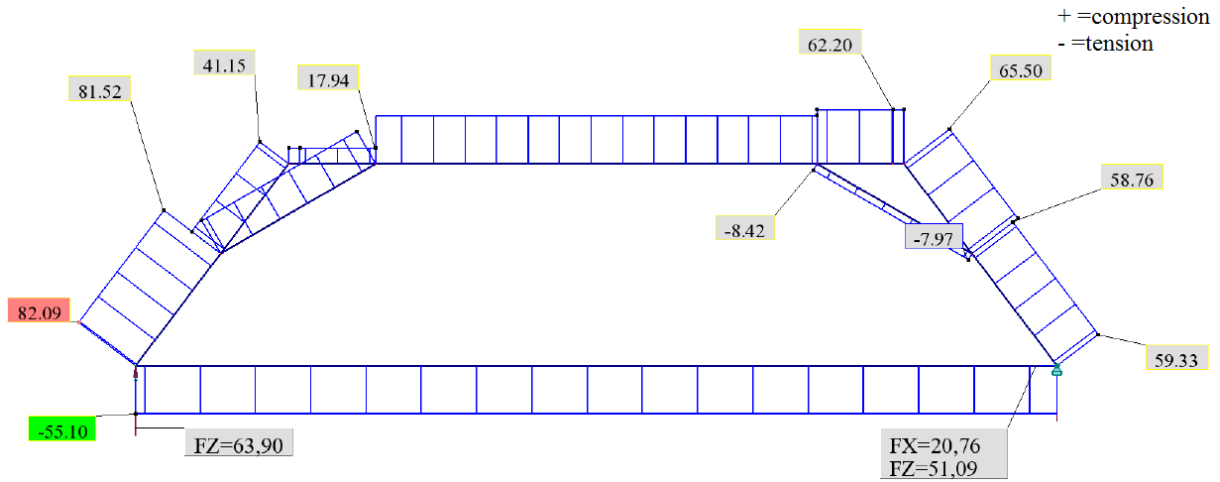
The total vertical support reaction B is:

$$B_v := B_{v1} + B_{v2} = 51.09 \text{ kN}$$

Horizontal support in B:

$$B_h := F_3 = 20.76 \text{ kN}$$

Normal forces and support reactions received from the FBD of the leaning trestle solved with finite element programme:



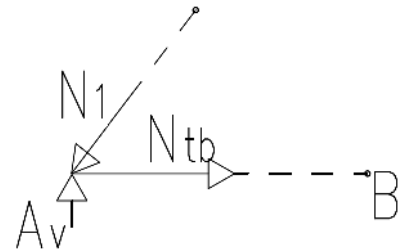
All the support reactions received from the FEM analysis match the ones done with hand calculation. The validity of the model is verified.

Normal force acting in the post of the leaning trestle in downwind face in the connection between the tie beam:

$$N_1 := 82.1 \text{ kN} \quad \textit{compression}$$

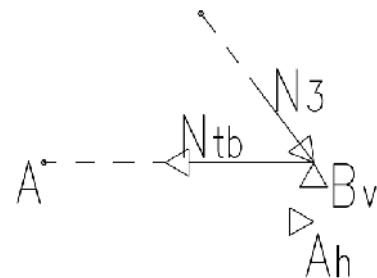
Normal force acting in the tie beam:

$$N_{tb} := 55.1 \text{ kN} \quad \textit{tension}$$



Normal force acting in the post of the leaning trestle in upwind face in the connection between the tie beam:

$$N_3 := 59.3 \text{ kN} \quad \textit{compression}$$

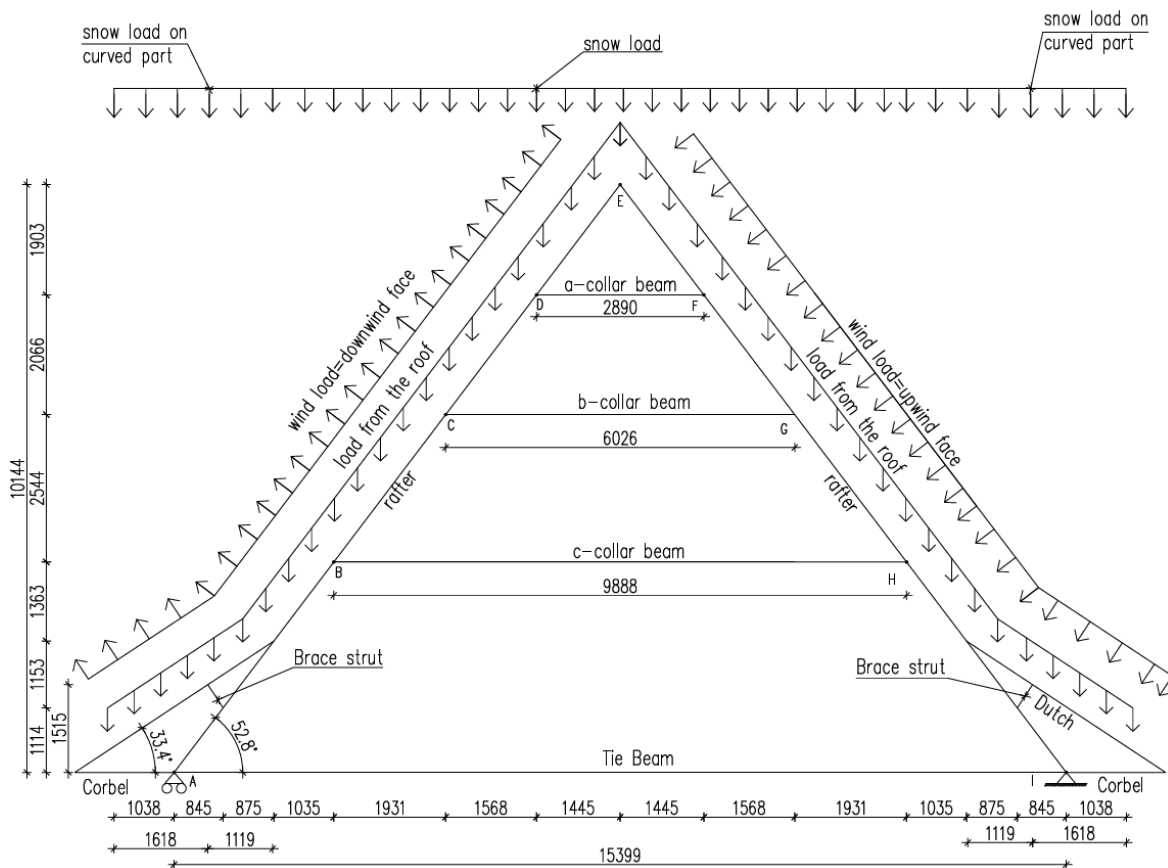


### B.3. The entire rafter frame

If one of the leaning trestles would loose its load bearing capacity the load paths would be reorganized and the loads are distributed to the masonry walls through the rafters as the load bearing capacity of the joists are unable to distribute the loads to the adjacent leaning trestles. In this chapter the normal forces acting in the part of the rafter penetrating into the masonry wall are calculated in a situation where one leaning trestle have lost its load bearing capacity.

The existing rafter frame was simplified and the curved part was changed to be straight with the mean inclination of 33.42 ° as shown in the FBD below. Also the FBD shows that the loads are not applied in the end of the eaves which is because the eaves are shorter in the existing structure but the FBD is a simplified version of the existing structure.

Free body diagram of the rafter frame:



Dimensions:  $L_{tot} := 15399 \text{ mm}$      $L_c := 9888 \text{ mm}$      $L_b := 6026 \text{ mm}$

$L_a := 2890 \text{ mm}$      $L_1 := 845 \text{ mm}$      $L_2 := 875 \text{ mm}$      $L_3 := 1035 \text{ mm}$      $L_4 := 1931 \text{ mm}$

$L_5 := 1568 \text{ mm}$      $L_6 := 1445 \text{ mm}$      $L_{d1} := 1618 \text{ mm}$      $L_{d2} := 1119 \text{ mm}$      $L_{d3} := 1038 \text{ mm}$

$h_{tot} := 10144 \text{ mm}$      $h_1 := 1114 \text{ mm}$      $h_2 := 1153 \text{ mm}$      $h_3 := 1363 \text{ mm}$      $h_6 := 1903 \text{ mm}$

$h_4 := 2544 \text{ mm}$      $h_5 := 2066 \text{ mm}$      $h_d := 1515 \text{ mm}$      $\alpha_1 := 52.8 \text{ deg}$      $\alpha_2 := 33.4 \text{ deg}$



As it can be seen the snow load, wind load and the weight of the roof on the "curved" part close to eaves are partly transferred to the masonry wall through corbels that support the eave structure and partly to the rafters through the brace strut and the connection of the Dutch and the rafter. It was estimated that half of the loads affecting the Dutch in the length of  $L_{d1}$  are subjected to the rafter and other half to the corbel. These uniform loads affecting to the rafter on the "curved" part are transferred as point loads that affect on the rafter frames in the calculation of vertical support reactions. The uplift due to wind loads acting below the eaves is not included in the calculations (mainly the corbels would have to bear these loads). The inner forces of the corbel is not solved in these calculations.

The internal forces are calculated with FEM programme. The FEM model is verified with hand calculated support reactions.

Calculating the support reactions by hand:

Calculating the vertical support reactions A and I and horizontal support reaction I in parts. The weight of the dutch and the brace strut is not taken into account in these calculations. The loads that are applied to the corbel and the weight of the corbel is not included.

$$A_{v1} := \frac{q_{s.d2} \cdot (L_{tot} - L_1 \cdot 2 - L_2 \cdot 2) \cdot \frac{L_{tot}}{2}}{L_{tot}} = 2.77 \text{ kN}$$

$$A_{v2} := \frac{(q_{w.d.GH2} - q_{w.d.IK2}) \cdot \sin(\alpha_1) \cdot \left( \frac{h_{tot} - h_1 - h_2}{\sin(\alpha_1)} \right) \cdot \left( \frac{h_{tot} - h_1 - h_2}{2} + h_1 + h_2 \right)}{L_{tot}} = 2.02 \text{ kN}$$

$$A_{v3} := \frac{q_{w.d.GH2} \cdot \cos(\alpha_1) \cdot \left( \frac{\frac{L_{tot}}{2} - L_1 - L_2}{\cos(\alpha_1)} \right) \cdot \left( \frac{\frac{L_{tot}}{2} - L_1 - L_2}{2} + L_1 + L_2 \right)}{L_{tot}} = 0.82 \text{ kN}$$

$$A_{v4} := \frac{q_{w.d.IK2} \cdot \cos(\alpha_1) \cdot \left( \frac{\frac{L_{tot}}{2} - L_1 - L_2}{\cos(\alpha_1)} \right) \cdot \left( \frac{L_{tot}}{2} + \frac{\frac{L_{tot}}{2} - L_1 - L_2}{2} \right)}{L_{tot}} = -0.79 \text{ kN}$$

$$A_{v5} := \frac{\frac{G_{rafter1}}{\cos(\alpha_1)} \cdot \frac{L_{tot}^2}{2} + G_{c.collar.beam1} \cdot L_c \cdot \frac{L_{tot}}{2} + G_{tb1} \cdot \frac{L_{tot}^2}{2}}{L_{tot}} = 5.91 \text{ kN}$$

$$A_{v6} := \frac{\frac{g_{k.R.d1}}{\cos(\alpha_1)} \cdot (L_c + L_3 \cdot 2) \cdot \frac{L_{tot}}{2}}{L_{tot}} = 4.71 \text{ kN}$$

$$A_{v7} := \frac{G_{b.collar.beam1} \cdot L_b \cdot \left( \frac{L_{tot}}{2} \right) + G_{a.collar.beam1} \cdot L_a \cdot \frac{L_{tot}}{2}}{L_{tot}} = 0.66 \text{ kN}$$

$$A_{v8} := \frac{\left( \frac{g_{k.R.d1} \cdot \frac{L_{d1}}{\cos(\alpha_2)}}{2} + \frac{g_{k.R.d1} \cdot \frac{L_{d2}}{\cos(\alpha_2)}}{2} \right) \cdot (L_{d1} - L_{d3})}{L_{tot}} = 0.03 \text{ kN}$$

$$A_{v9} := \frac{\left( \frac{g_{k.R.d1} \cdot \frac{L_{d1}}{\cos(\alpha_2)}}{2} + \frac{g_{k.R.d1} \cdot \frac{L_{d2}}{\cos(\alpha_2)}}{2} \right) \cdot (L_{tot} - (L_{d1} - L_{d3}))}{L_{tot}} = 0.75 \text{ kN}$$

$$A_{v10} := \frac{\frac{g_{k.R.d1} \cdot \frac{L_{d2}}{\cos(\alpha_2)}}{2} \cdot (L_1 + L_2)}{L_{tot}} + \frac{\frac{g_{k.R.d1} \cdot \frac{L_{d2}}{\cos(\alpha_2)}}{2} \cdot (L_{tot} - L_1 - L_2)}{L_{tot}} = 0.32 \text{ kN}$$

$$A_{v11} := \frac{\frac{L_{d2} \cdot q_{s.d2.1}}{2} \cdot (L_1 + L_2) + \frac{L_{d2} \cdot q_{s.d2.1}}{2} \cdot (L_{tot} - L_1 - L_2)}{L_{tot}} = 1 \text{ kN}$$

$$A_{v12} := \frac{\left( \frac{L_{d1} \cdot q_{s.d2.1}}{2} + \frac{L_{d2} \cdot q_{s.d2.1}}{2} \right) \cdot (L_{d1} - L_{d3})}{L_{tot}} = 0.09 \text{ kN}$$

$$A_{v13} := \frac{\left( \frac{L_{d1} \cdot q_{s.d2.1}}{2} + \frac{L_{d2} \cdot q_{s.d2.1}}{2} \right) \cdot (L_{tot} - (L_{d1} - L_{d3}))}{L_{tot}} = 2.36 \text{ kN}$$

$$A_{v14} := \frac{\frac{q_{w.d.GH2} \cdot \frac{L_{d2}}{\cos(\alpha_2)}}{2} \cdot \cos(\alpha_2) \cdot (L_1 + L_2)}{L_{tot}} = 0.03 \text{ kN}$$

$$A_{v15} := \frac{\left( \frac{q_{w.d.GH2} \cdot \frac{L_{d1}}{\cos(\alpha_2)}}{2} + \frac{q_{w.d.GH2} \cdot \frac{L_{d2}}{\cos(\alpha_2)}}{2} \right) \cdot \cos(\alpha_2) \cdot (L_1 + L_2 - L_{d2})}{L_{tot}} = 0.02 \text{ kN}$$

$$A_{v16} := \frac{\frac{q_{w.d.IK2} \cdot \frac{L_{d2}}{\cos(\alpha_2)}}{2} \cdot \cos(\alpha_2) \cdot (L_{tot} - L_1 - L_2)}{L_{tot}} = -0.1 \text{ kN}$$

$$A_{v17} := \frac{\left( \frac{q_{w.d.IK2} \cdot \frac{L_{d1}}{\cos(\alpha_2)}}{2} + \frac{q_{w.d.IK2} \cdot \frac{L_{d2}}{\cos(\alpha_2)}}{2} \right) \cdot \cos(\alpha_2) \cdot (L_{tot} - L_1 - L_2 + L_{d2})}{L_{tot}} = -0.25 \text{ kN}$$

$$A_{v18} := \frac{\left( \frac{q_{w.d.GH2} \cdot \frac{L_{d2}}{\cos(\alpha_2)}}{2} - \frac{q_{w.d.IK2} \cdot \frac{L_{d2}}{\cos(\alpha_2)}}{2} \right) \cdot \sin(\alpha_2) \cdot (h_1 + h_2)}{L_{tot}} = 0.03 \text{ kN}$$

$$A_{v19} := \frac{\left( \frac{q_{w.d.GH2} \cdot \frac{L_{d1}}{\cos(\alpha_2)}}{2} + \frac{q_{w.d.GH2} \cdot \frac{L_{d2}}{\cos(\alpha_2)}}{2} \right) \cdot \sin(\alpha_2) \cdot h_d}{L_{tot}} = 0.04 \text{ kN}$$

$$A_{v20} := \frac{\left( \frac{q_{w.d.IK2} \cdot \frac{L_{d1}}{\cos(\alpha_2)}}{2} + \frac{q_{w.d.IK2} \cdot \frac{L_{d2}}{\cos(\alpha_2)}}{2} \right) \cdot \sin(\alpha_2) \cdot h_d}{L_{tot}} = 0.02 \text{ kN}$$

$$A_{v111} := A_{v1} + A_{v2} + A_{v3} + A_{v4} + A_{v5} + A_{v6} + A_{v7} + A_{v8} + A_{v9} + A_{v10} = 17.19 \text{ kN}$$

$$A_{v222} := A_{v11} + A_{v12} + A_{v13} + A_{v14} + A_{v15} + A_{v16} + A_{v17} + A_{v18} + A_{v19} + A_{v20} = 3.24 \text{ kN}$$

$$\text{Total vertical support reaction in support A: } \rightarrow A_v := A_{v111} + A_{v222} = 20.44 \text{ kN}$$

Vertical support in I:

$$I_{v1} := q_{w.d.GH2} \cdot \cos(\alpha_1) \cdot \left( \frac{L_{tot}}{2} - L_1 - L_2 \right) + q_{w.d.IK2} \cdot \cos(\alpha_1) \cdot \left( \frac{L_{tot}}{2} - L_1 - L_2 \right) = 1.53 \text{ kN}$$

$$I_{v2} := \frac{G_{rafter1}}{\cos(\alpha_1)} \cdot L_{tot} + G_{c.collar.beam1} \cdot L_c + \frac{g_{k.R.d1}}{\cos(\alpha_1)} \cdot (L_c + L_3 \cdot 2) = 15.7 \text{ kN}$$

$$I_{v3} := G_{b.collar.beam1} \cdot L_b + G_{a.collar.beam1} \cdot L_a + \frac{g_{k.R.d1} \cdot \frac{L_{d1}}{\cos(\alpha_2)}}{2} \cdot 2 + g_{k.R.d1} \cdot \frac{L_{d2}}{\cos(\alpha_2)} \cdot 2 = 3.51 \text{ kN}$$

$$I_{v4} := \left( L_{d2} + \frac{L_{d1}}{2} \right) \cdot q_{s.d2.1} \cdot 2 + G_{tb1} \cdot L_{tot} = 12.43 \text{ kN}$$

$$I_{v5} := \frac{q_{w.d.IK2} \cdot \frac{L_{d2}}{\cos(\alpha_2)}}{2} \cdot \cos(\alpha_2) = -0.11 \text{ kN}$$

$$I_{v6} := \left( \frac{q_{w.d.IK2} \cdot \frac{L_{d1}}{\cos(\alpha_2)}}{2} + \frac{q_{w.d.IK2} \cdot \frac{L_{d2}}{\cos(\alpha_2)}}{2} \right) \cdot \cos(\alpha_2) = -0.26 \text{ kN}$$

$$I_{v7} := \frac{q_{w.d.GH2} \cdot \frac{L_{d2}}{\cos(\alpha_2)}}{2} \cdot \cos(\alpha_2) = 0.25 \text{ kN}$$

$$I_{v8} := \left( \frac{q_{w.d.GH2} \cdot \frac{L_{d1}}{\cos(\alpha_2)}}{2} + \frac{q_{w.d.GH2} \cdot \frac{L_{d2}}{\cos(\alpha_2)}}{2} \right) \cdot \cos(\alpha_2) = 0.61 \text{ kN}$$

$$I_{v9} := q_{s.d2} \cdot (L_{tot} - L_1 \cdot 2 - L_2 \cdot 2) = 5.55 \text{ kN}$$

Total vertical support in I:

$$I_v := I_{v1} + I_{v2} + I_{v3} + I_{v4} + I_{v5} + I_{v6} + I_{v7} + I_{v8} + I_{v9} - A_v = 18.77 \text{ kN}$$

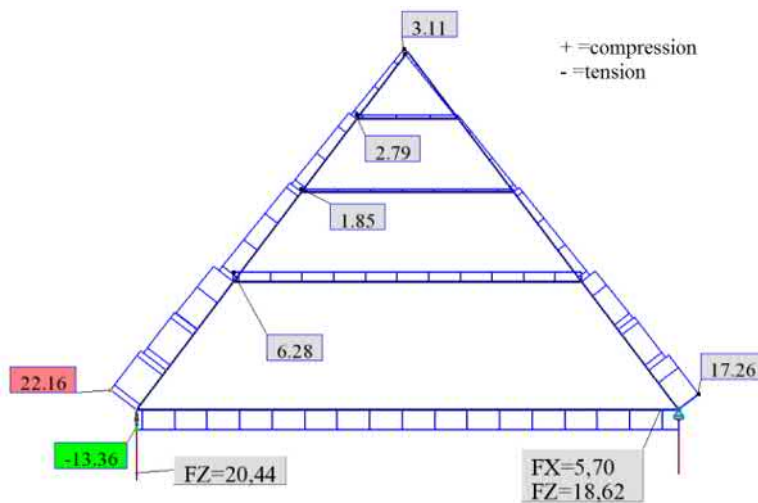
Horizontal support I in parts:

$$I_{h1} := (q_{w.d.GH2} \cdot \cos(\alpha_2) - q_{w.d.IK2} \cdot \cos(\alpha_2)) \cdot \left( \frac{(h_1 + h_2) - \frac{\tan(\alpha_2) \cdot (L_{d1})}{2}}{\sin(\alpha_2)} \right) = 1.68 \text{ kN}$$

$$I_{h2} := (q_{w.d.GH2} \cdot \cos(\alpha_1) - q_{w.d.IK2} \cdot \cos(\alpha_1)) \cdot \left( \frac{h_{tot} - h_1 - h_2}{\sin(\alpha_1)} \right) = 3.81 \text{ kN}$$

$$I_h := I_{h1} + I_{h2} = 5.49 \text{ kN}$$

Normal forces and support reactions received from the FBD of the rafter frame with finite element model:



Verifying the support reactions:

Downwind face:

$$\text{Vertical support reaction: } FZ := A_v = 20.44 \text{ kN} \quad \Rightarrow \text{OK!}$$

Upwind face:

$$\text{Vertical support: } FZ := 18.62 \quad I_v = 18.77 \text{ kN} \quad \Rightarrow \text{Small difference. OK!}$$

$$\text{Horizontal support: } FX := 5.7 \text{ kN} \quad I_h = 5.49 \text{ kN} \quad \Rightarrow \text{Small difference. OK!}$$

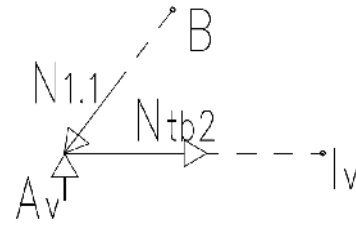
Although all of the support reactions were not identical when comparing the FEM model and hand calculations the difference was so small that the FEM model is reliable.

Internal force in the rafter at downwind face:

$$N_{1.1} := 22.2 \text{ kN} \quad (\text{compression})$$

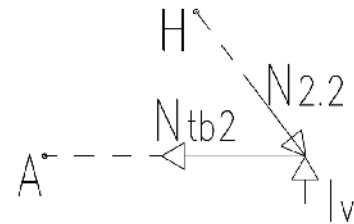
Tension force in the tie beam:

$$N_{tb2} := 13.4 \text{ kN} \quad (\text{tension})$$



Internal force in the rafter at upwind face:

$$N_{2.2} := 17.3 \text{ kN} \quad (\text{compression})$$



## C. Structural capacity

In this chapter the structural capacity of the existing structural members penetrating into the masonry wall are analysed in ULS with the existing design guidelines. The type of connections between timber members inside the masonry wall are not known. Due to this only the capacity of the cross sections inside the masonry wall are analysed.

### C.1. Material properties

Instantaneous wind load is acting >  $k_{mod} := 1.1$  (RIL 205-1-2017, table 3.1)

Lumber >  $\gamma_m := 1.3$  (RIL 205-1-2017, table 2.12)

### C.2. Design values

Strength of structural members in the existing roof structures are C24 based on the rough estimation according to the SFS 5878 insta 142. SFS 5878 is used to evaluate the strength class of new timber members. The structural capacity of the existing timber members is evaluated as if they would be new. This is because load history or other characteristics that might have been altered during time in timber members are not included.

Compression strength parallel to grain: (EN 338, table 1)

$$f_{c.0.k} := 21 \text{ MPa} \quad f_{c.0.d} := \frac{f_{c.0.k}}{\gamma_m} \cdot k_{mod} = 17.77 \text{ MPa}$$

Compression strength perpendicular to grain:

$$f_{c.90.k} := 2.5 \text{ MPa} \quad f_{c.90.d} := \frac{f_{c.90.k}}{\gamma_m} \cdot k_{mod} = 2.12 \text{ MPa}$$

Tension strength parallel to grain:

$$f_{t.0.k} := 14.5 \text{ MPa} \quad f_{t.0.d} := \frac{f_{t.0.k}}{\gamma_m} \cdot k_{mod} = 12.27 \text{ MPa}$$

### C.3. Calculating the required dimensions of the leaning trestle

Minimum cross section for the post and tie beam of the leaning trestle in ULS are calculated with the calculated normal forces:



**Tie beam:**

Dimensions of the cross section:  $b := 250 \text{ mm}$        $h := 250 \text{ mm}$

## 1. Tension parallel to grain:

Utility rate: 
$$\frac{N_{tb}}{f_{t.0.d} \cdot b \cdot h} = 0.07 \quad \Rightarrow 7\%$$

Required  $h_{min}$  when  $b := 220 \text{ mm}$  is: 
$$h_{min} := \frac{N_{tb}}{f_{t.0.d} \cdot b} = 20.41 \text{ mm}$$

Required cross section for the tie beam: 
$$A_{req} := b \cdot h_{min} = 44.91 \text{ cm}^2$$

**Post:**

Dimensions of the cross section:  $b := 220 \text{ mm}$        $h := 250 \text{ mm}$

## 1. Compression parallel to grain:

Utility rate: 
$$\frac{N_1}{f_{c.0.d} \cdot b \cdot h} = 0.08 \quad \Rightarrow 8\%$$

Required  $h_{min}$  when  $b := 220 \text{ mm}$  is: 
$$h_{min} := \frac{N_1}{f_{c.0.d} \cdot b} = 21 \text{ mm}$$

Required cross section area for the tie beam: 
$$A_{req} := b \cdot h_{min} = 46.2 \text{ cm}^2$$

2. Compression on an angle to grain in the connection (RIL 205-1-2017, 6.2.2)  
between the tie beam and the post inside the masonry wall:

$k_{c.90} := 1$  (RIL 205-1-2017, 6.15)

Utility rate: 
$$\frac{\frac{N_1}{b \cdot h}}{\frac{f_{c.0.d}}{\frac{f_{c.0.d}}{k_{c.90} \cdot f_{c.90.d}} \cdot \sin(\alpha_1) + \cos(\alpha_1)}} = 0.61 \quad \Rightarrow 61\%$$

Required  $h_{min}$  when  
 $b := 220 \text{ mm}$ : 
$$h_{min} := \frac{N_1}{\frac{f_{c.0.d}}{\frac{f_{c.0.d}}{k_{c.90} \cdot f_{c.90.d}} \cdot \sin(\alpha_1) + \cos(\alpha_1)} \cdot b} = 153.22 \text{ mm}$$

-> The utility rate for the post of the leaning trestle is 61% and the required cross section dimension h would be 154 mm when b is 220 mm.

## C.4. Rafter frame

Same design values are used with rafters as were used with the leaning trestle when performance of the rafter inside the masonry wall is calculated:

Dimensions of rafter:  $b := 170 \text{ mm}$   $h := 170 \text{ mm}$

### 1. Compression parallel to grain

$$\text{Utility rate: } \frac{N_{1.1}}{\frac{b \cdot h}{f_{c.0.d}}} = 0.04 \quad \Rightarrow 4\%$$

$$\text{Required } h_{min} \text{ when } b := 170 \text{ mm is: } h_{min} := \frac{N_{1.1}}{f_{c.0.d} \cdot b} = 7.35 \text{ mm}$$

### 2. Compression on an angle to grain in the connection (RIL 205-1-2017, 6.2.2) between the tie beam and the post inside the masonry wall:

$$k_{c.90} := 1 \quad (\text{RIL 205-1-2017, 6.15})$$

$$\text{Utility rate: } \frac{\frac{N_{1.1}}{b \cdot h}}{\frac{f_{c.0.d}}{k_{c.90} \cdot f_{c.90.d}} \cdot \sin(\alpha_1) + \cos(\alpha_1)} = 0.32 \quad \Rightarrow 32\%$$

$$\text{Required } h_{min} \text{ when } b := 170 \text{ mm: } h_{min} := \frac{N_{1.1}}{\frac{f_{c.0.d}}{k_{c.90} \cdot f_{c.90.d}} \cdot \sin(\alpha_1) + \cos(\alpha_1)} \cdot b = 53.62 \text{ mm}$$

-> The utility rate for the rafter is 32% and the required cross section dimension h would be 54 mm when b is 170 mm.

Appendix B.

Mikko Nurkka

**Rot Report on Louhisaari Manor's Roof Structures**

## Table of contents

Table of contents.....	2
1 Introduction.....	3
2 Materials and methods .....	3
2.1 Visual inspection.....	3
2.2 Resistance drillings .....	3
3 Results.....	4
3.1 Rotten timber members .....	4
3.2 Mapping of rotten timber members.....	5
3.3 Condition of timber members .....	9
3.4 Resistance drilling diagrams .....	11
3.4.1 Tie beam ends in the southwest side.....	11
3.4.2 Tie beams ends in the northeast side .....	26
3.4.3 Posts of the leaning trestles.....	34

## 1 Introduction

This report is based on the visual inspection that was performed in the Louhisaari manor in the 15 of March 2019 and resistance drillings that were performed in the 30 of March in 2019.

## 2 Materials and methods

### 2.1 Visual inspection

The visual inspection was performed in the third floor and in the attic of Louhisaari manor. Primarily the timber members that are penetrating to the masonry wall were investigated (tie beams, rafters and posts). Assisting instruments such as hammer and knife were used during the visual inspections in the attic if necessary. Knife was used to verify the stage of decay and hammer to discover hidden rot with tapping method.

### 2.2 Resistance drillings

The resistance drillings were performed in the 30<sup>th</sup> of March 2019 by arborist Teppo Suoranta with Resistograph (IML RESI PD400) which has a maximum drilling depth of 40 cm. The diameter of the drilling needle is 3 mm and the shaft is 1.5 mm. The drillings were performed approximately in an angle of 45° in relation to perpendicular to the timber member with approximately +/-10° error margin. Figure 1 shows the basic principle how the resistance drilling was performed on the tie beam.

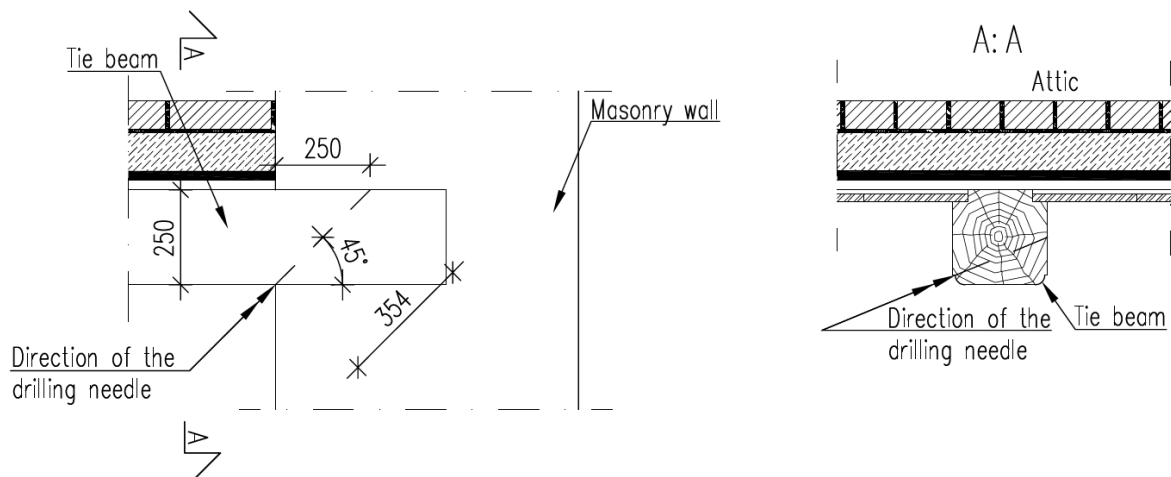


Figure 1. Schematic drawing how the resistance drilling was performed to the tie beams in the third floor. The rafter and the post connect to the tie beam inside the masonry wall even though it is not presented in this figure.

The penetration depth depends on number of issues that have to be taken into account. For eg. the drill bit is automatically pulled back if it meets timber with significantly high or low resistance. This kind of high resistance can be for eg. a knot and low resistance for eg. extremely rotten wood. In addition, the Resistographs timber contacting surface has a detector that has to be pressed inward during the drilling or the drill bit will be automatically pulled back. Sometimes this detector was released due to the challenging position in which the drilling was performed. When one of these errors occurred during the drilling the structural member was redrilled to achieve proper results.

The small diameter of the Resistographs drilling shaft (1.5 mm) makes it flexible and due to this it is possible that the drilling needle starts to follow possible cracks inside the timber and would falsely show decreased density of the timber. High propagation speed of the drill and blunt drill bit can cause this effect to take place. A propagation speed of 100 cm/min was used and the drill bit was changed if it was damaged to prevent this unwanted event from occurring. This potential error was also evaluated during the resistance drillings and if doubt arised the drilling was performed again to verify the results received from the drilling. However, it was found after the results were received from the drillings that a couple of the results were not as explicit as was intended.

The used rotation speed was 2500 rpm which is suitable for this kind of work according to the experience of Teppo Suoranta. If the rotation speed would be too high it would affect on the direction of the drill bit when it would enter into a crack. It causes the drill bit to bounce when it dashes into solid wood after going through a crack.

53 tie beams were drilled in the third floor. Tie beams that are located in the banqueting hall with original paintings were excluded from the drillings. 16 out of 20 posts were drilled from the attic. One post (PI) from the southwest and three posts (PI-PIII) from the northeast side were left undrilled.

### 3 Results

#### 3.1 Rotten timber members

Only one rotten timber member was found during the visual inspection from the third floor which was located in the storage room in the stairway to the attic. Visual rot was not found from any of the tie beams that are painted. The timber members in the attic are rotten mainly on the prats that penetrate into the masonry. Only one timber member was found rotten from the higher parsts of the roof. Examples of highly rotten timber members penetrating into the masonry wall in the attic are shown in the figures 2, 3, 4 and 5.



Figure 2. Left: post of the leaning trestle (VIII), rafter (S4), cross bracing and the diagonal timber member that reaches to the top of the gable. Structural opening has been made on the right side of the post. Right: showing the stage of decay more detailed.





Figure 3. Rotten rafter S18 penetrating to the masonry wall.



Figure 4. Left: rotten rafter S26 penetrating to the masonry wall. Right: rotten rafter S29 penetrating to the masonry wall.



Figure 5. Left: post of the leaning trestle (PIIIII), rafter (S41), cross bracing and the diagonal timber member that reaches to the top of the gable. Right: showing the stage of decay more detailed. Rafter has lost its entire cross section.

### 3.2 Mapping of rotten timber members

Figure 6 shows the mapping of rotten rafters and posts in the attic near the floor level based on the visual inspections. Figure 7 shows the condition of posts according the resistance drillings. Figure 8 shows the condition of tie beams in the third floor according the resistance drillings.

PI-PIIIII, VI-VIII, VO-VOOOO = Leaning trestle  
 S = Rafter  
 (LT) = Rafter which is in the same line with the leaning trestle  
 Circle = Structural opening

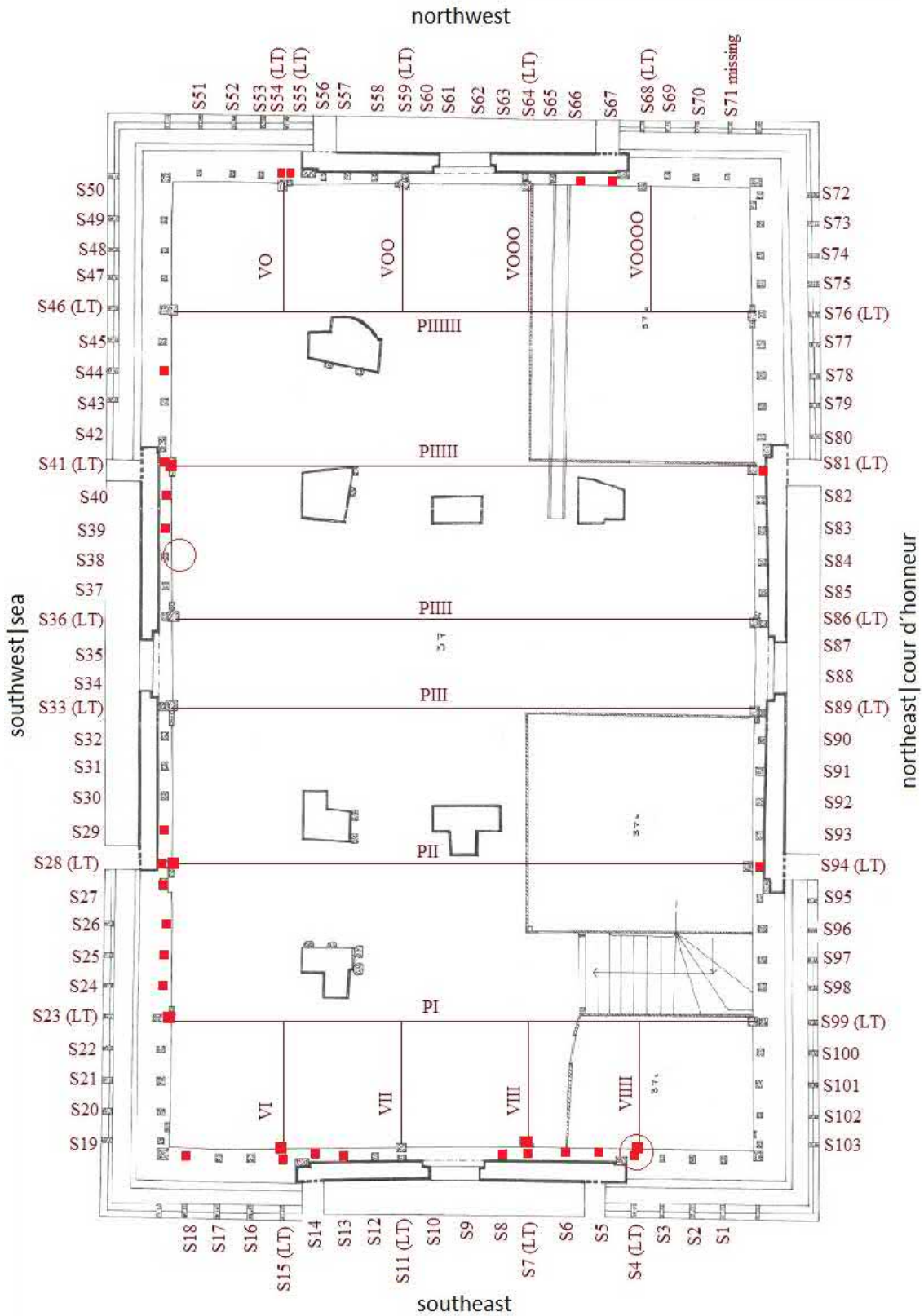


Figure 6. The mapping of rotten timber members (rafters and posts) in the attic near the floor level based on the visual inspection. Rotten members are shown in the figure with red markings.





Axx-xx L=tie beam end on the southwest side  
 Axx-xx K=tie beam end on the northwest side

- =rot/extremely soft wood
- =decreased density or small amount of rot
- =not investigated
- =no defects

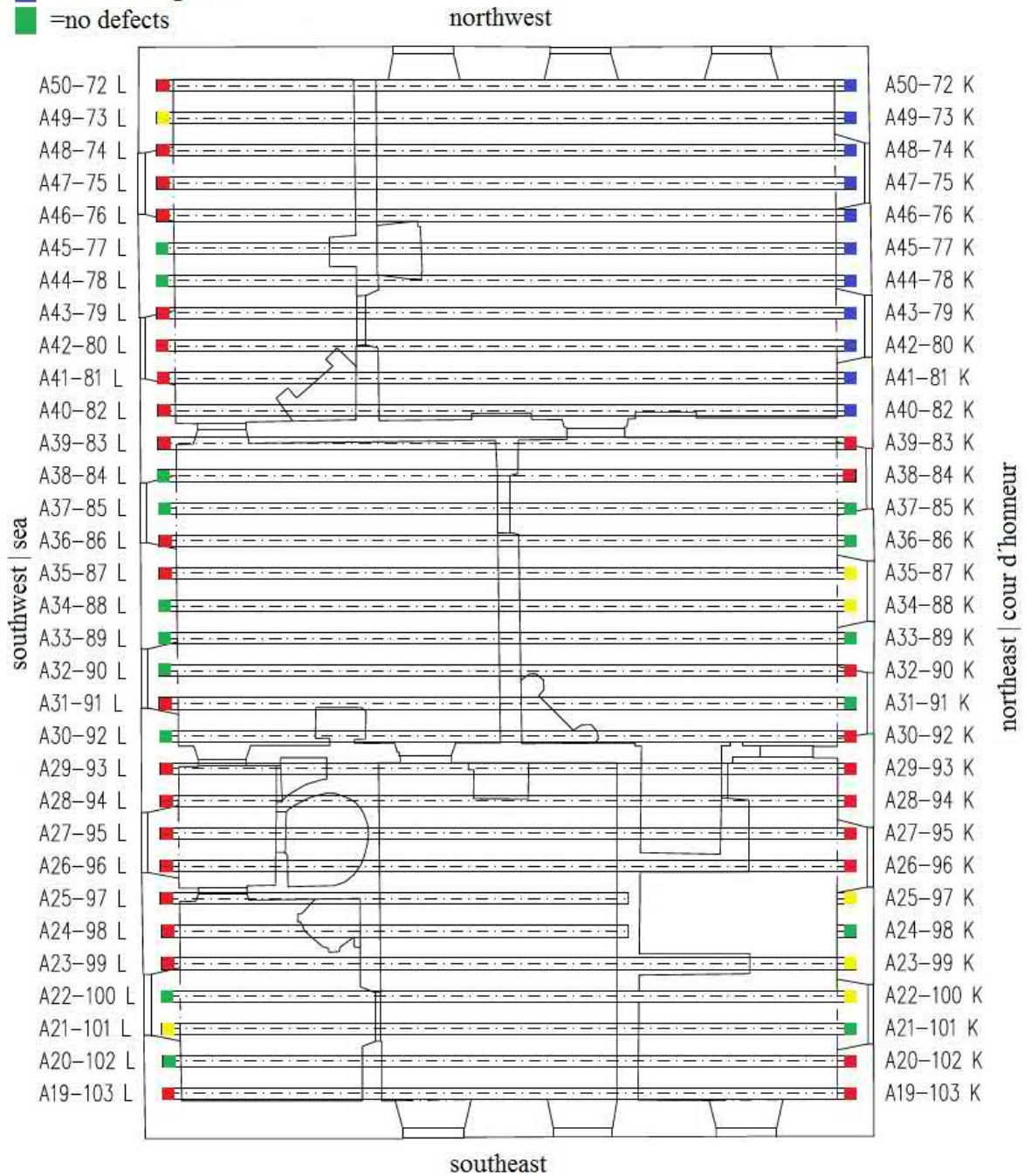


Figure 8. Condition of the tie beam ends in the third floor according the resistance drillings.

### 3.3 Condition of timber members

The condition of timber members that were investigated during the visual inspection and resistance drillings are shown in the tables below.



Table 1. The condition of posts according the resistance drillings and visual inspection on the left side of the table. The condition of rafters on the shorter side of the roof according to the visual inspection on the right side of the table.

	=extremely soft/rotten
	=decreased density/small amount of rot
X	=cut above the masonry
-	=not investigated

Post	Resistance drilling	Visual inspection
	Condition (Figure 7)	Condition (Figure 6)
VI		
VII		
VIII		
VIII		
PI-sw	-	
PII-sw		
PIII-sw		
PIII-sw		
PIII-sw		
PIII-sw		
VO		
VOO		
VOOO		
VOOOO		
PI-ne	-	-
PII-ne	-	
PIII-ne	-	
PIII-ne		
PIII-ne		
PIII-ne		
PIII-ne		

Visual inspection			
Rafter	Condition (Figure 6)	Rafter	Condition (Figure 6)
S1		S51	
S2		S52	
S3		S53	
S4		S54	
S5		S55	
S6		S56	
S7		S57	
S8		S58	X
S9	X	S59	
S10	X	S60	X
S11		S61	X
S12		S62	X
S13		S63	X
S14		S64	
S15		S65	
S16		S66	
S17		S67	
S18		S68	
		S69	
		S70	
		S71	Missing

Table 2. The condition of tie beams according the resistance drillings and corresponding rafters according to the visual inspection. Southwest side on the left and northeast side on the right.

	=extremely soft/rotten
	=decreased density/small amount of rot
X	=cut above the masonry
-	=not investigated

Resistance drilling		Visual inspection/tapping	
Tie beam end	Condition (Figure 9)	Rafter	Condition (Figure 6)
A19-103 L		S19	
A20-102 L		S20	
A21-101 L		S21	
A22-100 L		S22	
A23-99 L		S23	
A24-98 L		S24	
A25-97 L		S25	
A26-96 L		S26	
A27-95 L		S27	
A28-94 L		S28	
A29-93 L		S29	
A30-92 L		S30	
A31-91 L		S31	
A32-90 L		S32	
A33-89 L		S33	
A34-88 L		S34	X
A35-87 L		S35	X
A36-86 L		S36	
A37-85 L		S37	
A38-84 L		S38	
A39-83 L		S39	
A40-82 L		S40	
A41-81 L		S41	
A42-70 L		S42	X
A43-79 L		S43	
A44-78 L		S44	
A45-77 L		S45	
A46-76 L		S46	
A47-75 L		S47	
A48-74 L		S48	
A49-73 L		S49	
A50-72 L		S50	

Resistance drilling		Visual inspection	
Tie beam end	Condition (Figure 9)	Rafter	Condition (Figure 6)
A39-83 K		S83	
A38-84 K		S84	
A37-85 K		S85	
A36-86 K		S86	
A35-87 K		S87	X
A34-88 K		S88	X
A33-89 K		S89	
A32-90 K		S90	
A31-91 K		S91	
A30-92 K		S92	
A29-93 K		S93	
A28-94 K		S94	
A27-95 K		S95	
A26-96 K		S96	
A25-97 K		S97	
A24-98 K		S98	-
A23-99 K		S99	-
A22-100 K		S100	
A21-101 K		S101	
A20-102 K		S102	
A19-103 K		S103	
		S72	
		S73	
		S74	
		S75	
		S76	
		S77	
		S78	
		S79	
		S80	
		S81	
		S82	

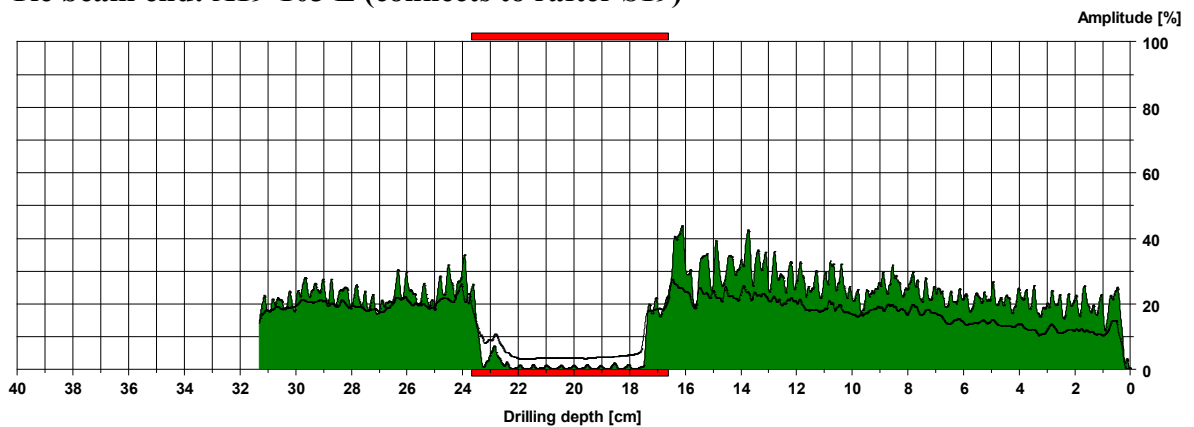
### 3.4 Resistance drilling diagrams

The drillings have been analysed by the arborist Teppo Suoranta. The markings in the diagrams stand for:

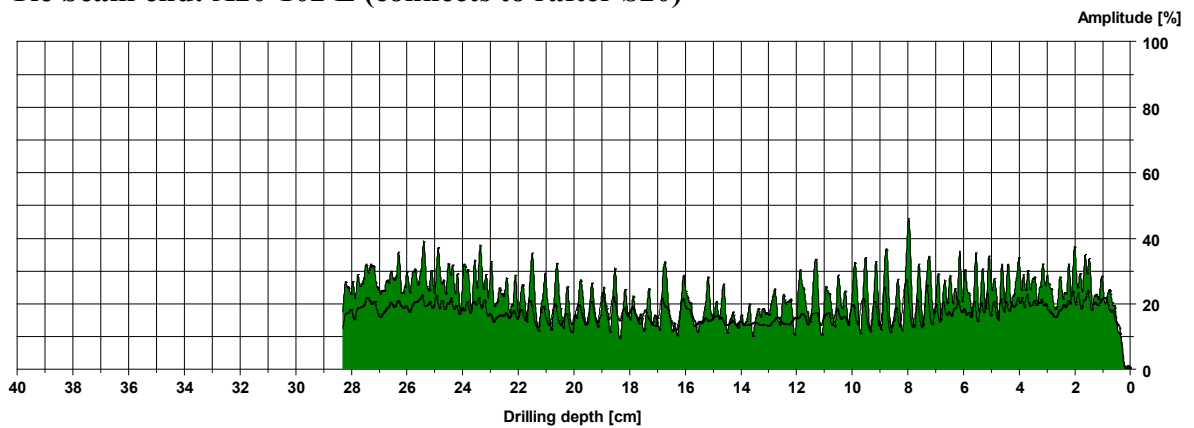
1. Red=extremely soft/rotten wood
2. Yellow=decreased density/small amount of rot
3. Blue=Hard wood
4. Good or normal quality of wood is not marked

#### 3.4.1 Tie beam ends in the southwest side

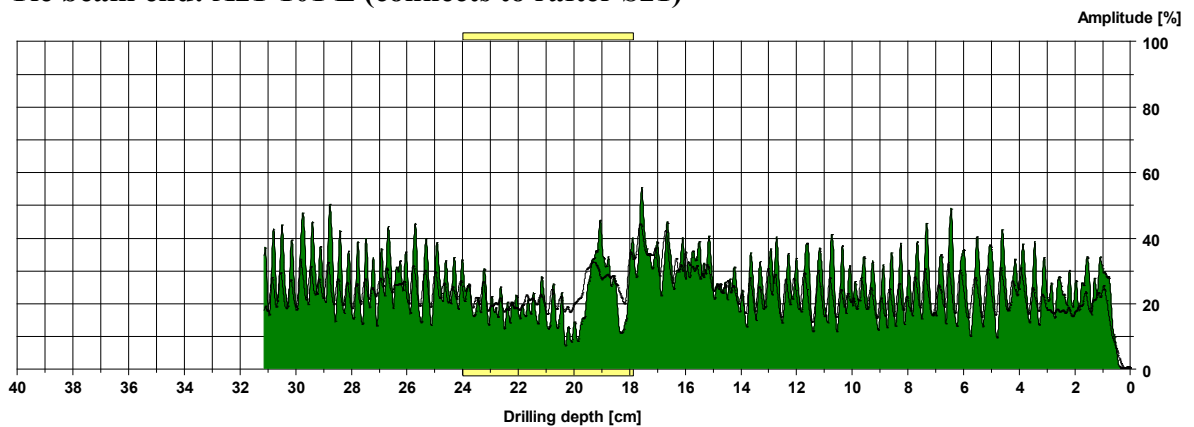
Tie beam end: A19-103 L (connects to rafter S19)



Tie beam end: A20-102 L (connects to rafter S20)

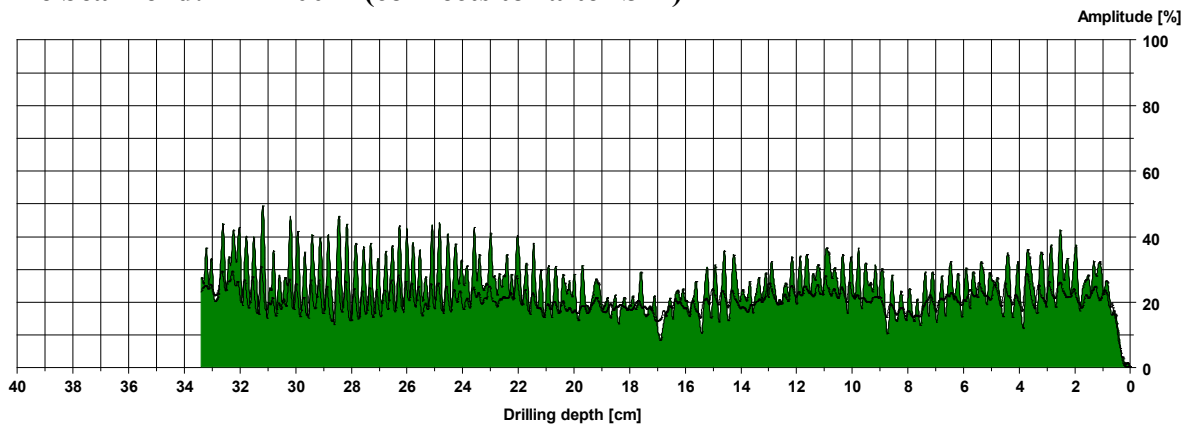


Tie beam end: A21-101 L (connects to rafter S21)

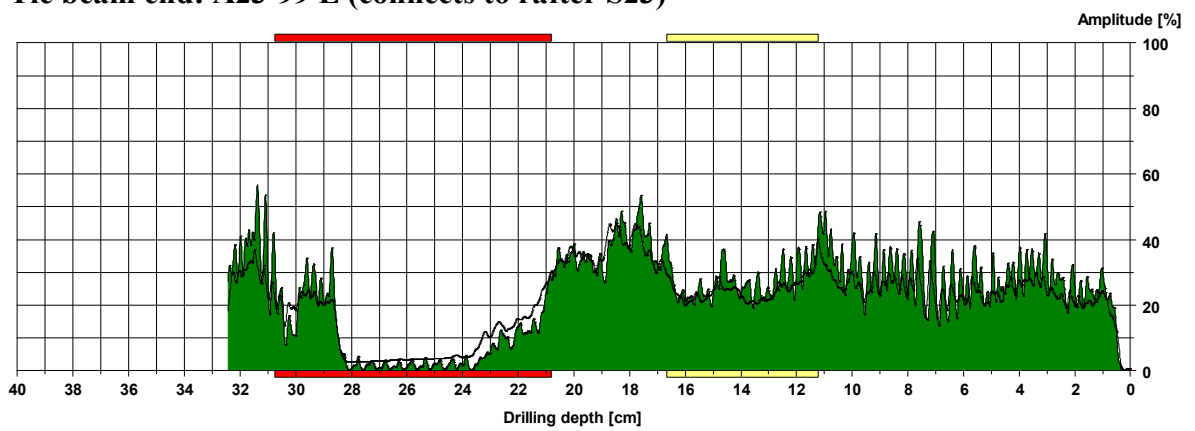




**Tie beam end: A22-100 L (connects to rafter S22)**

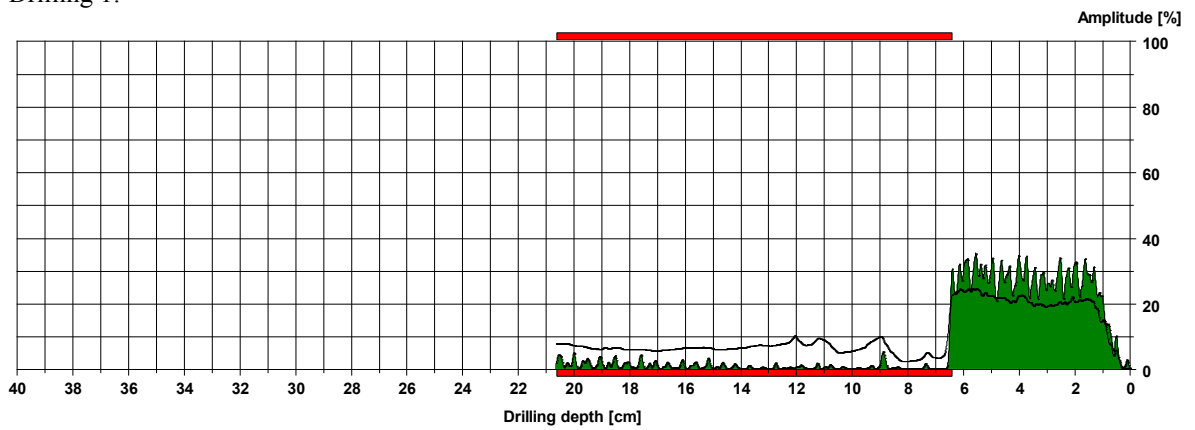


**Tie beam end: A23-99 L (connects to rafter S23)**

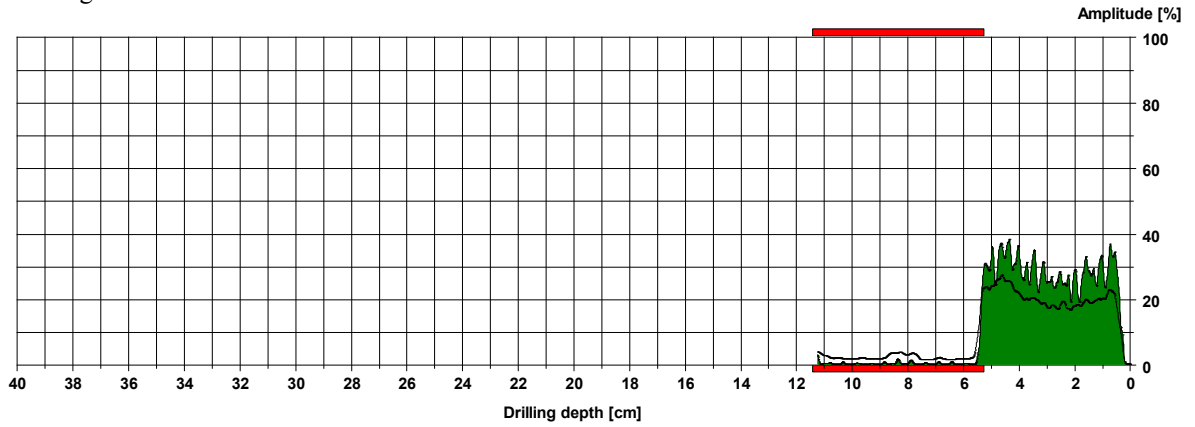


**Tie beam end: A24-98 L (connects to rafter S24)**

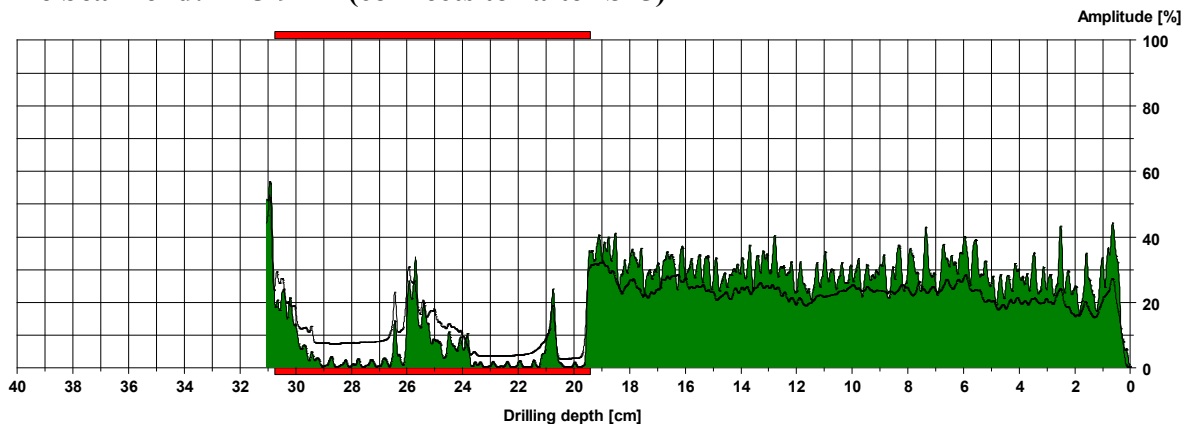
Drilling 1:



Drilling 2:

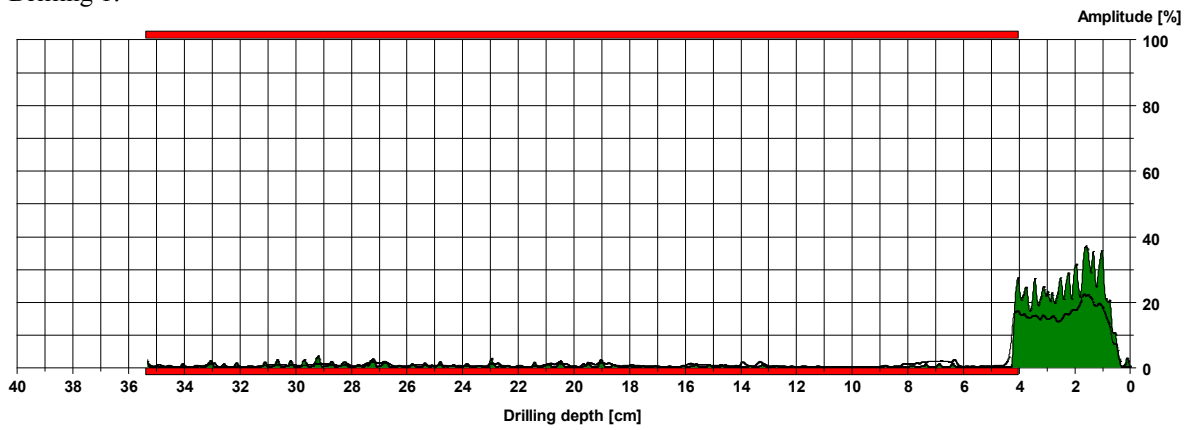


Tie beam end: A25-97 L (connects to rafter S25)

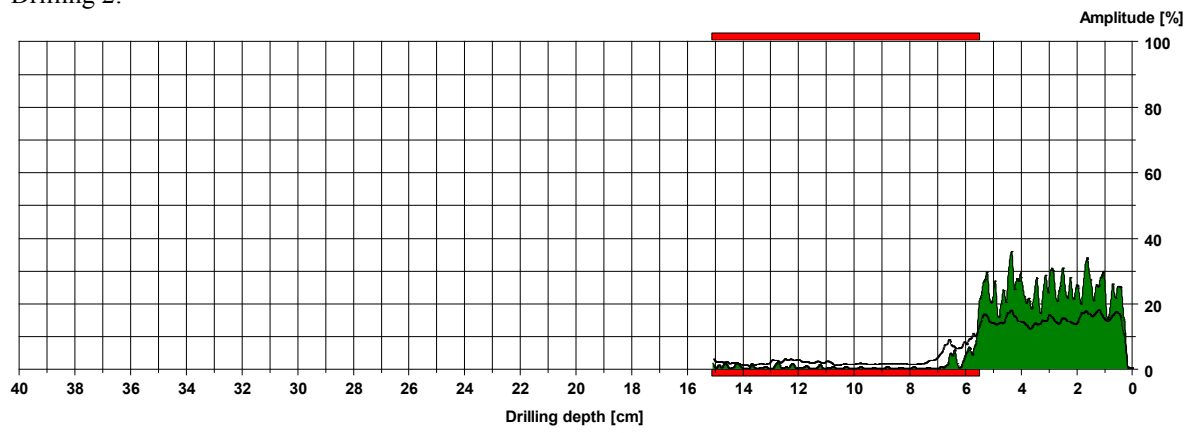


Tie beam end: A26-96 L (connects to rafter S26)

Drilling 1:

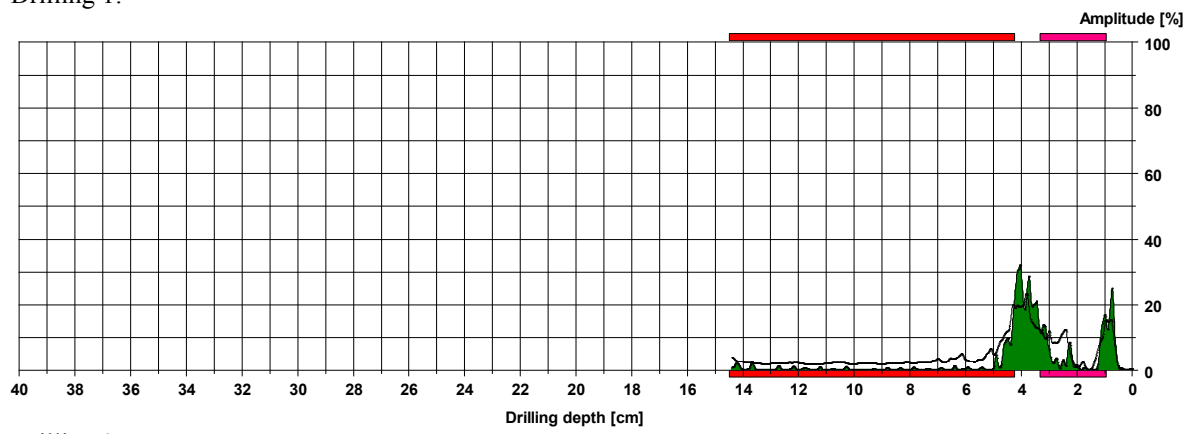


Drilling 2:

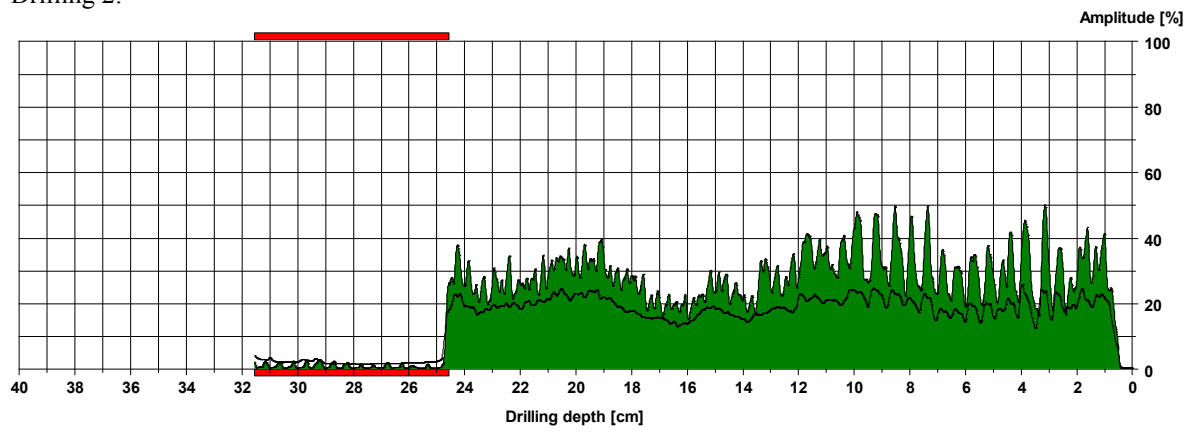


**Tie beam end: A27-95 L (connects to rafter S27)**

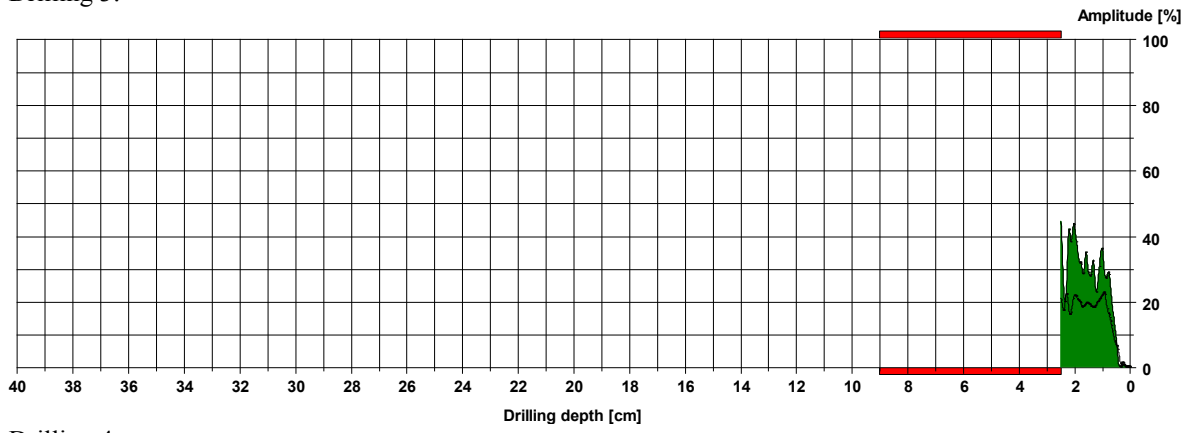
Drilling 1:



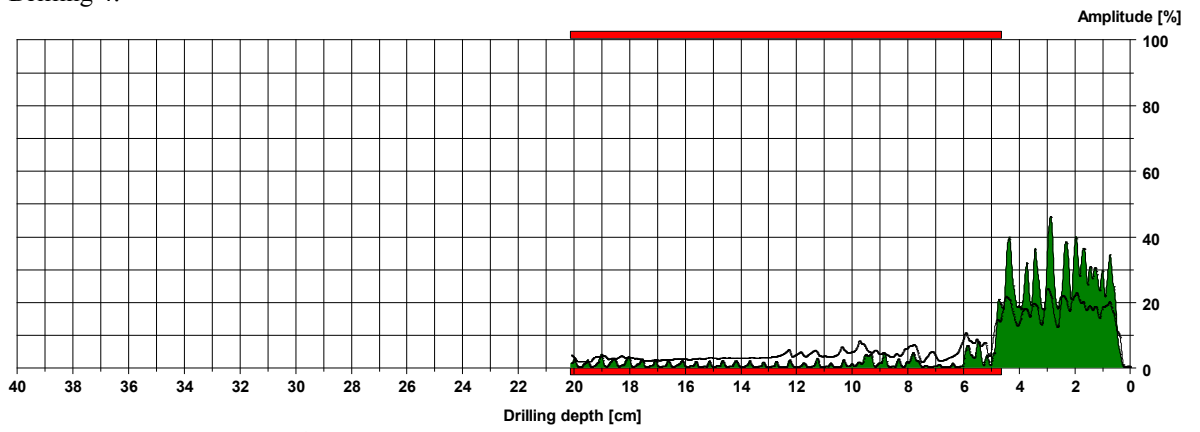
Drilling 2:



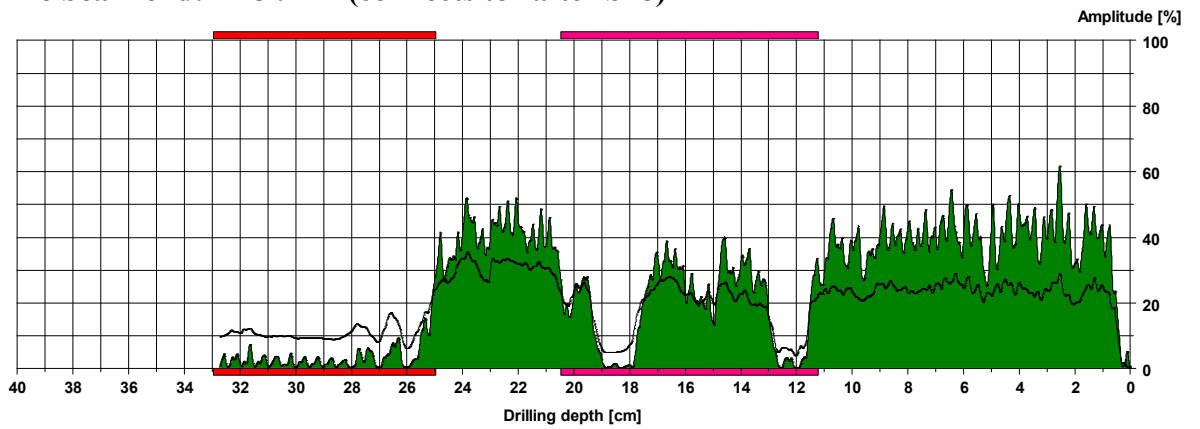
Drilling 3:



Drilling 4:

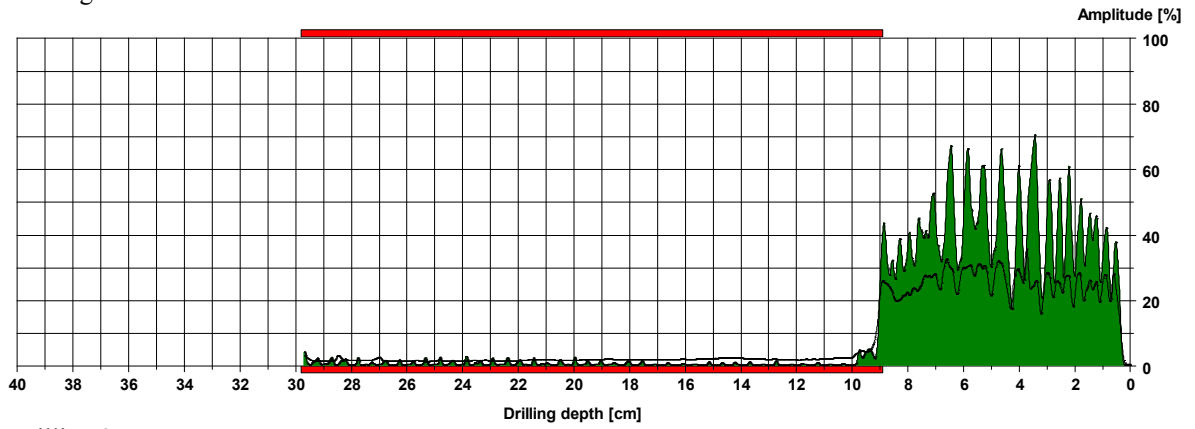


Tie beam end: A28-94 L (connects to rafter S28)

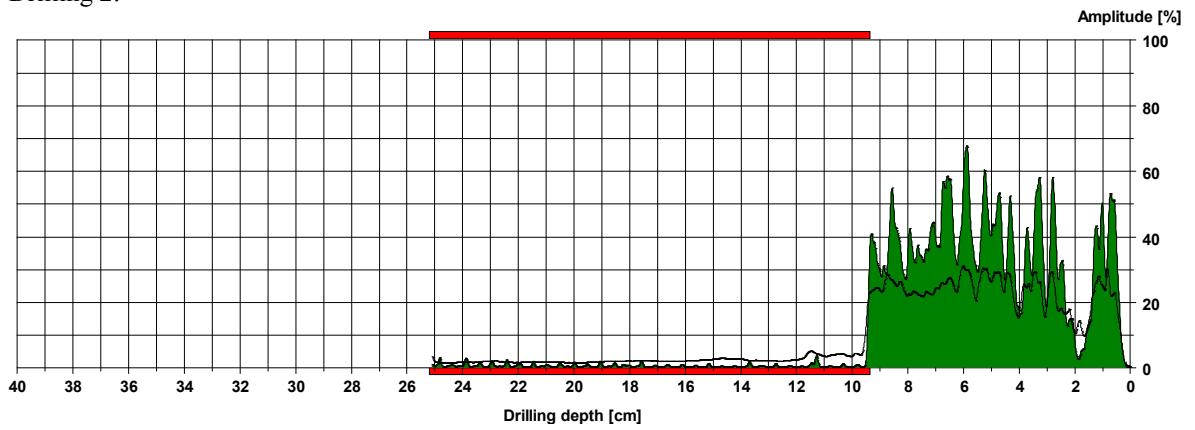


**Tie beam end: A29-93 L (connects to rafter S29)**

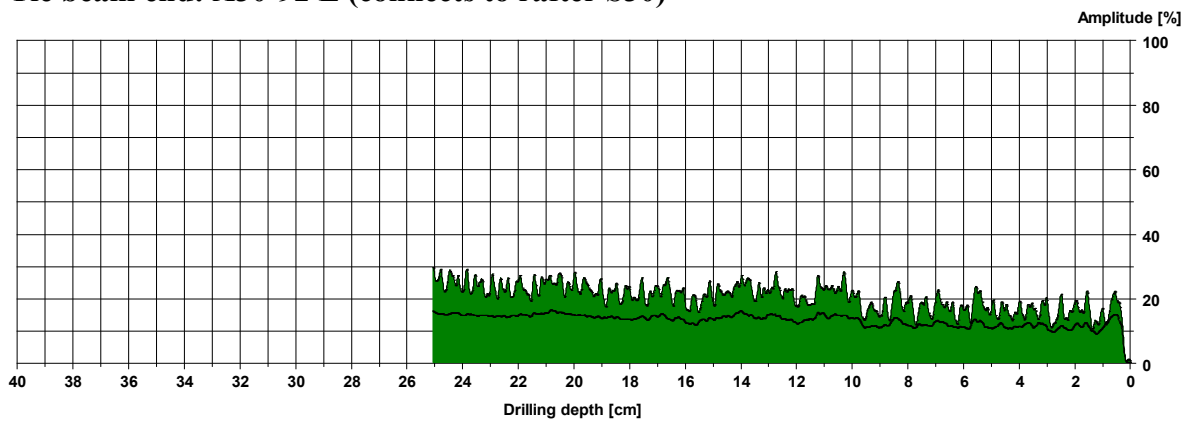
Drilling 1:



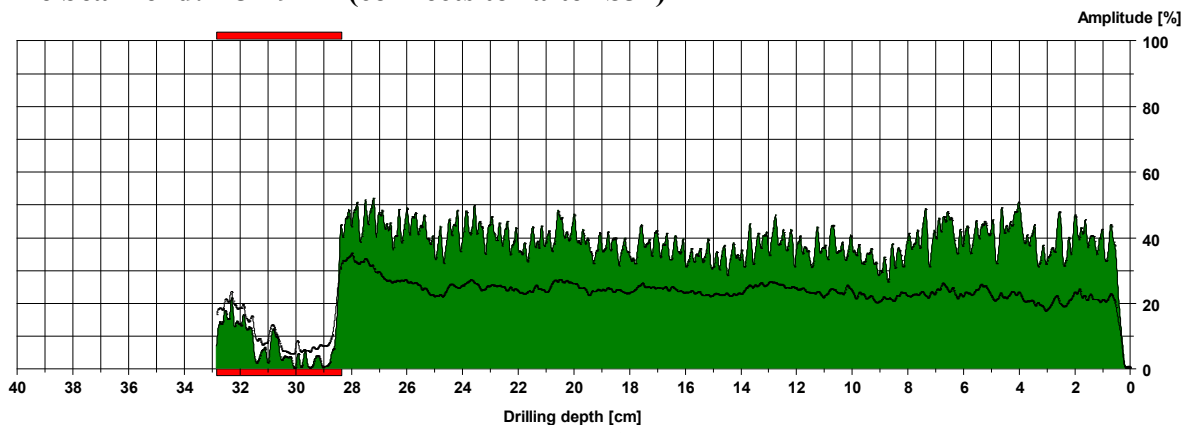
Drilling 2:



**Tie beam end: A30-92 L (connects to rafter S30)**

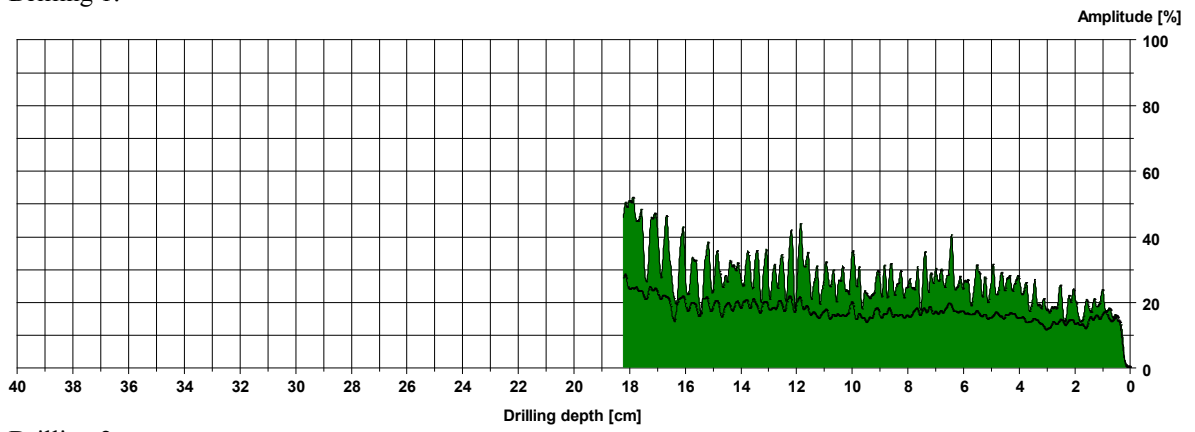


**Tie beam end: A31-91 L (connects to rafter S31)**

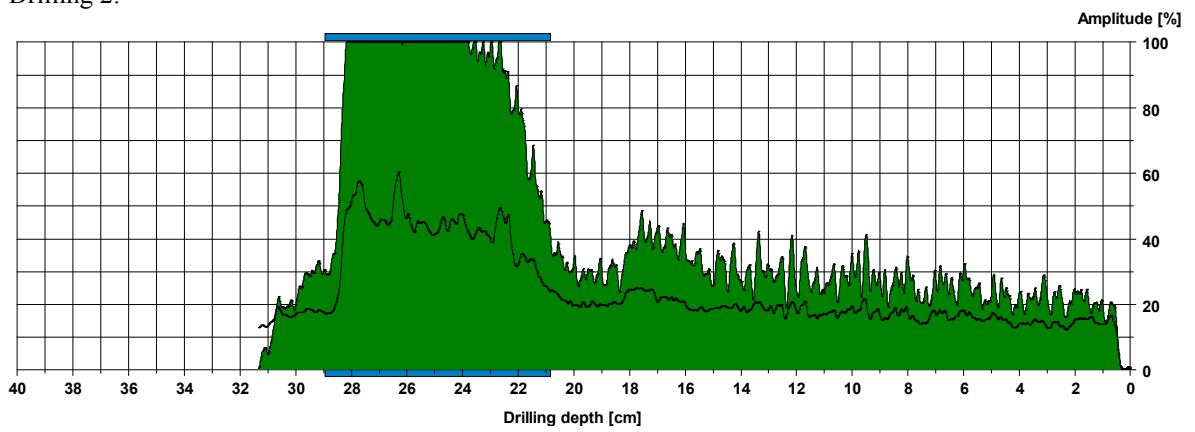


**Tie beam end: A32-90 L (connects to rafter S32)**

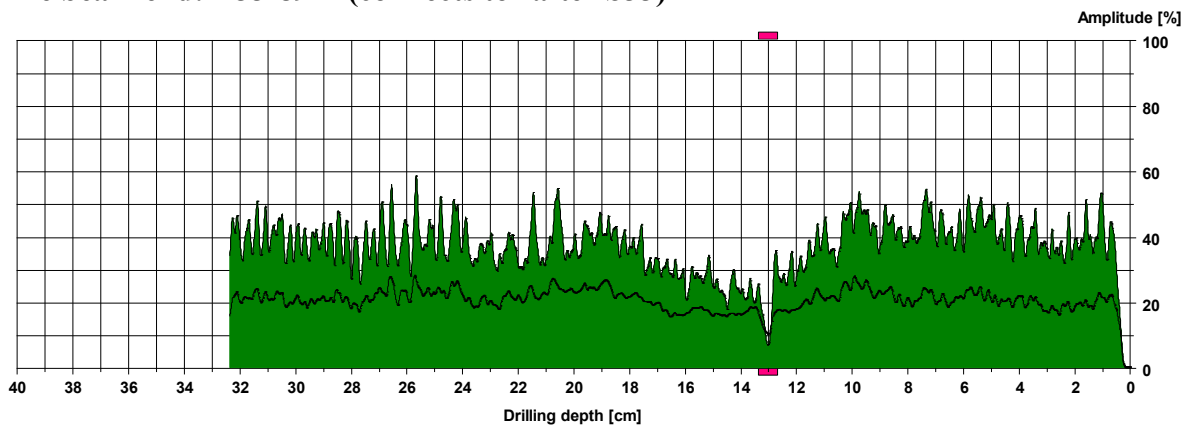
Drilling 1:



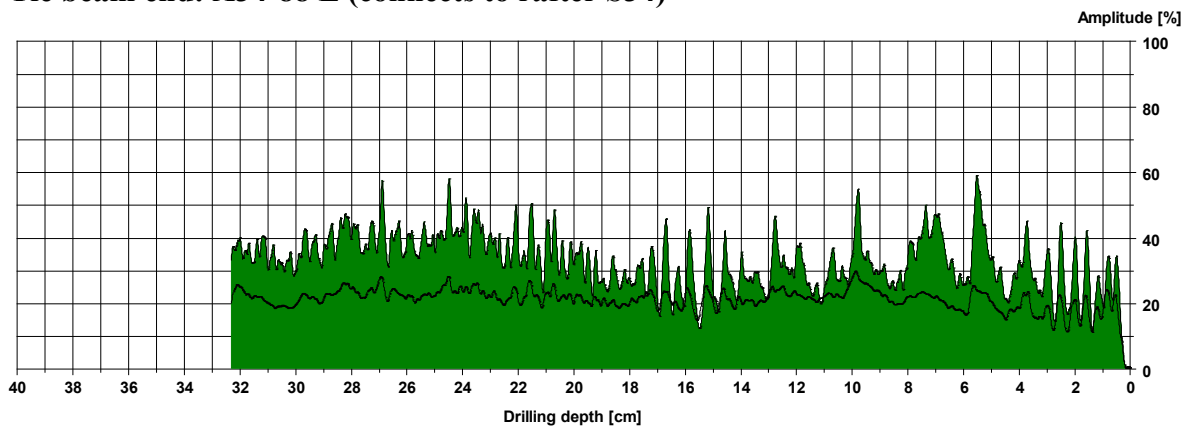
Drilling 2:



**Tie beam end: A33-89 L (connects to rafter S33)**

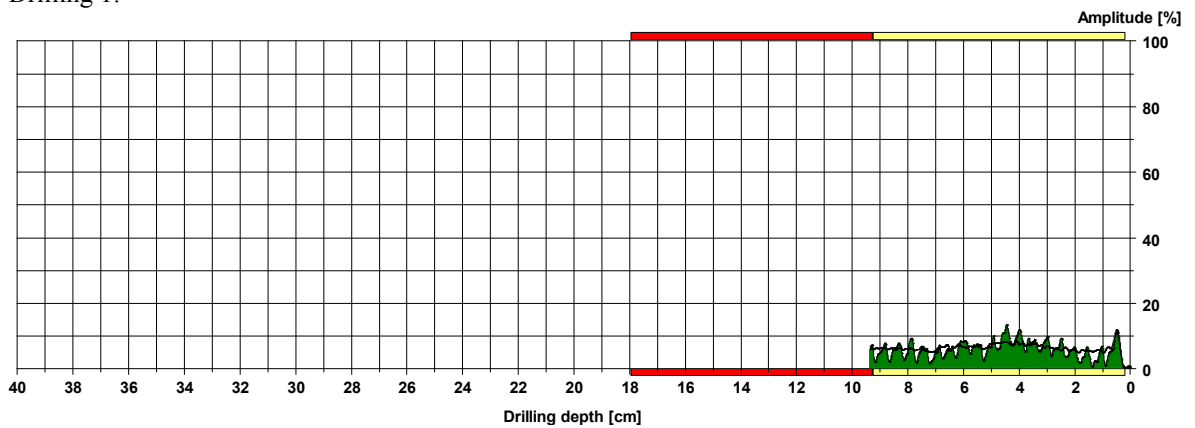


**Tie beam end: A34-88 L (connects to rafter S34)**



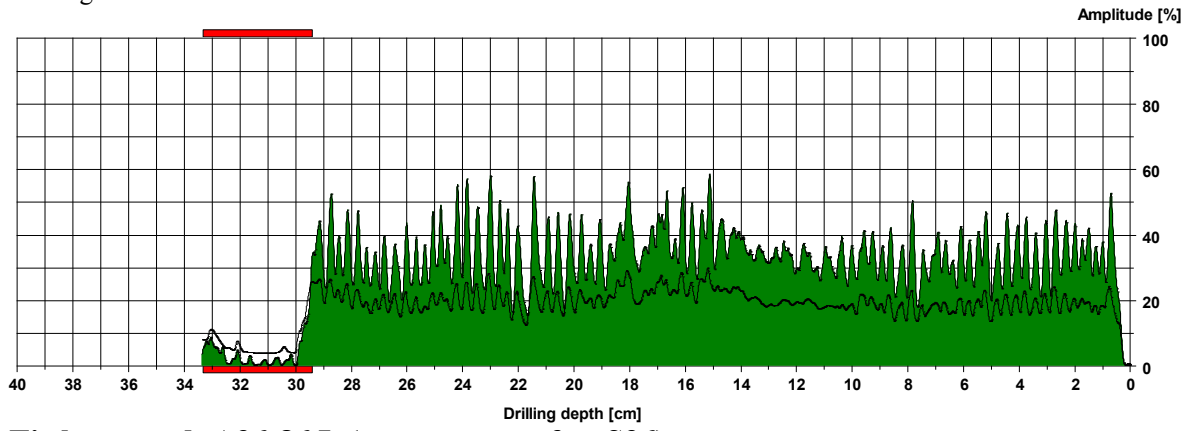
**Tie beam end: A35-87 L (connects to rafter S35)**

Drilling 1:



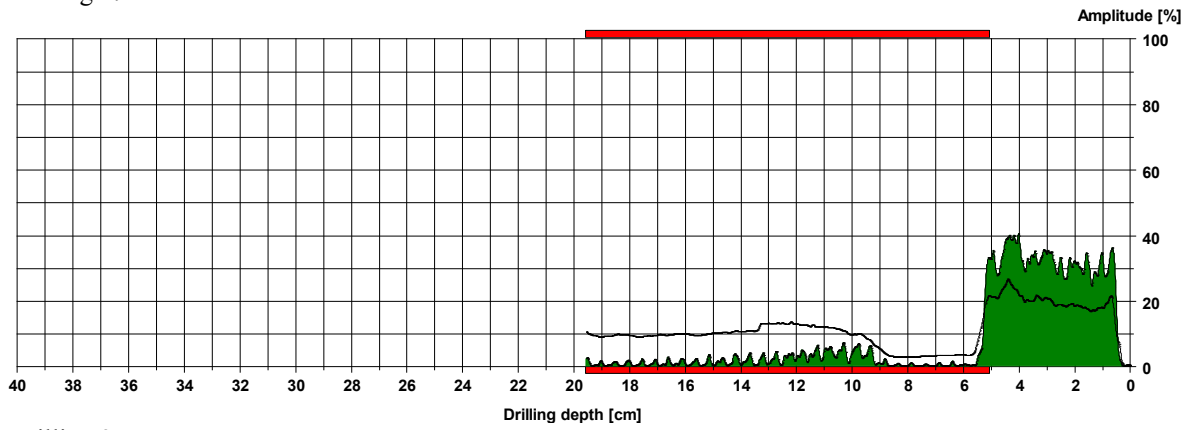


Drilling 2:

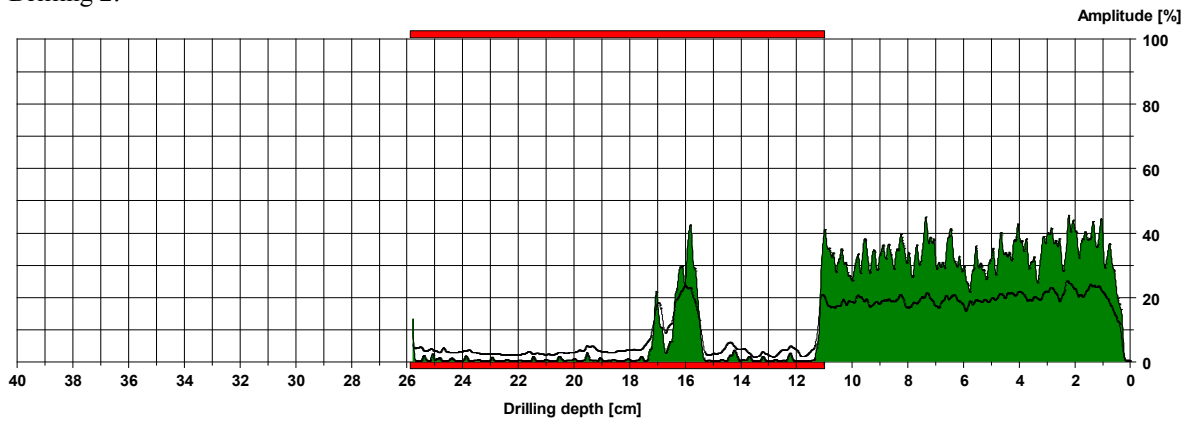


**Tie beam end: A36-86 L (connects to rafter S36)**

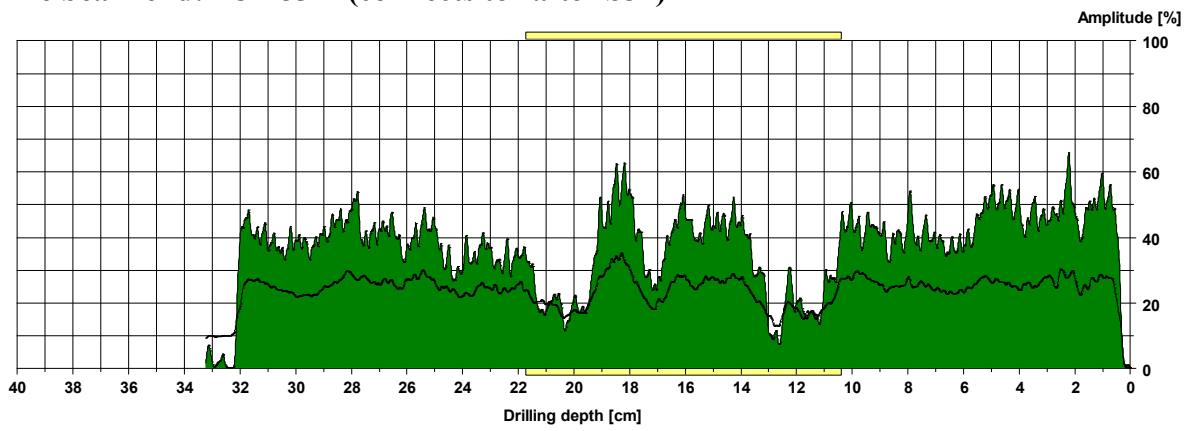
Drilling 1:



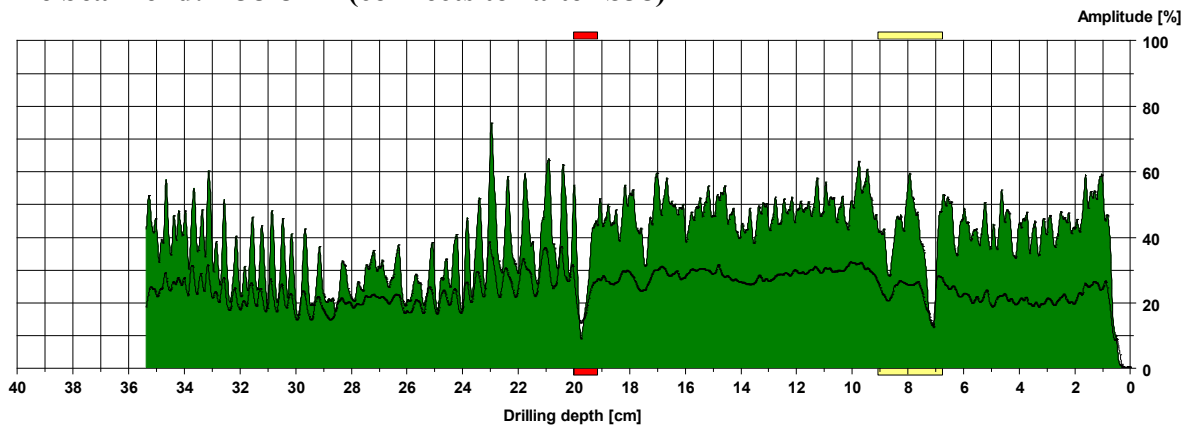
Drilling 2:



**Tie beam end: A37-85 L (connects to rafter S37)**

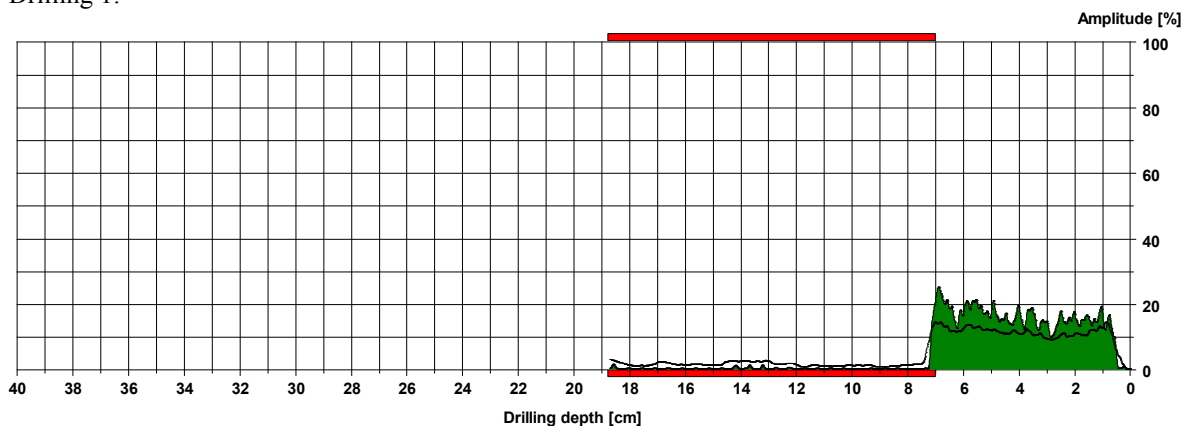


**Tie beam end: A38-84 L (connects to rafter S38)**

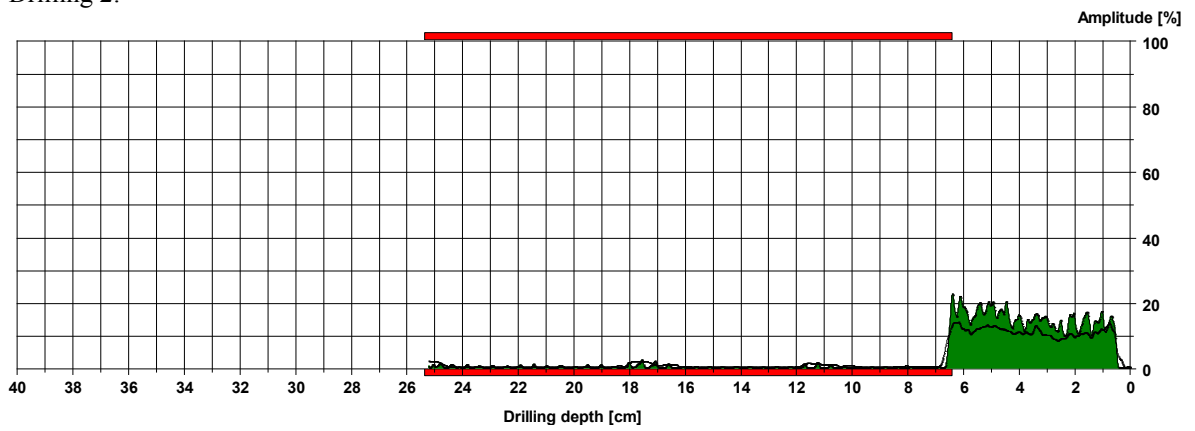


**Tie beam end: A39-83 L (connects to rafter S39)**

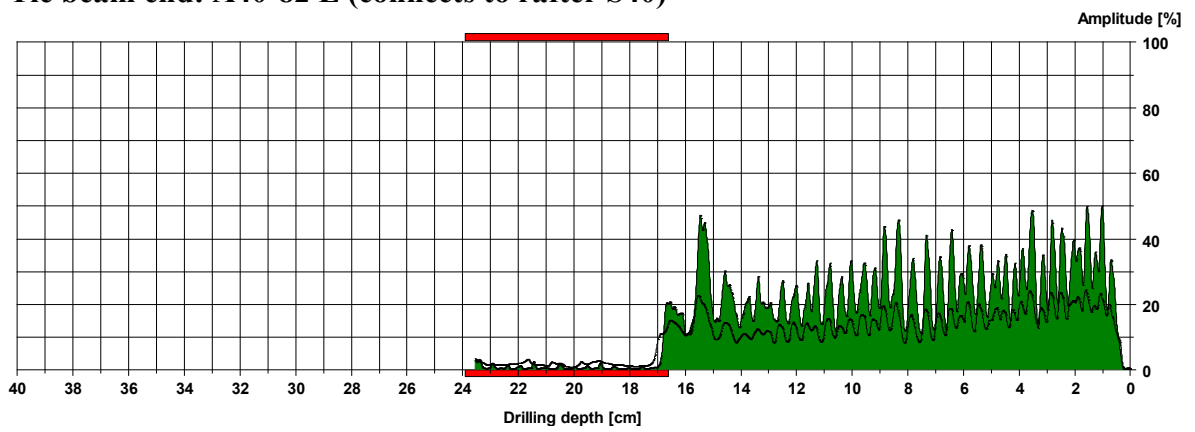
Drilling 1:



Drilling 2:

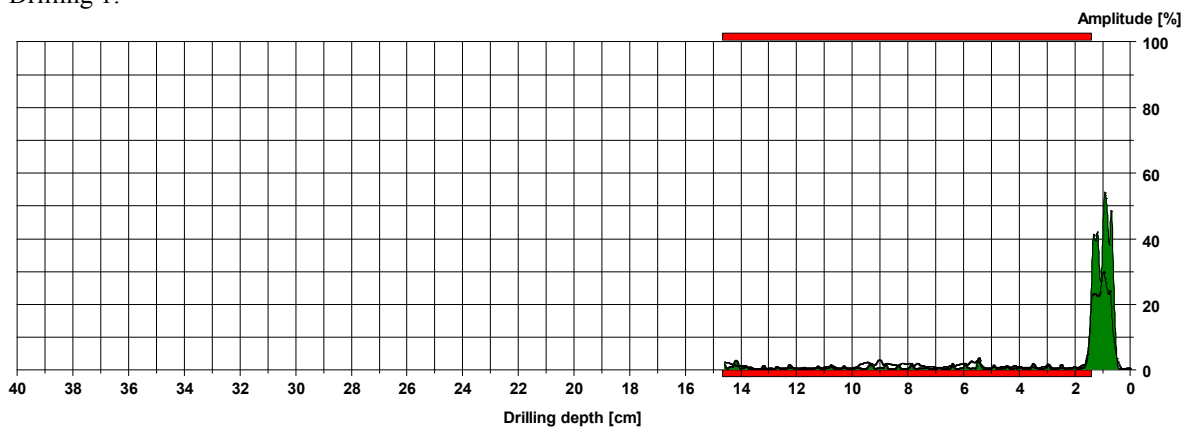


**Tie beam end: A40-82 L (connects to rafter S40)**

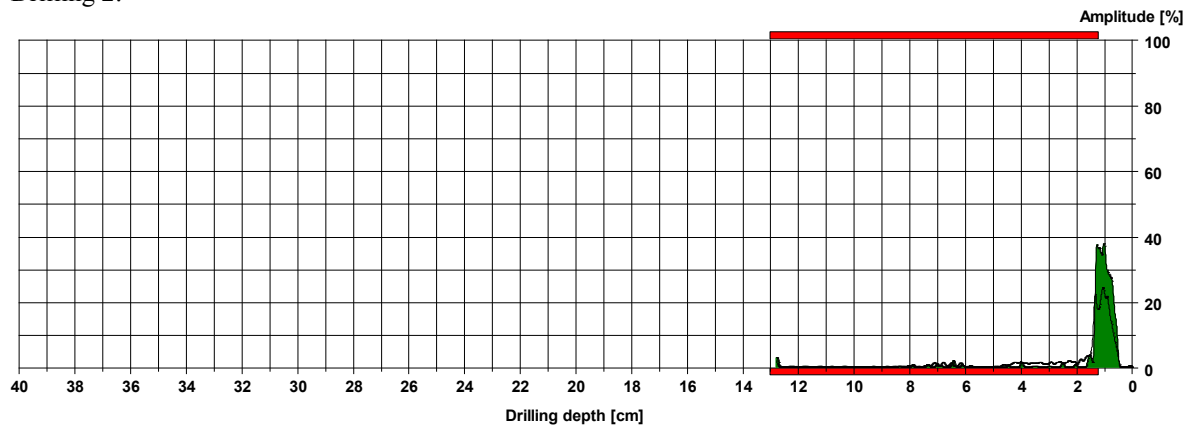


**Tie beam end: A41-81 L (connects to rafter S41)**

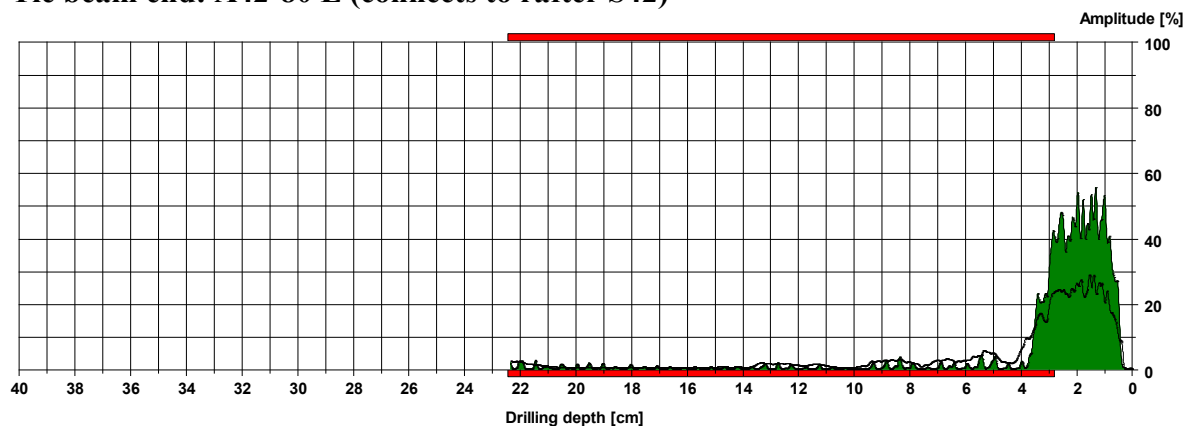
Drilling 1:



Drilling 2:

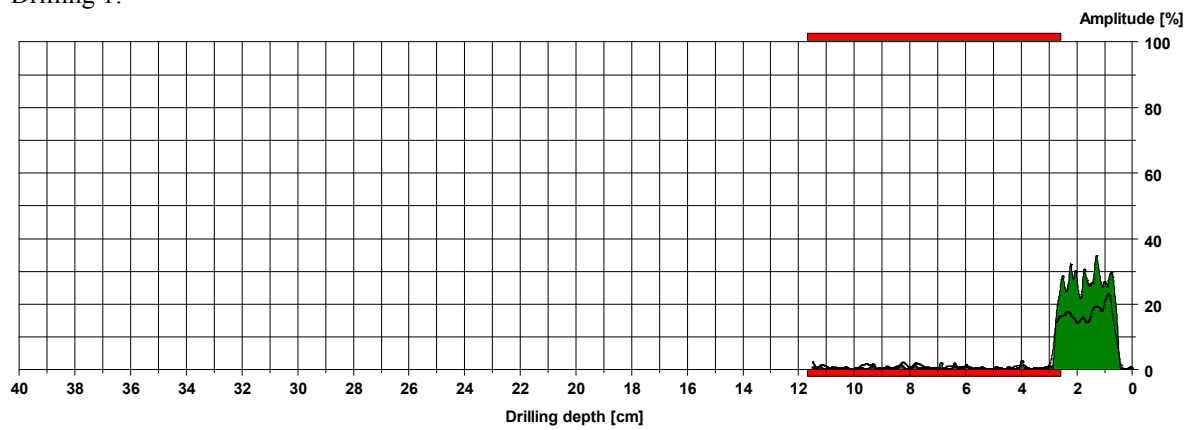


**Tie beam end: A42-80 L (connects to rafter S42)**

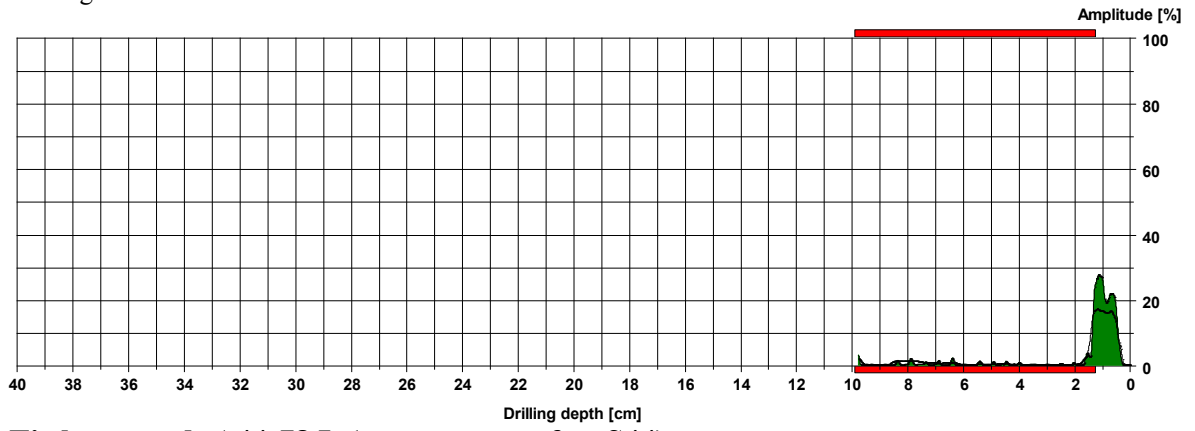


**Tie beam end: A43-79 L (connects to rafter S43)**

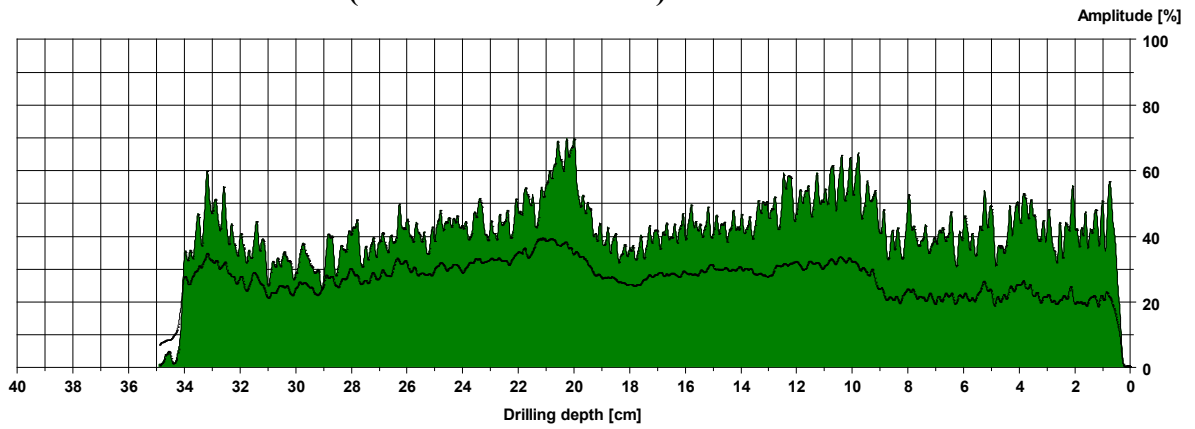
Drilling 1:



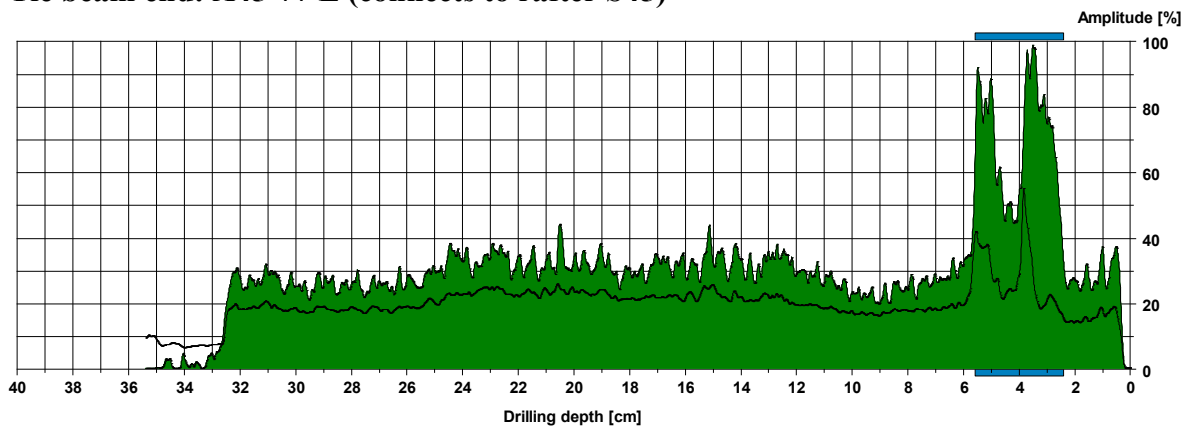
Drilling 2:



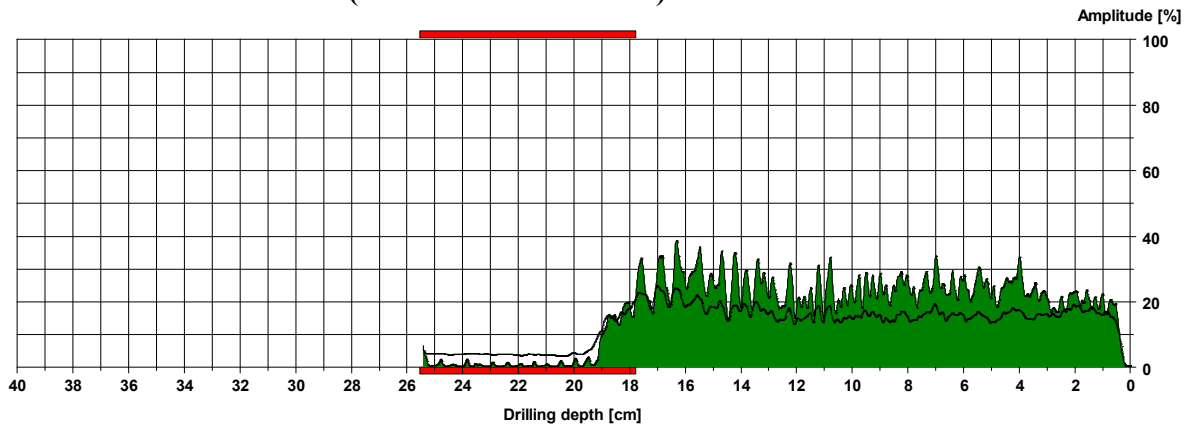
**Tie beam end: A44-78 L (connects to rafter S44)**



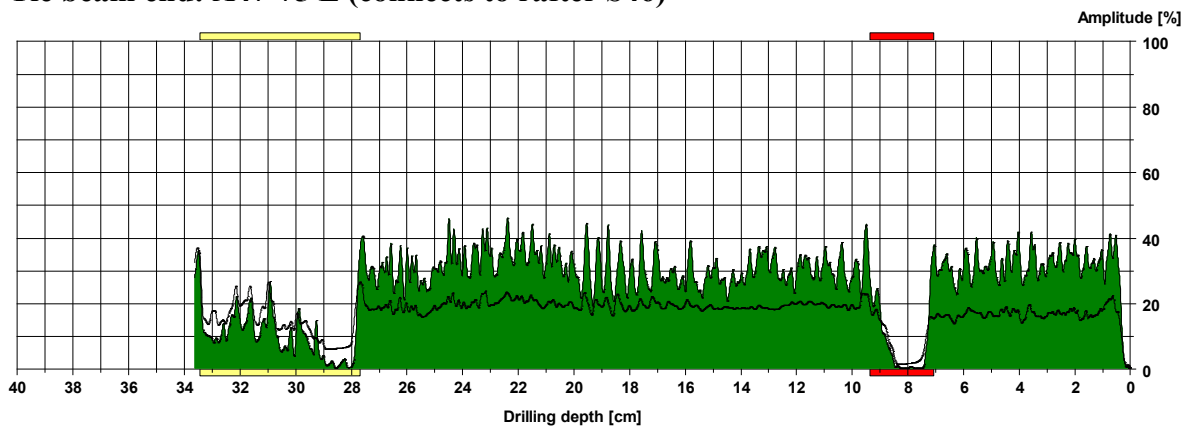
**Tie beam end: A45-77 L (connects to rafter S45)**



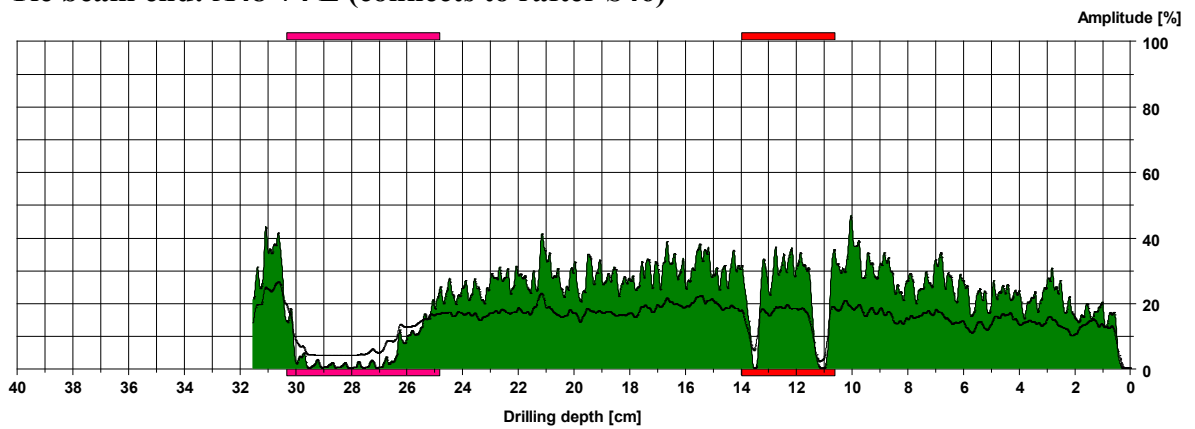
**Tie beam end: A46-76 L (connects to rafter S46)**



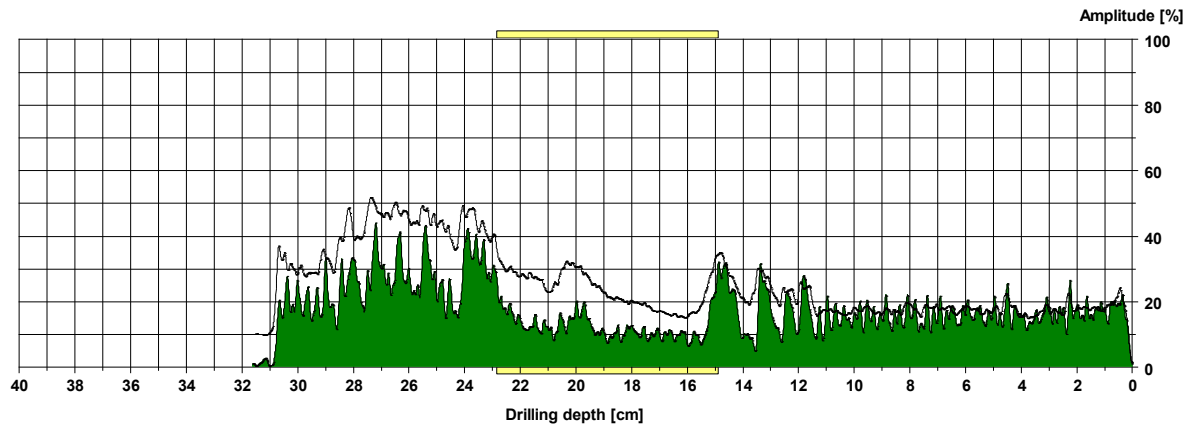
**Tie beam end: A47-75 L (connects to rafter S46)**



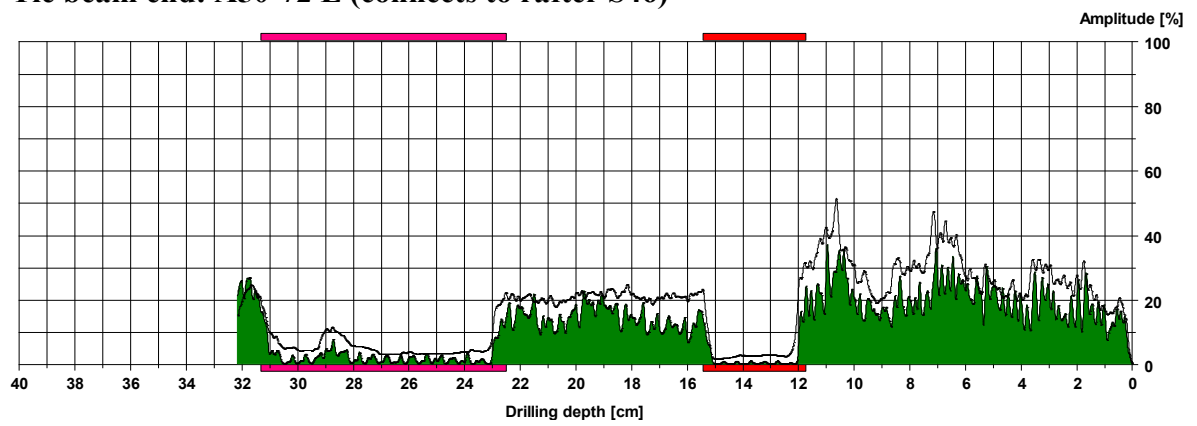
**Tie beam end: A48-74 L (connects to rafter S46)**



**Tie beam end: A49-73 L (connects to rafter S46)**

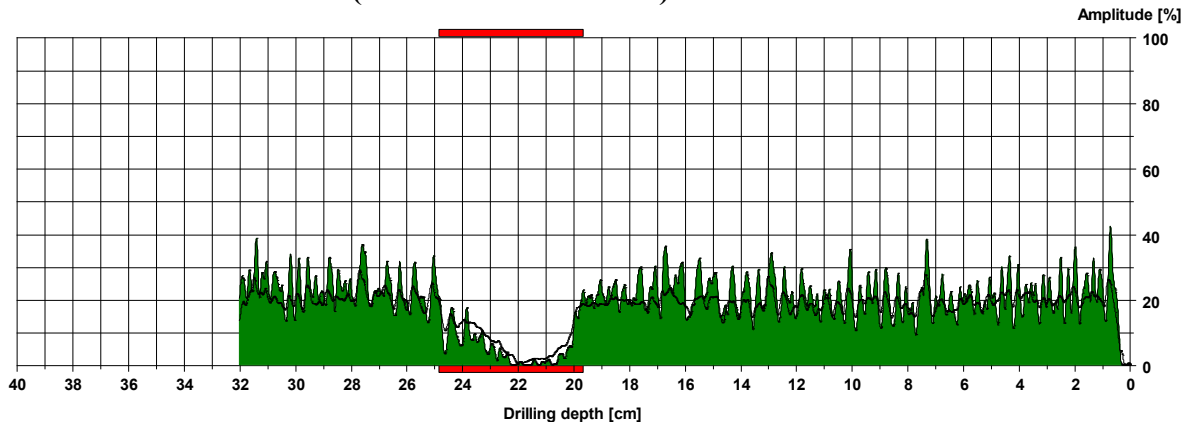


**Tie beam end: A50-72 L (connects to rafter S46)**

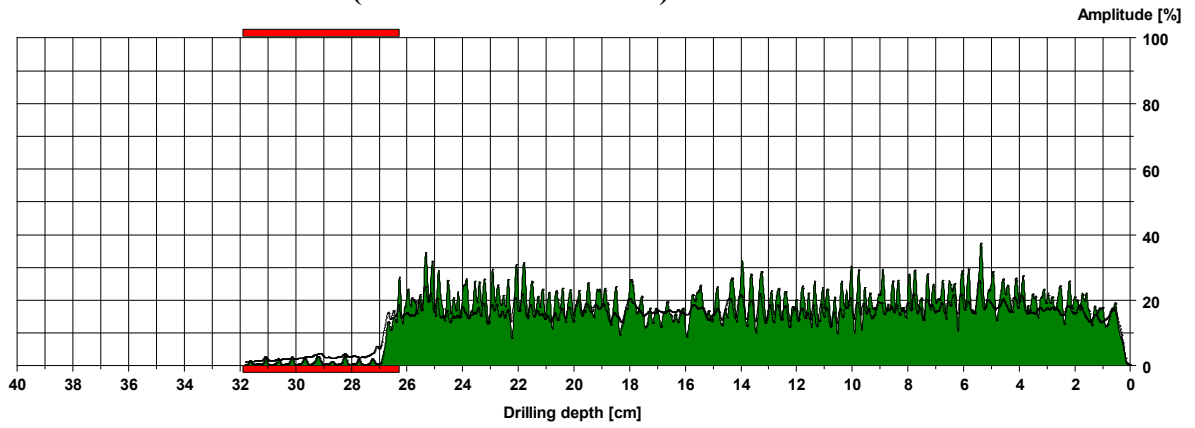


### 3.4.2 Tie beams ends in the northeast side

Tie beam end: A39-83 K (connects to rafter S83)

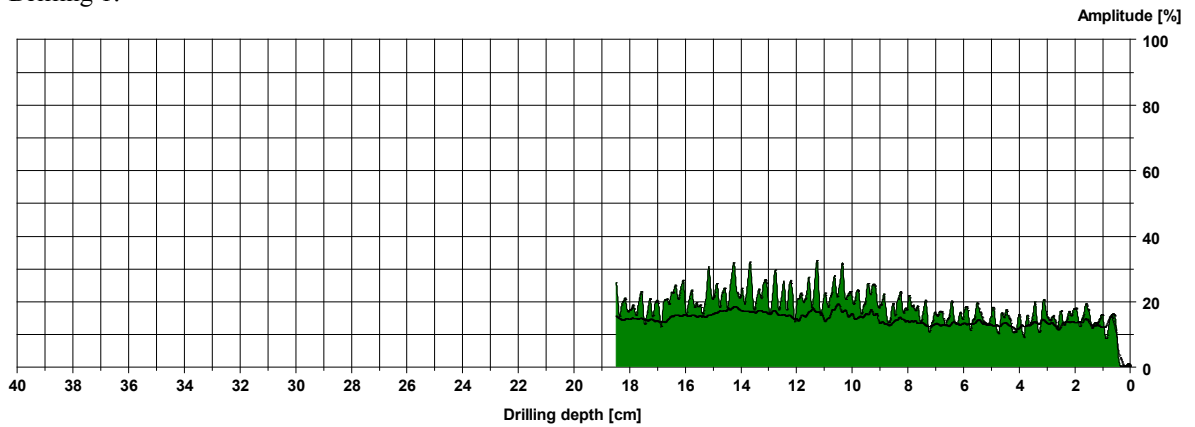


Tie beam end: A38-84 K (connects to rafter S84)



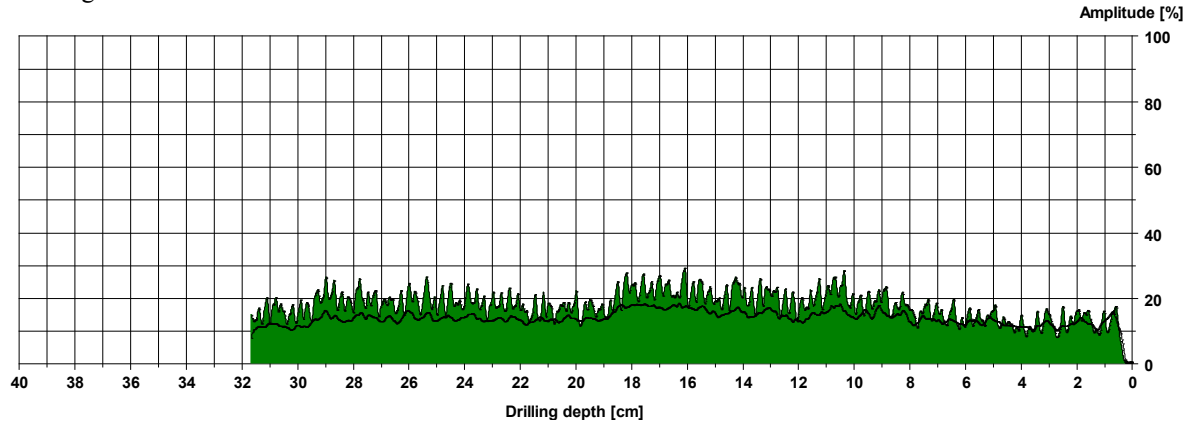
Tie beam end: A37-85 K (connects to rafter S85)

Drilling 1:

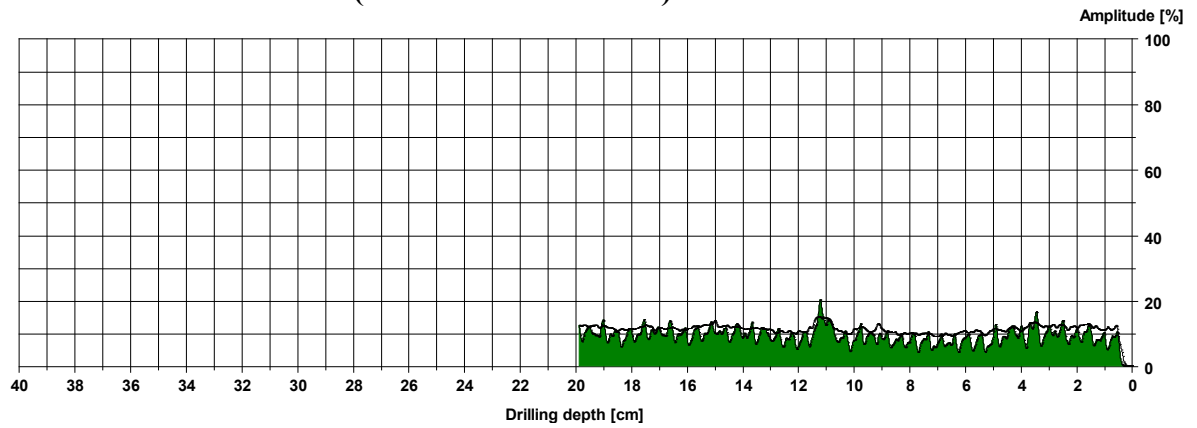




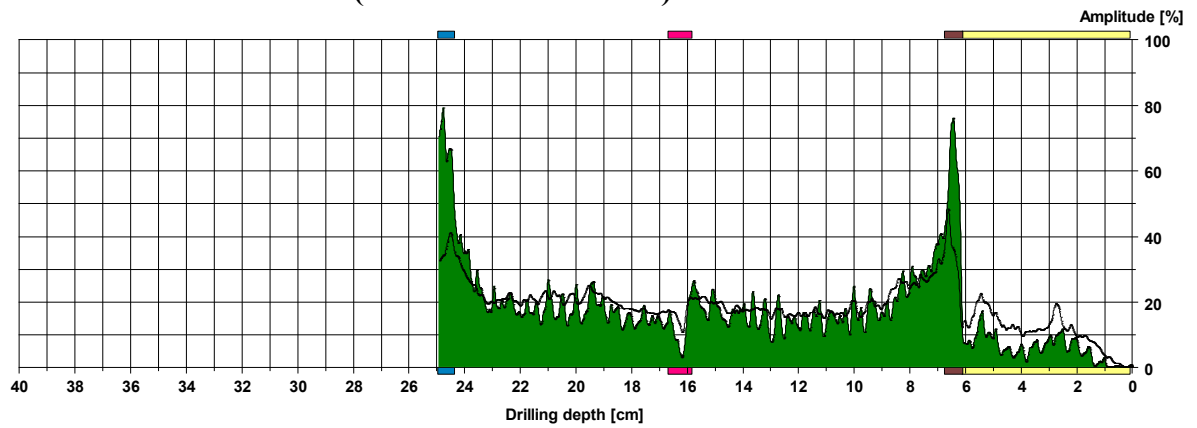
Drilling 2:



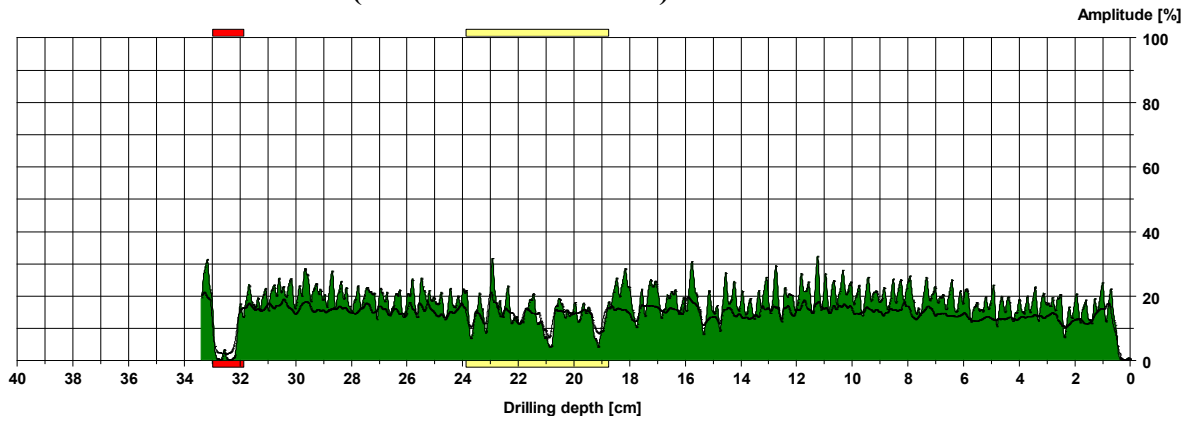
**Tie beam end: A36-86 K (connects to rafter S86)**



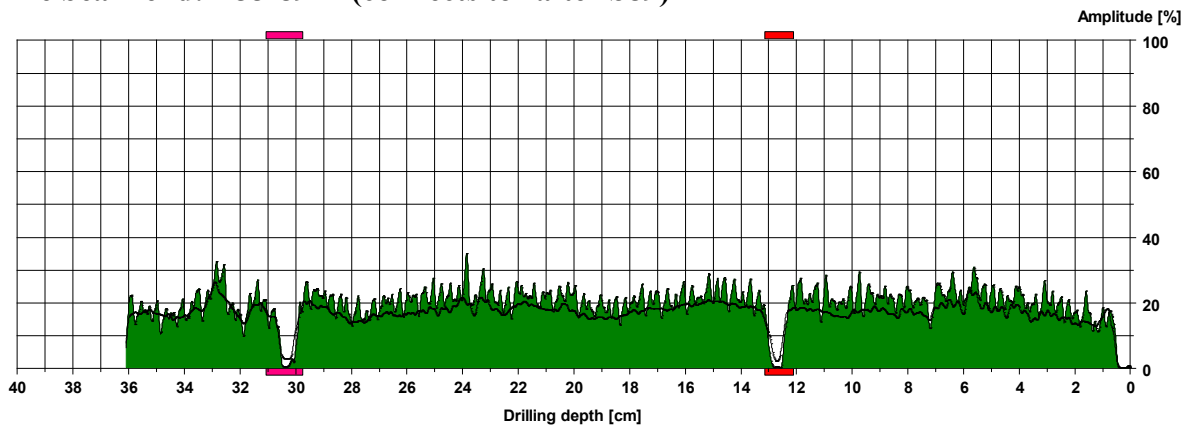
**Tie beam end: A35-87 K (connects to rafter S87)**



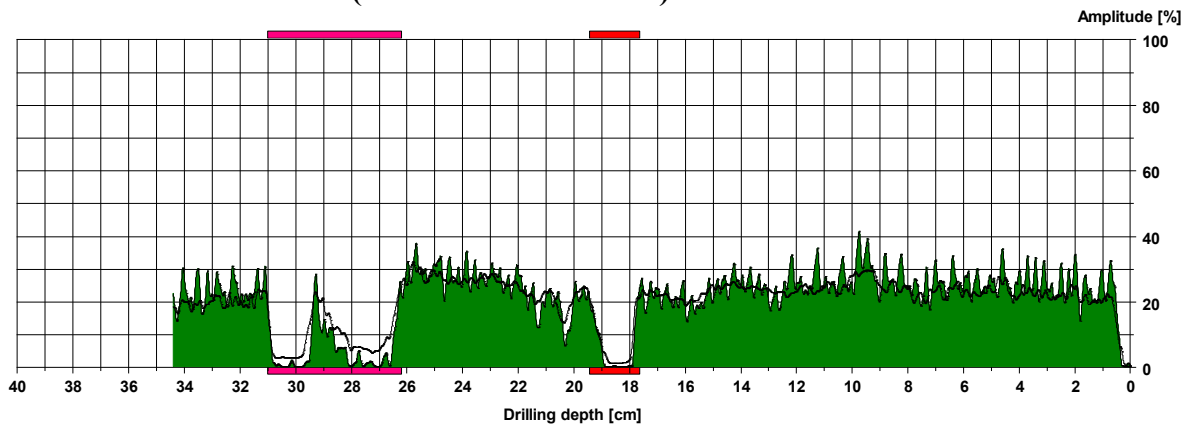
**Tie beam end: A34-88 K (connects to rafter S88)**



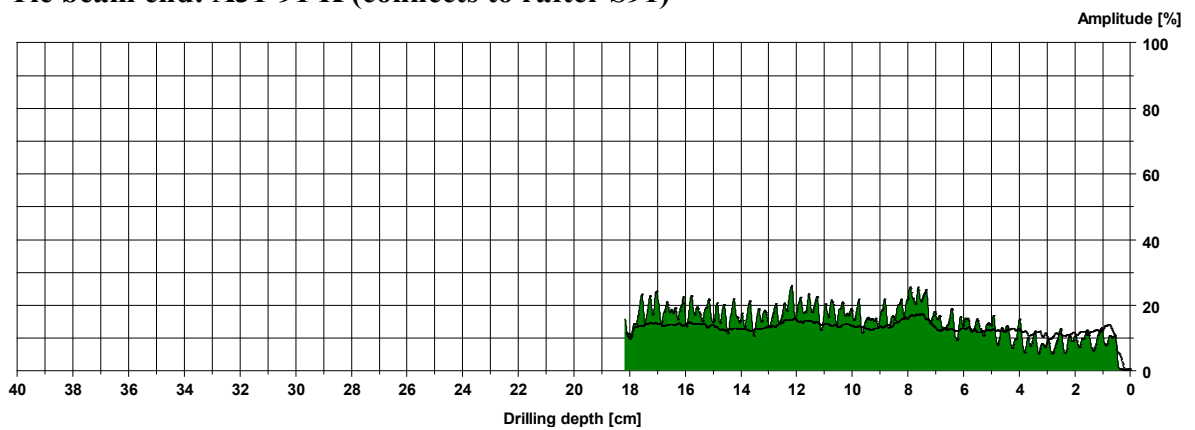
**Tie beam end: A33-89 K (connects to rafter S89)**



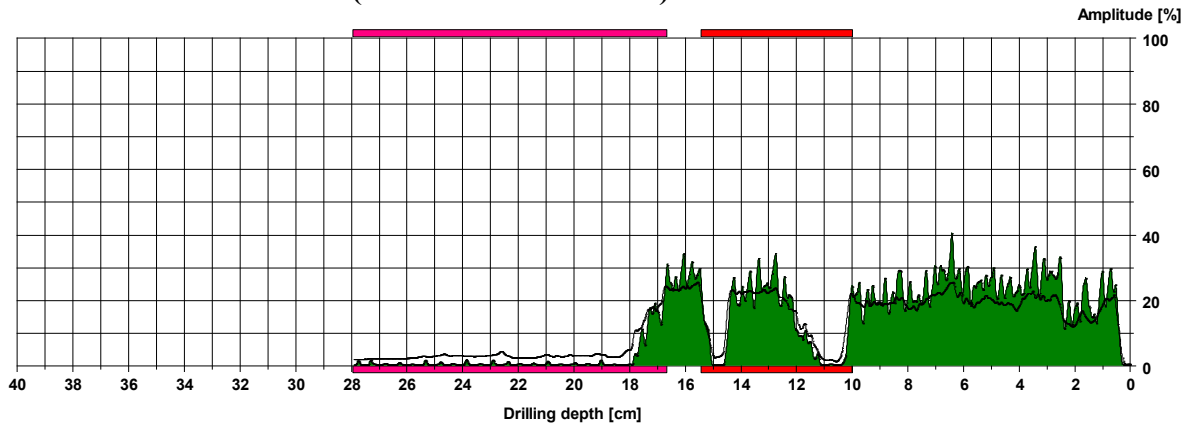
**Tie beam end: A32-90 K (connects to rafter S90)**



**Tie beam end: A31-91 K (connects to rafter S91)**

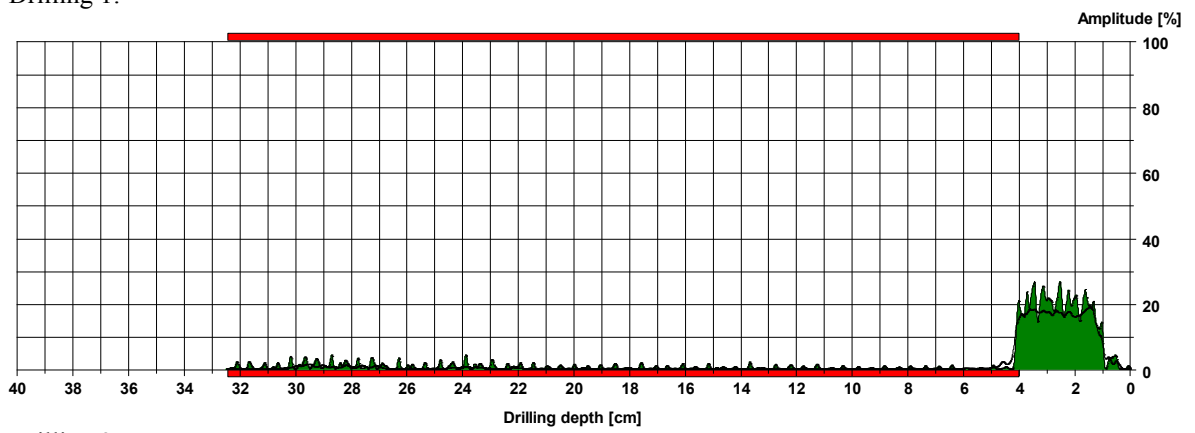


**Tie beam end: A30-92 K (connects to rafter S92)**

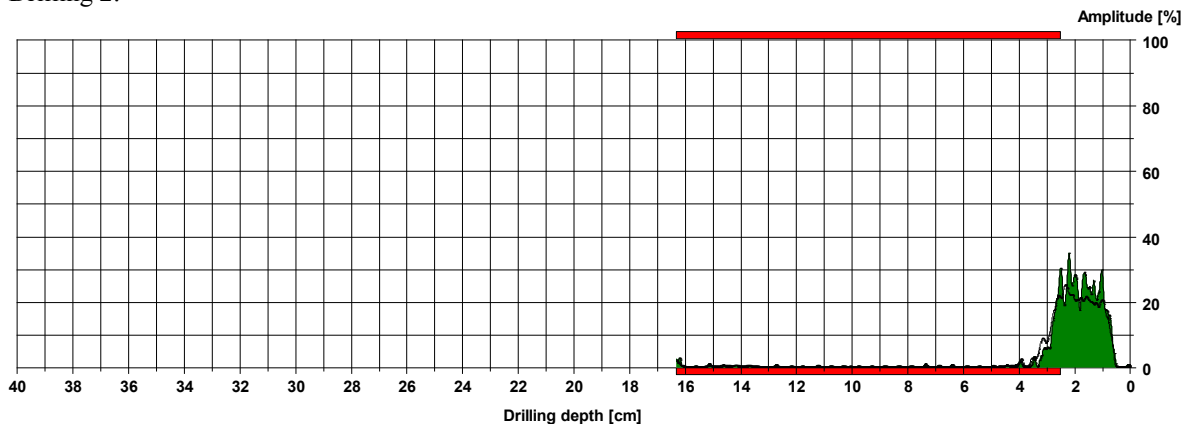


**Tie beam end: A29-93 K (connects to rafter S93)**

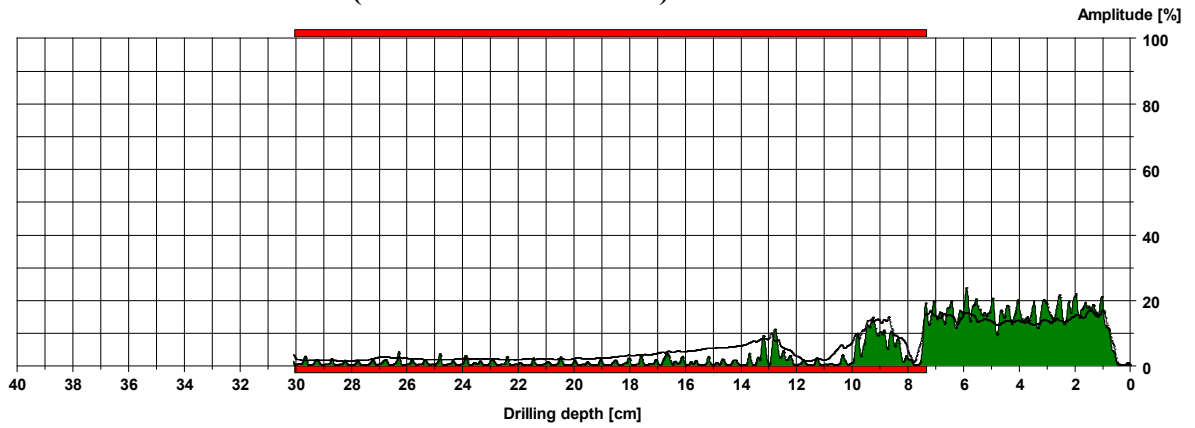
Drilling 1:



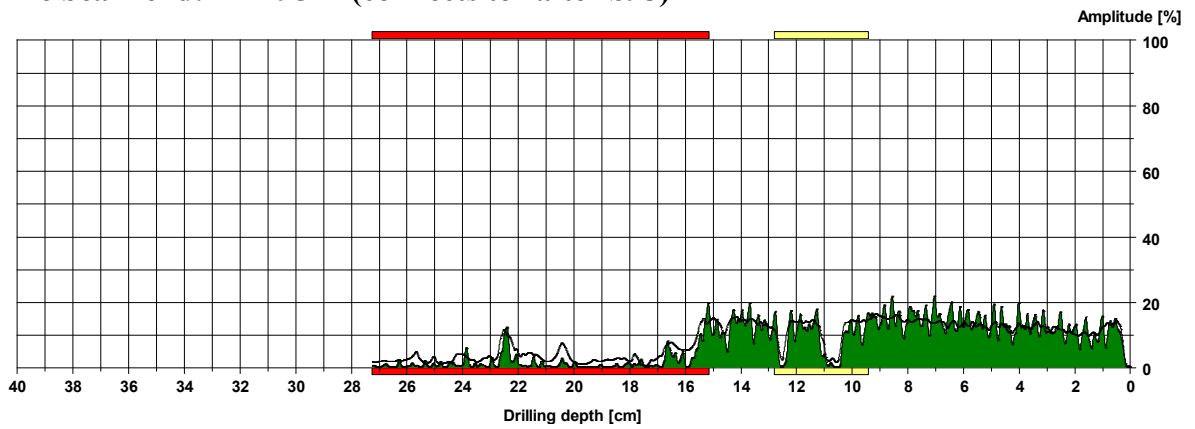
Drilling 2:



**Tie beam end: A28-94 K (connects to rafter S94)**

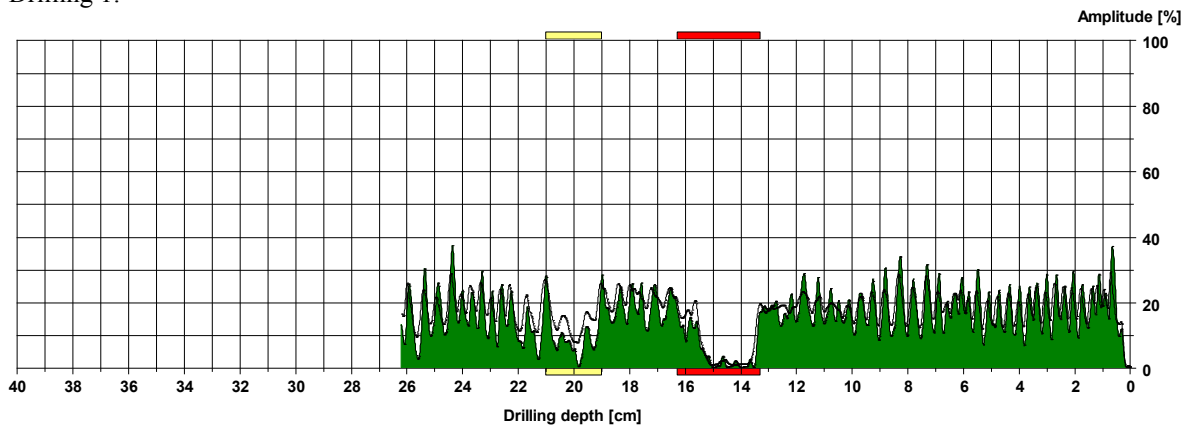


**Tie beam end: A27-95 K (connects to rafter S95)**

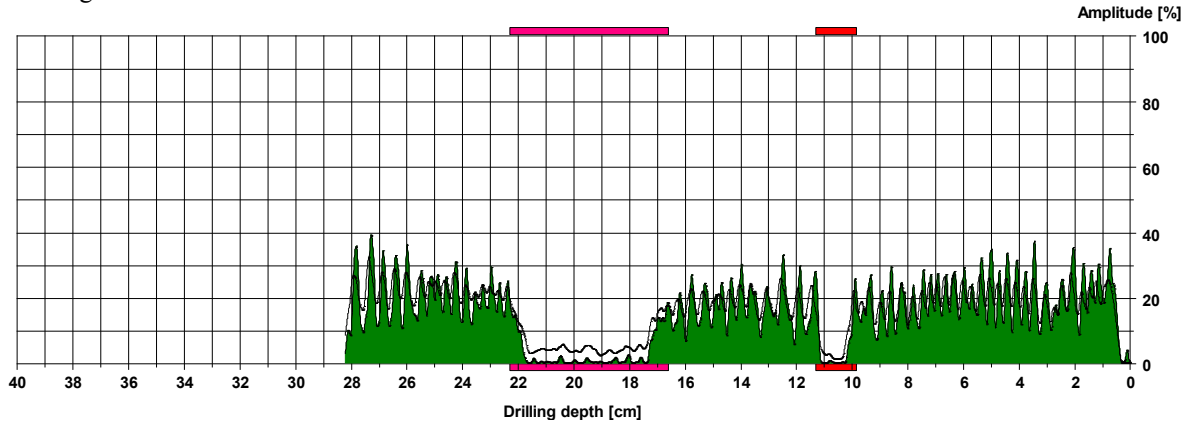


**Tie beam end: A26-96 K (connects to rafter S96)**

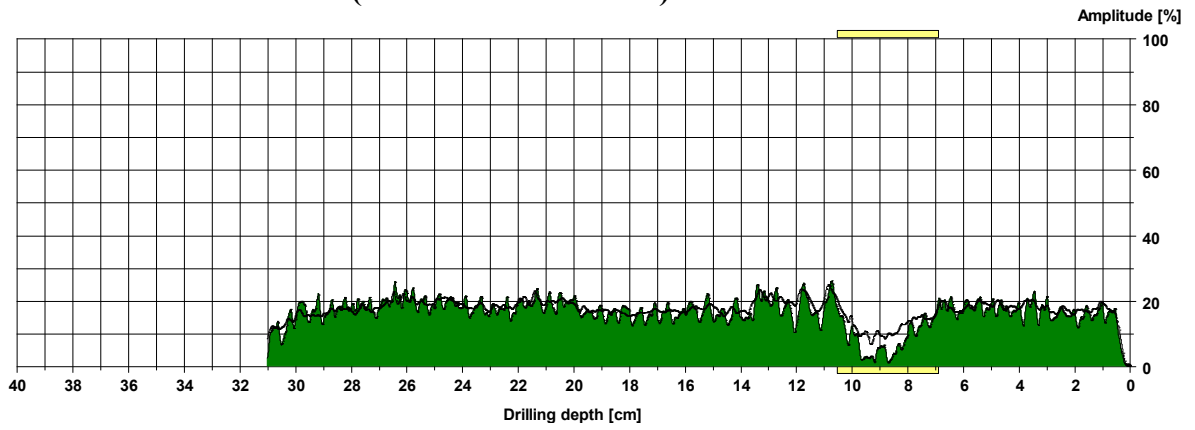
Drilling 1:



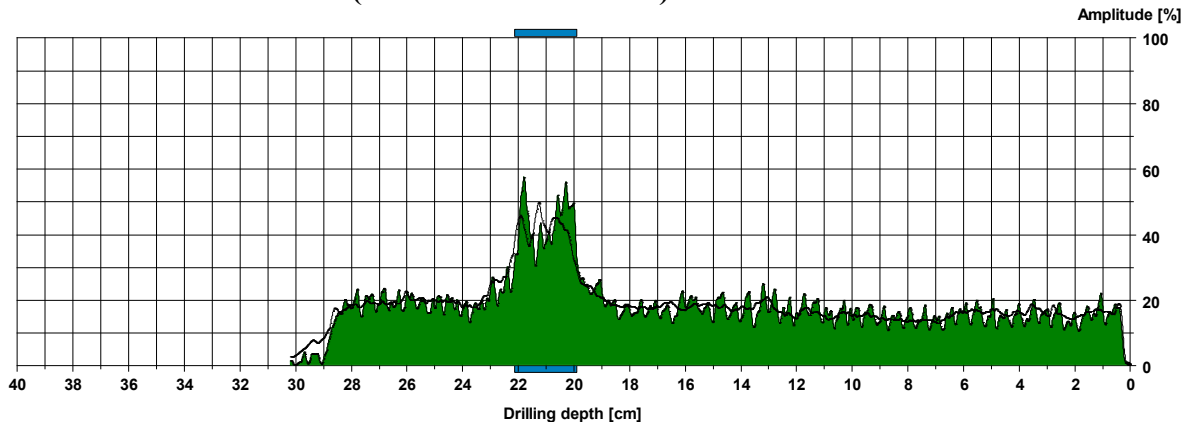
Drilling 2:



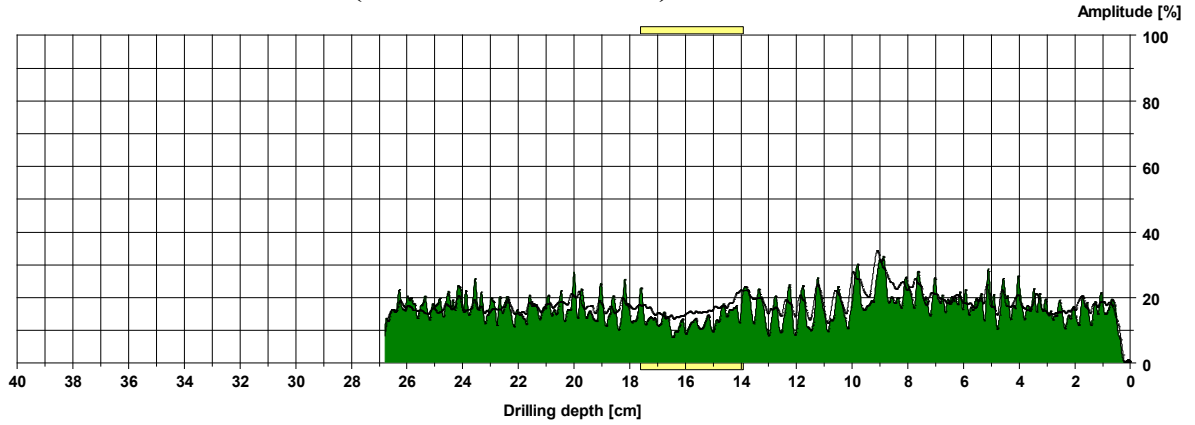
**Tie beam end: A25-97 K (connects to rafter S97)**



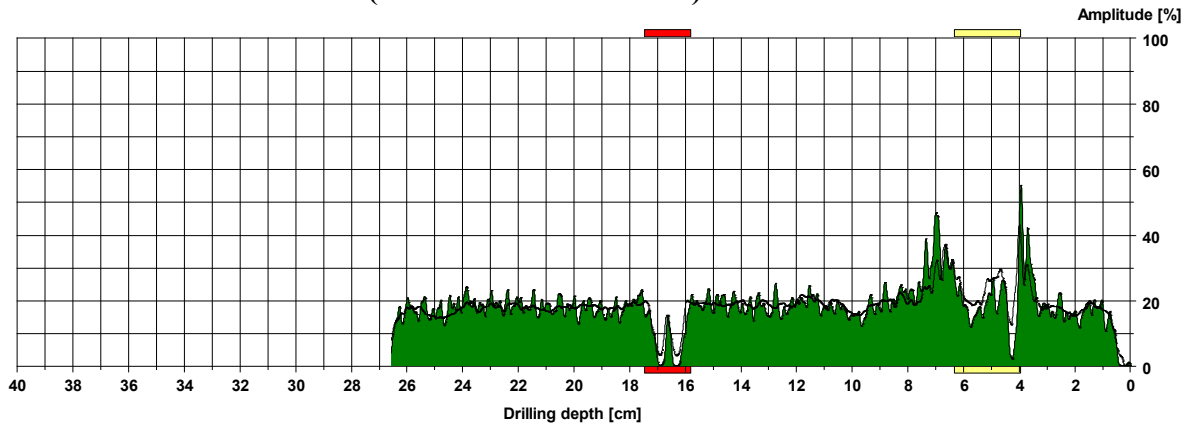
**Tie beam end: A24-98 K (connects to rafter S98)**



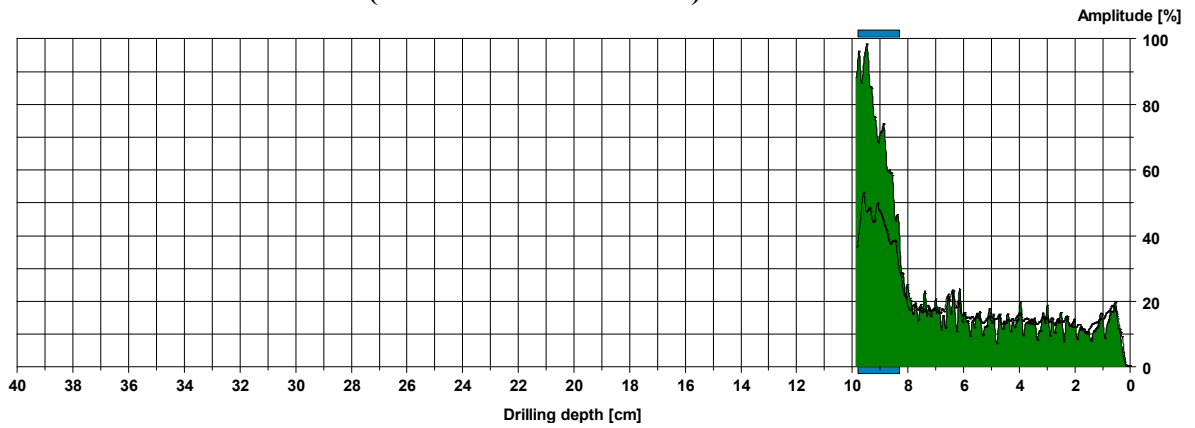
**Tie beam end: A23-99 K (connects to rafter S99)**



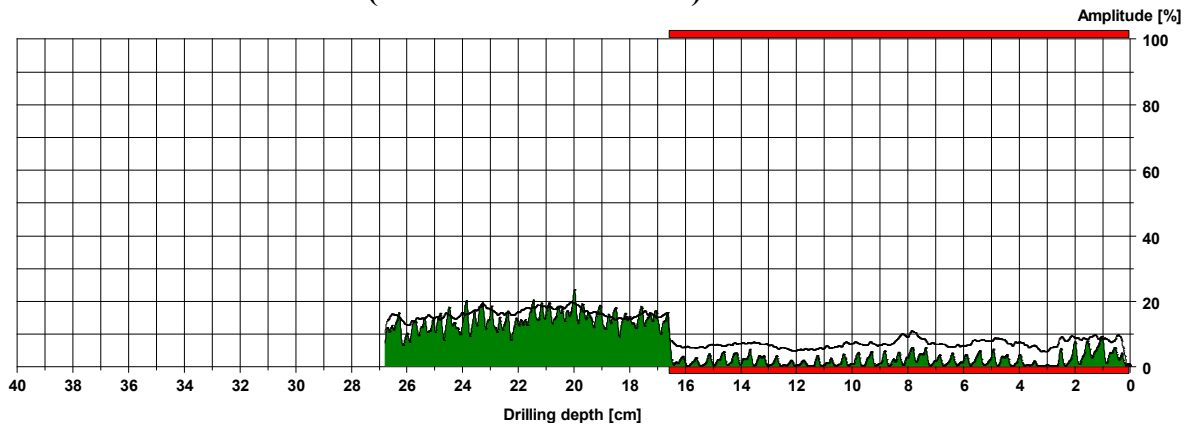
**Tie beam end: A22-100 K (connects to rafter S100)**



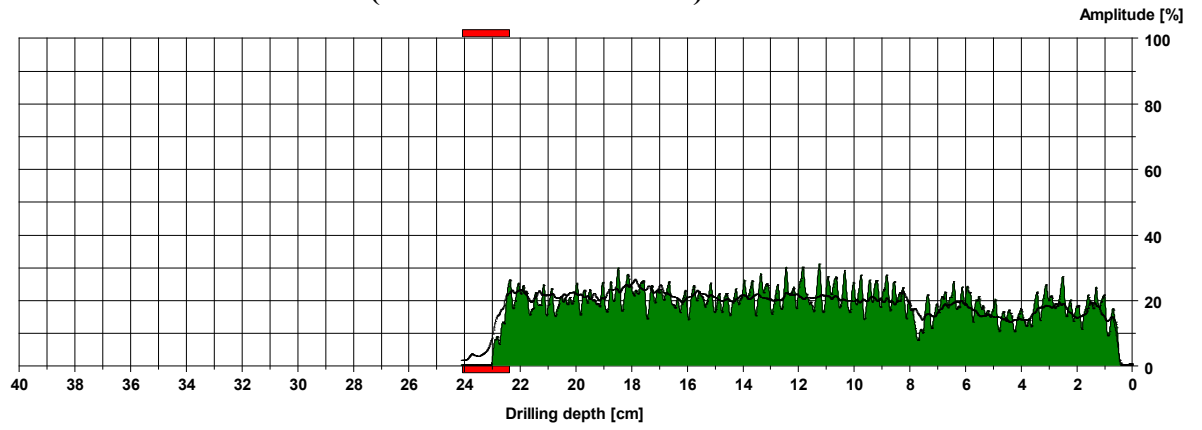
**Tie beam end: A21-101 K (connects to rafter S101)**



**Tie beam end: A20-102 K (connects to rafter S102)**

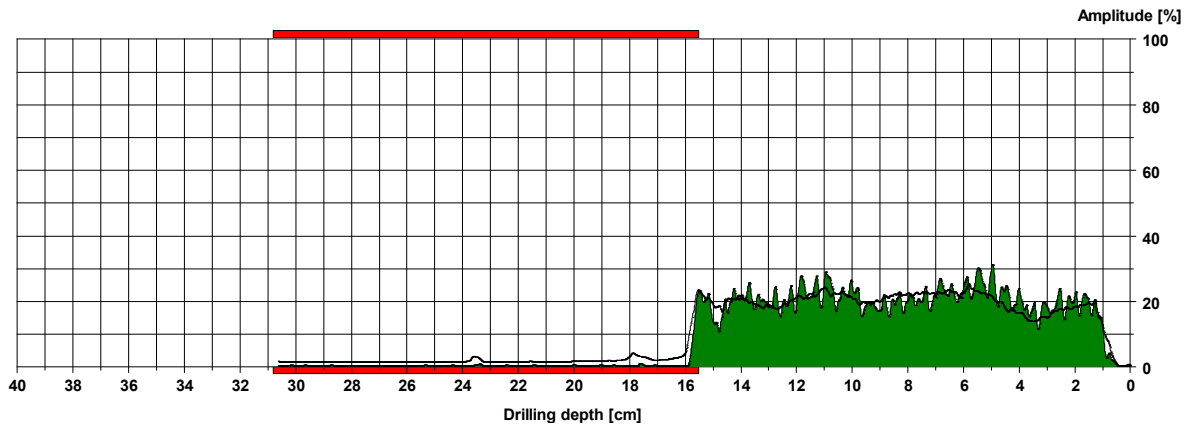


**Tie beam end: A19-103 K (connects to rafter S103)**



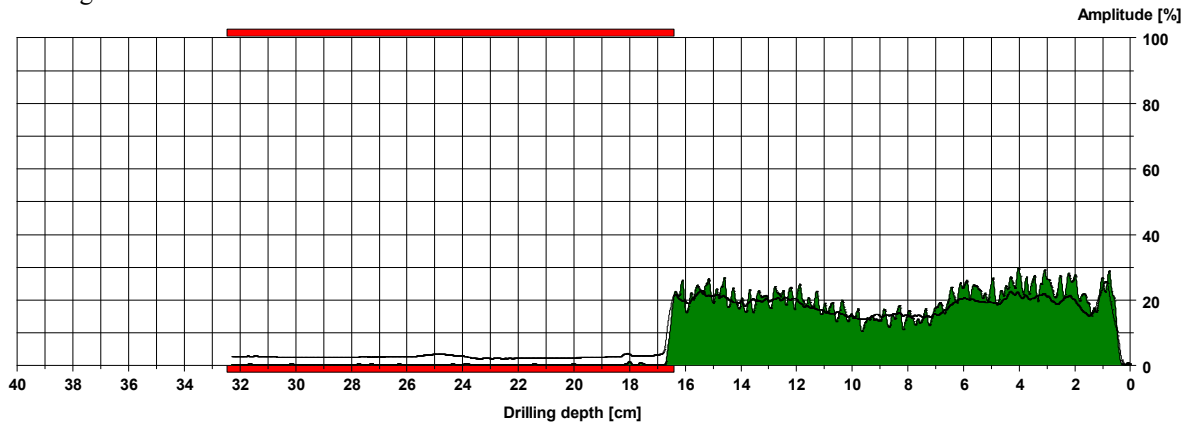
### 3.4.3 Posts of the leaning trestles

#### Post in VI

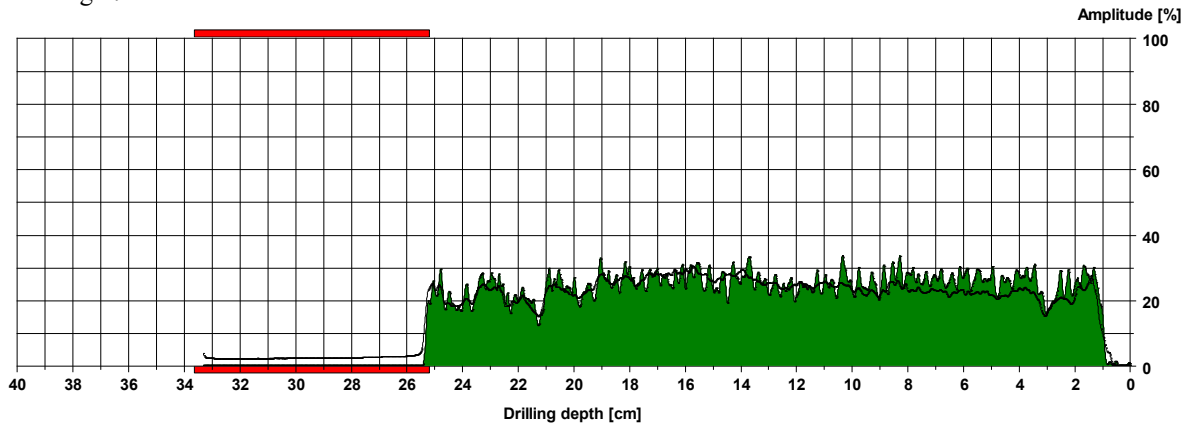


#### Post in VII

Drilling 1:

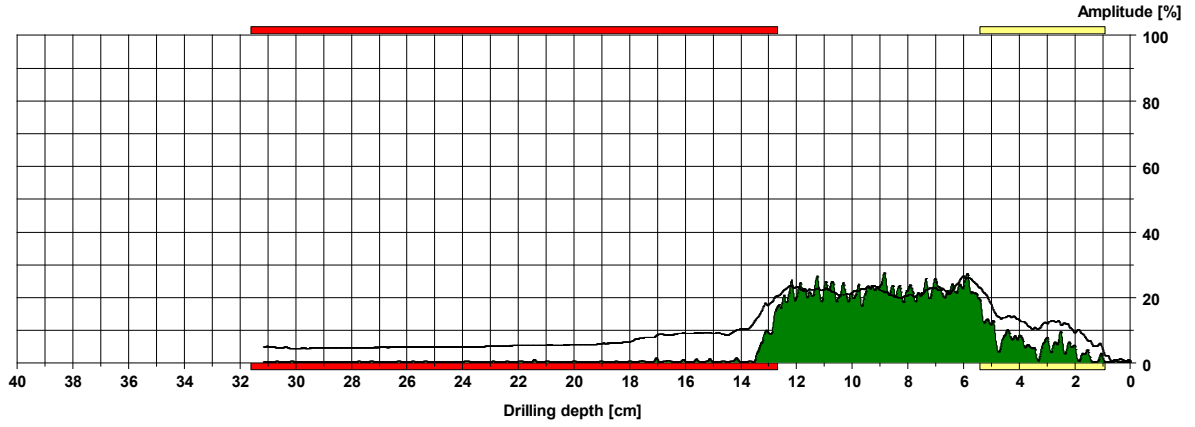


Drilling 2:



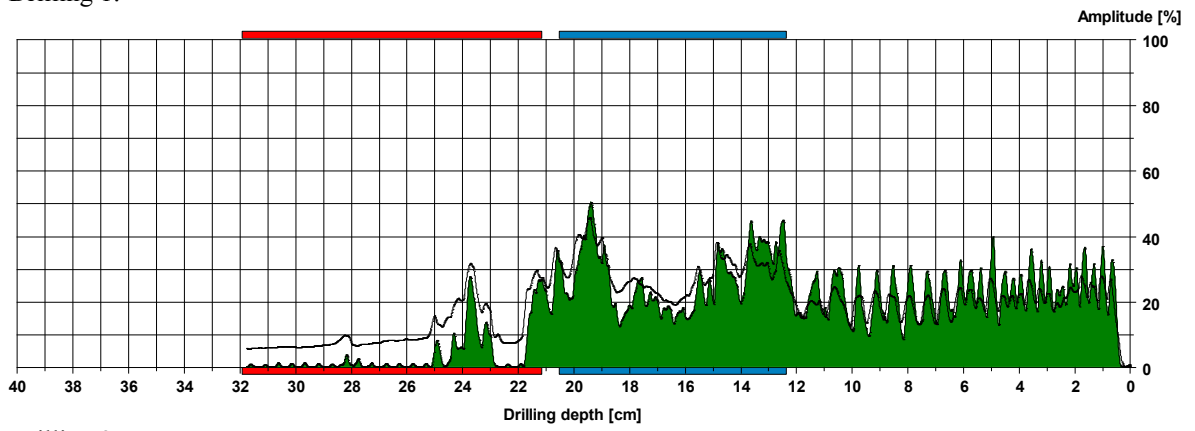


**Post in VIII**

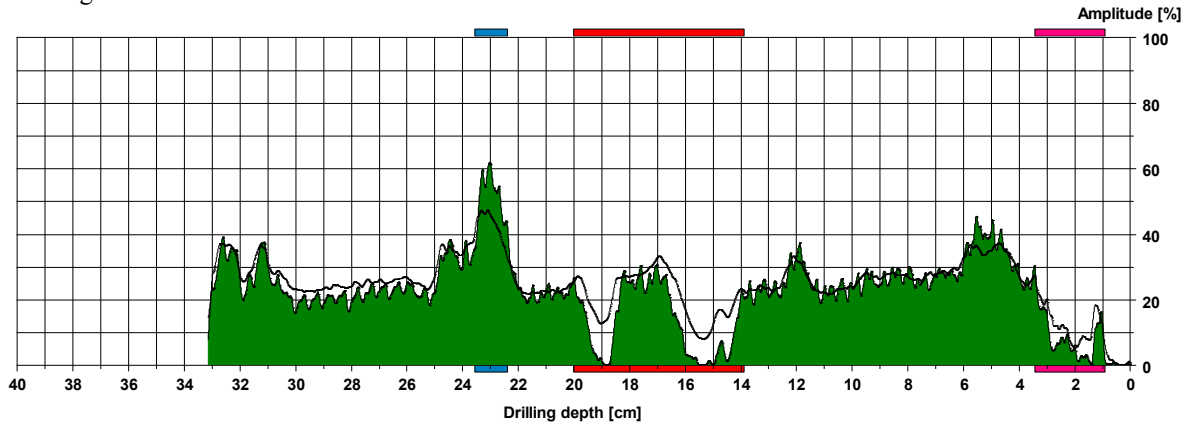


**Post in VIII**

Drilling 1:

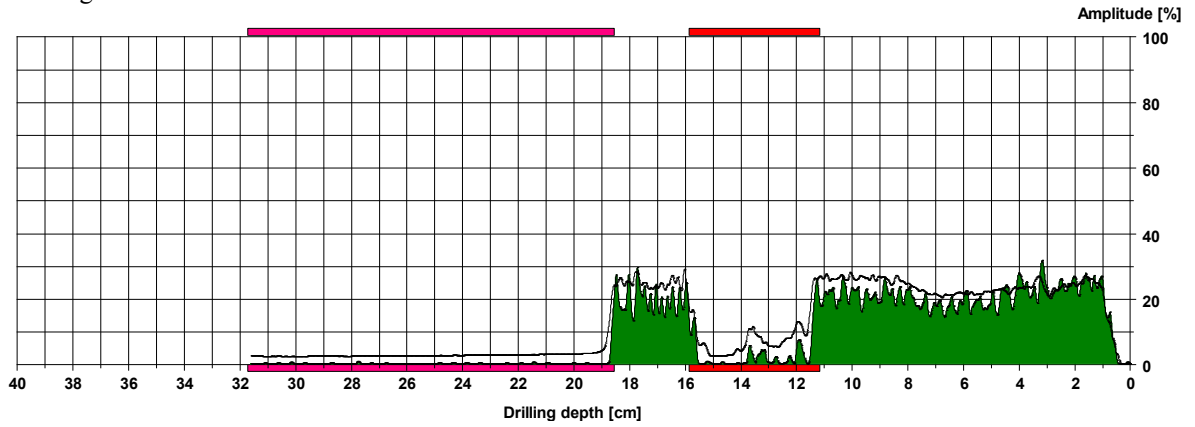


Drilling 2:

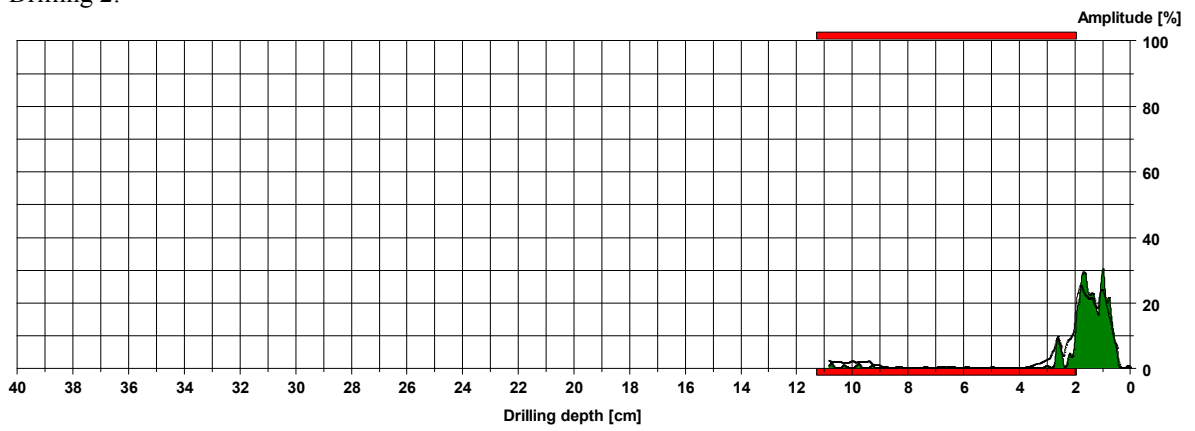


**Post in the southwest side of PII**

Drilling 1:

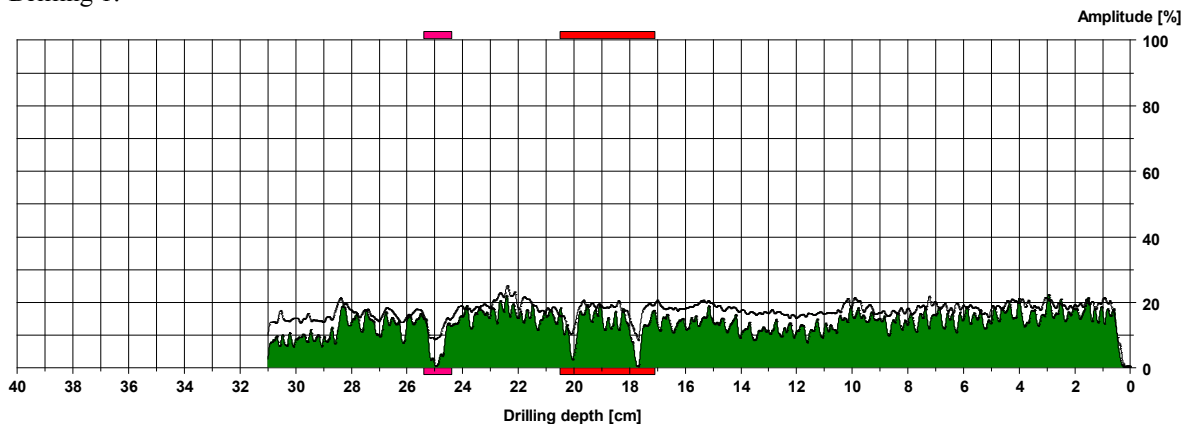


Drilling 2:

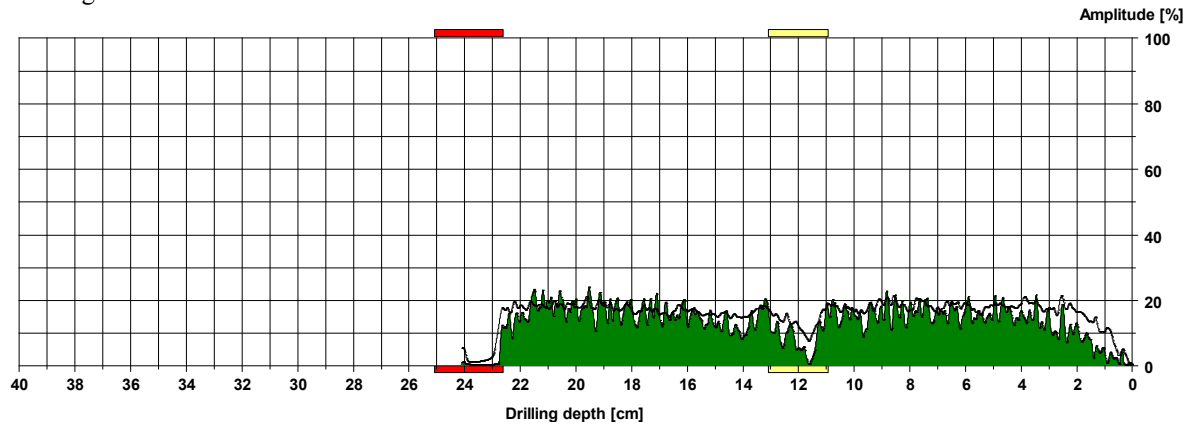


**Post in the southwest side of PIII**

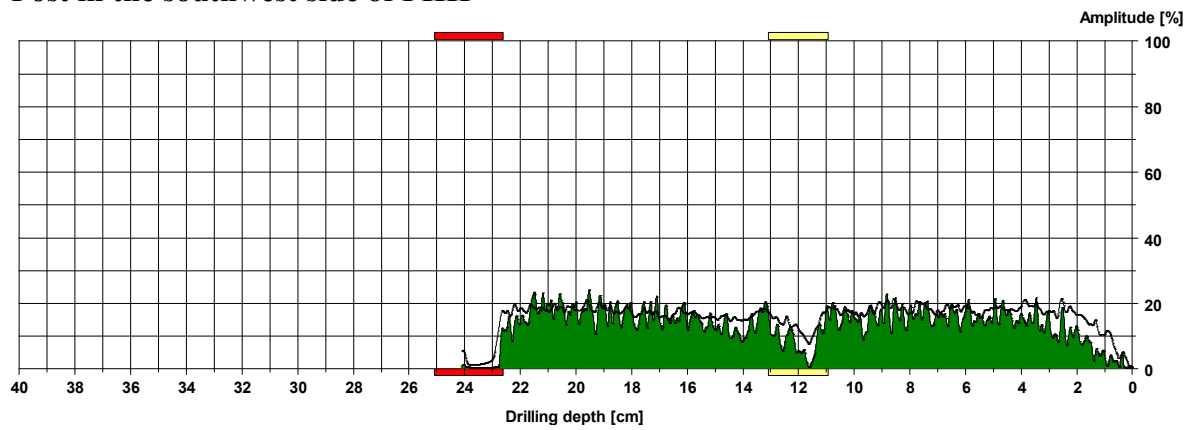
Drilling 1:



Drilling 2:

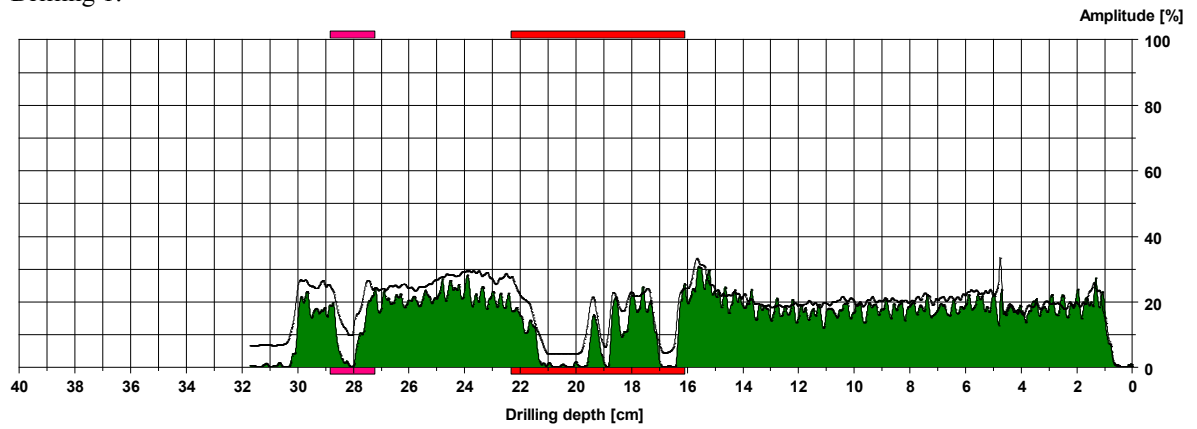


**Post in the southwest side of PIII**

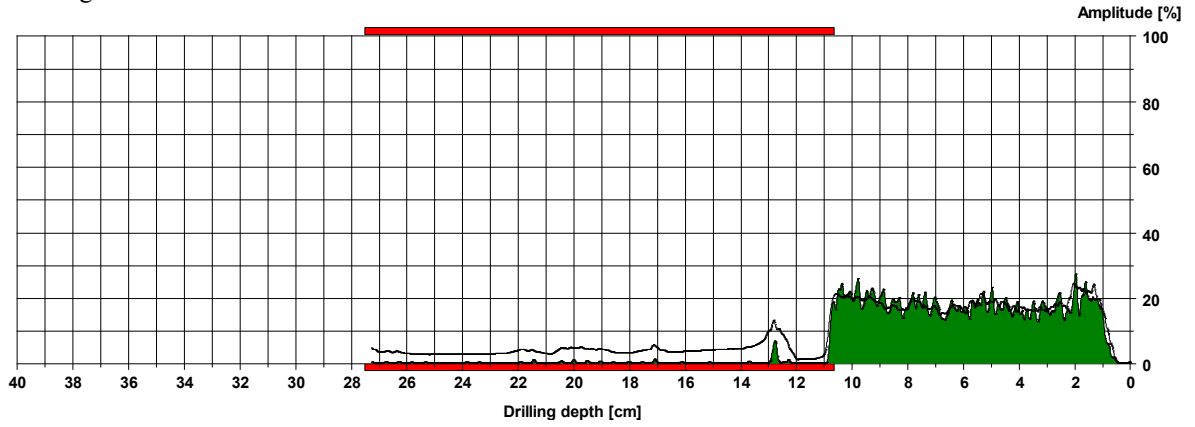


**Post in the southwest side of PIIII**

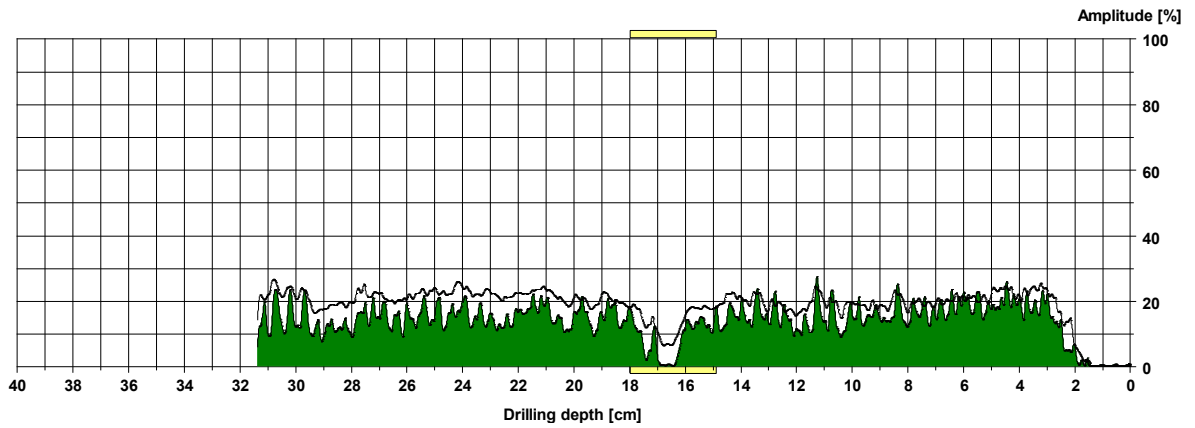
Drilling 1:



Drilling 1:

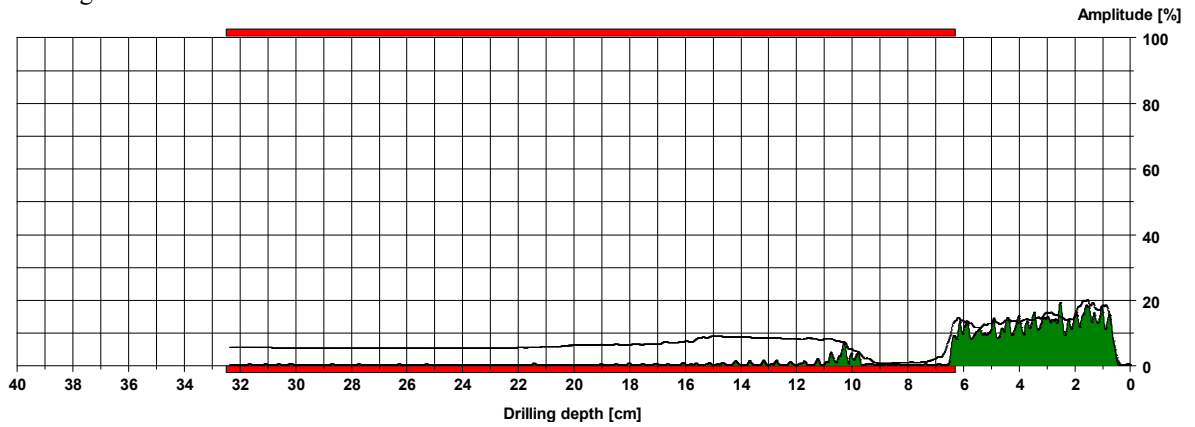


Post in the southwest side of PIIIII

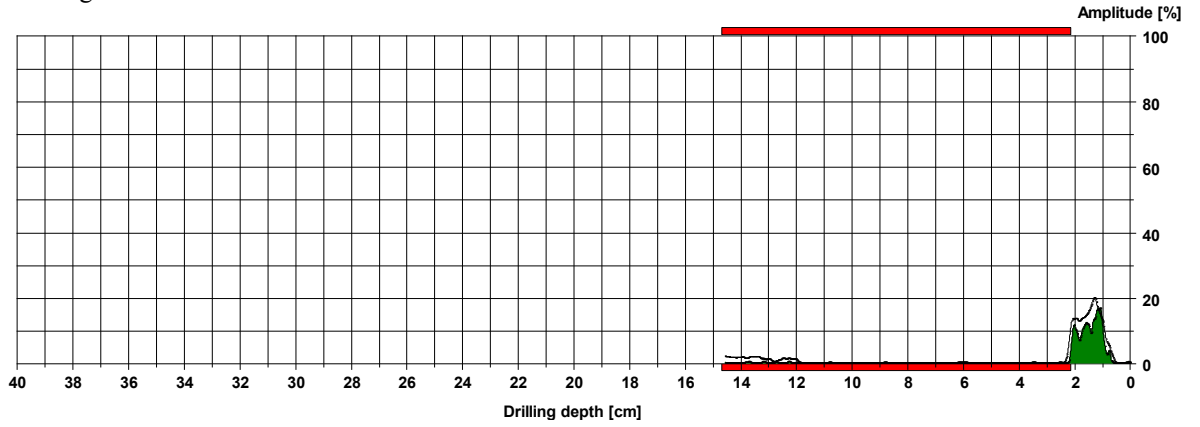


Post in VO

Drilling 1:

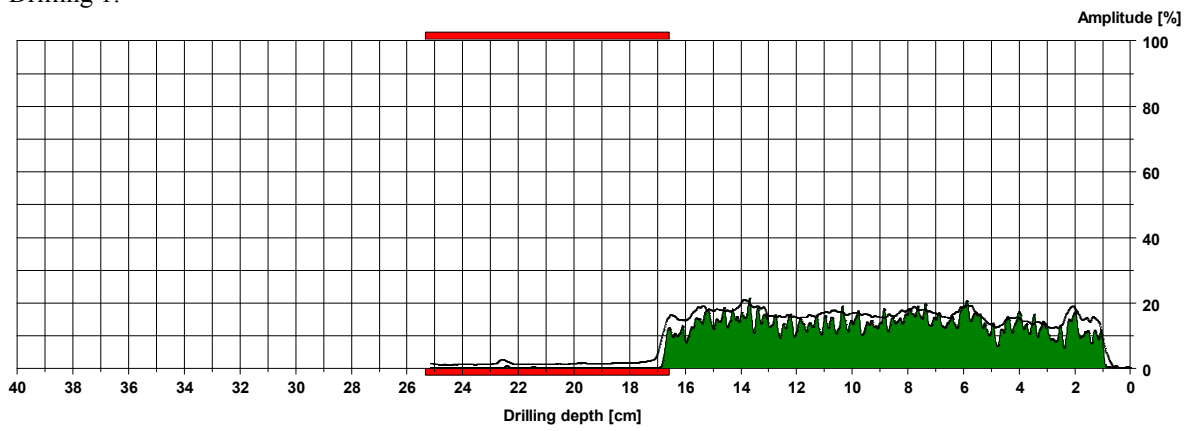


Drilling 2:

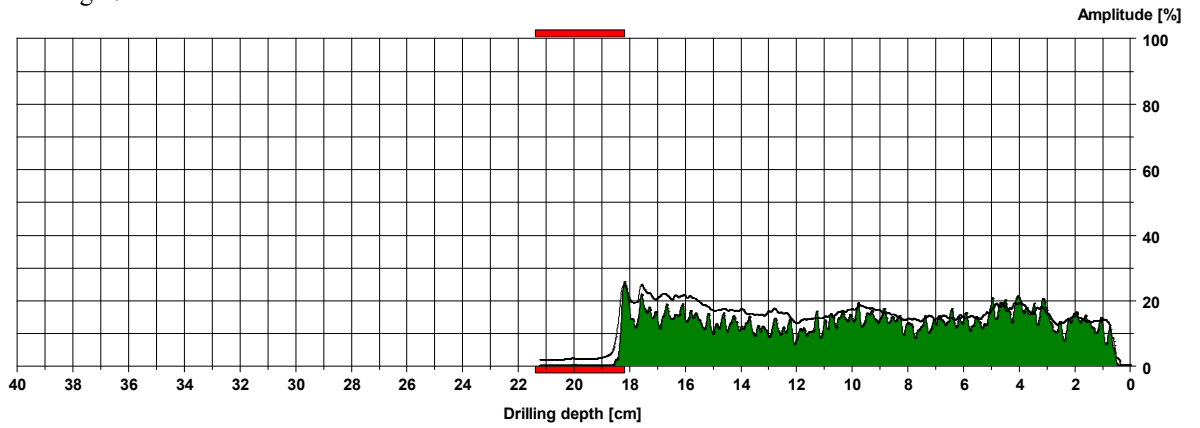


**Post in VOO**

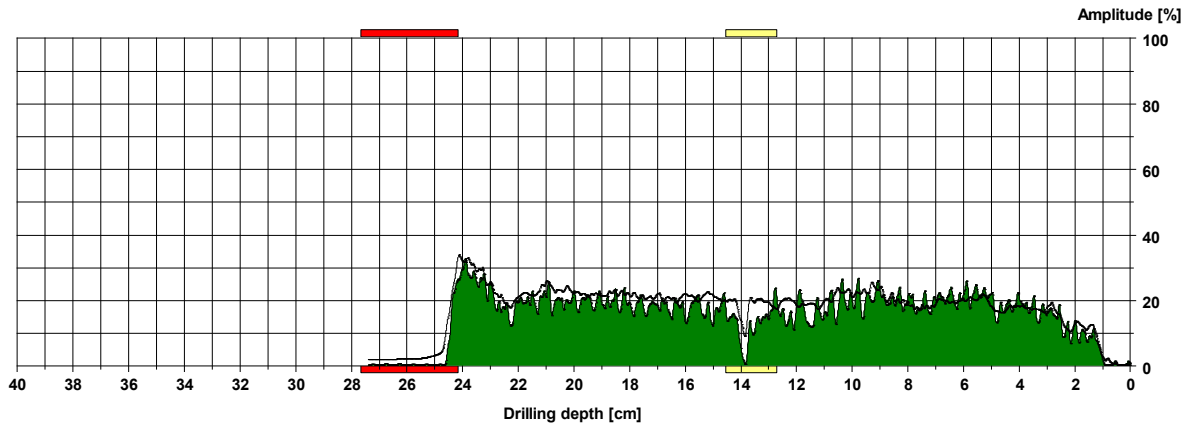
Drilling 1:



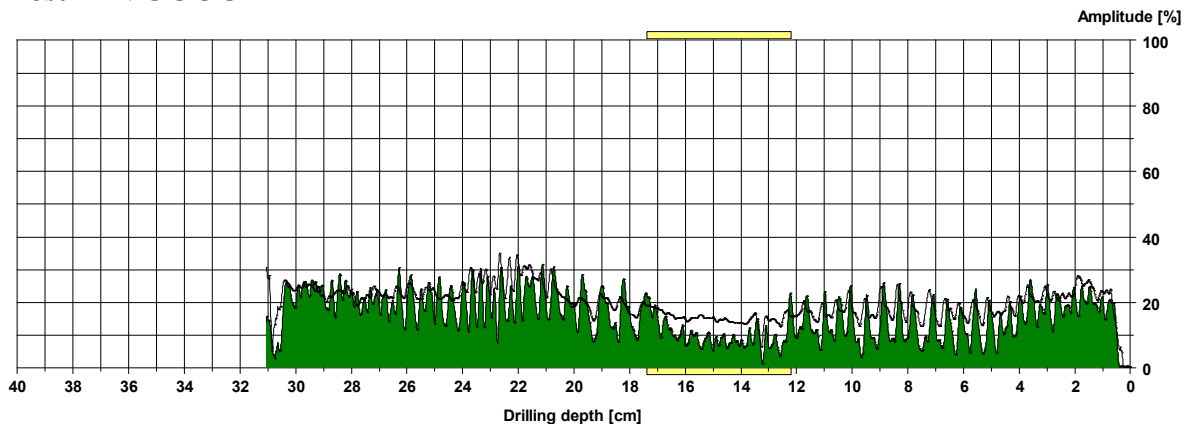
Drilling 2:



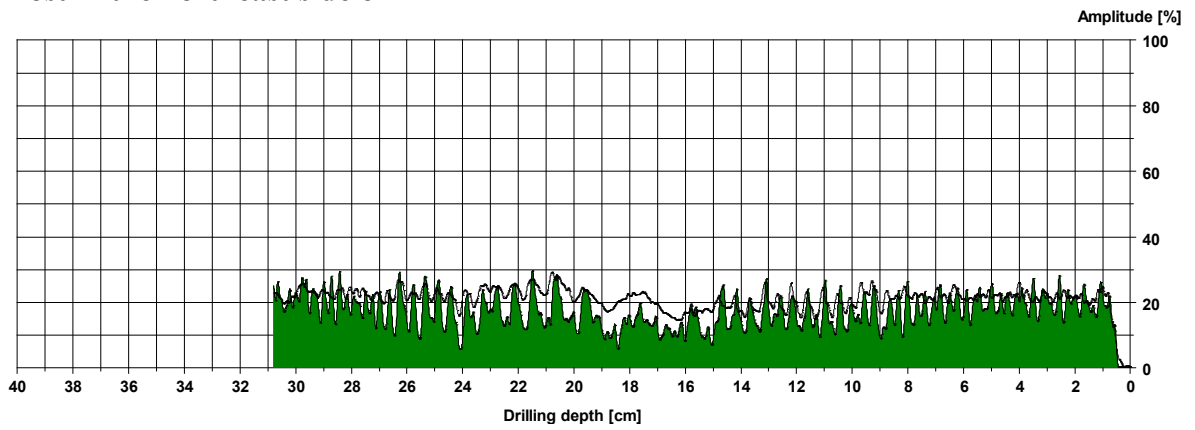
**Post in VOOO**



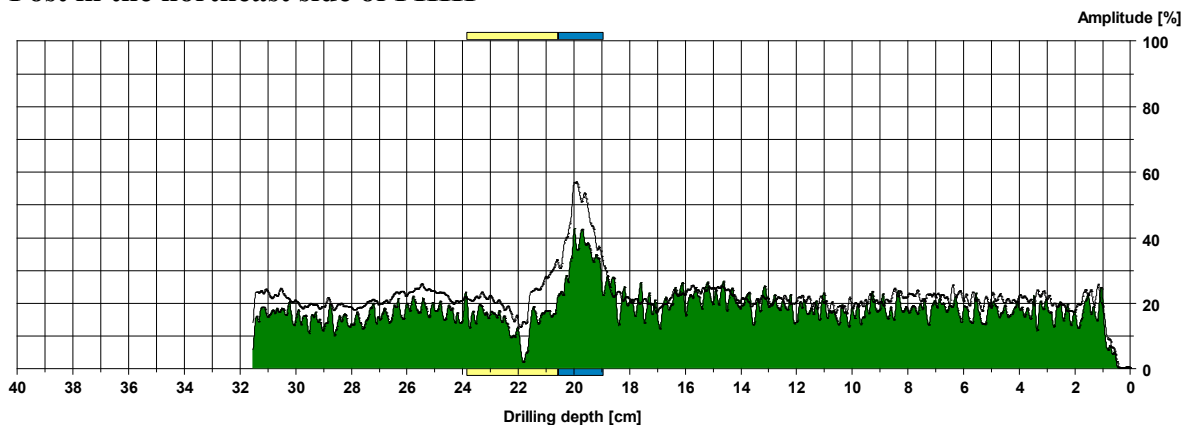
**Posti in VOOOO**



**Post in the northeast side of PIIII**



**Post in the northeast side of PIIII**



**Post in the northeast side of PIIIII**

